Residual restoration of DNA lesions in *Deinococcus radiodurans* mutants indicate presence of a bypass UV-repair process

Von der Fakultät für Mathematik und Naturwissenschaften der Carl von Ossietzky Universität Oldenburg zur Erlangung des Grades und Titels einer

Doktorin der Naturwissenschaften
Dr. rer. nat.

angenommene Dissertation

von
Ulrike Pogoda de la Vega, geb. de la Vega

geboren am 1976-04-20
in
Manhattan, New York, USA

Gutachterin: Dr. habil. Anna A. Gorbushina

Zweitgutachterin: Prof. Dr. Luise Berthe-Corti

Drittgutachterin: Dr. Petra Rettberg

Tag der Disputation: 17.04.2008

Eidesstattliche Erklärung

Hiermit versichere ich, die vorliegende Arbeit selbständig angefertigt und keine anderen als die angegebenen Quellen und Hilfsmittel benutzt zu haben.

Wörtliche und sinngemäße Zitate sind als solche gekennzeichnet.

Ich erkläre mich damit einverstanden, dass die Dissertation zu wissenschaftlichen Zwecken ausgeliehen werden kann.

15. Januar 2008 Ulrike Pogoda de la Vega

In short but very accurate, a statement describing the excitement of scientific discovery

> *"What we lacked with resources, we made up with enthusiasm."*
> (Aziz Sancar)

Publications

Part of the experiments of this dissertation have been published in advance.

U. Pogoda de la Vega, P. Rettberg, G. Reitz (2007) Simulation of the Martian UV radiation climate and its effect on *Deinococcus radiodurans*. 36^{th} COSPAR Scientific Assembly, Advances in Space Research 40 (11), pp. 1672—1677

R. Moeller, G. Horneck, **U. Pogoda de la Vega**, P. Rettberg, E. Stackebrandt, G. Reitz, R. Okayasu, T. Berger (2006) DNA damaging effects of heavy ion and X-ray irradiation of *Bacillus subtilis* spores. Int. Journal of Astrobiology 5, pp. 87 (abstract)

U. Pogoda de la Vega, P. Rettberg, T. Douki, J. Cadet, G. Horneck (2005), Sensitivity to polychromatic UV-radiation of strains of *Deinococcus radiodurans* differing in their DNA repair capacity. Int. Journal of Radiation Biology 81, pp. 601–611

U. Pogoda de la Vega, P. Rettberg, T. Douki, J. Cadet, G. Horneck (2004) UV-induced lesions and inactivation of *D. radiodurans*: wavelength-dependent correlation. EMBO Conference on Molecular Microbiology, Topic *Exploring prokaryotic diversity*, p. 65, Heidelberg, Germany (abstract)

U. Pogoda de la Vega, P. Rettberg and G. Horneck (2004) Effect of repair capability on UV resistance of *Deinococcus radiodurans*. Proceedings of the 7^{th} annual meeting of the German Society for Radiation Biology (GBS Gesellschaft für Biologische Strahlenforschung), Darmstadt, Germany, ISBN 3-00-013476-X (abstract)

P. Rettberg, **U. Pogoda de la Vega** and G. Horneck (2004) *Deinococcus radiodurans* – a model organism for life under Martian conditions. Proceedings of the 3^{rd} European Workshop on Exo-Astrobiology. Mars: The search for Life, ESA SP-545, pp. 59--62

CONTENTS

1. INTRODUCTION

Owing to its contamination of a can of meat that had expected to be sterile after it had been treated with 4,000 Gray (Gy) of γ rays, *Deinococcus radiodurans* R1 was isolated and described by Anderson in the 1950's of the past century [Anderson et al., 1956]. The sterilizing dose applied is approximately 250 times higher than that typically used to kill *Escherichia coli*, a representative of radiation sensitive bacterium [Battista, 1997]. Since then *D. radiodurans'* immanent radio resistance[1] and its accurate repair of fragmented DNA following $\gamma-$radiation has made this non-spore forming bacterium the investigation object of preference.

Radiation in general causes complex damage to various cell components, including nucleic acids, proteins and membranes. The damage can be caused either directly by the radiation or indirectly by free radicals produced by it as it passes through the cell [Mrazek, 2002]. Of the multiple lesions, DNA injury has the greatest impact on cell viability. Due to its size, genomic DNA occupies the largest fraction of the cell volume, therefore representing the most probable target to be hit. In addition, the genome exhibits little redundancy since it belongs to the small number molecules. Furthermore, considering the genome's omnipotent regulatory function in a single-cell organism, partial loss of functionality would result in a cellular collapse [Cox & Battista, 2005]. Hence, DNA damage is one of the key ramifications of ultra violet (UV) radiation on present day Earth. Cockell and Andrady (1999) identified three cardinal interrelated mechanisms that terrestrial organisms use for dealing with UV radiation: avoidance, protection and repair.

D. radiodurans meets all mentioned features: it indeed avoids UV radiation since it usually inhabits soil [Moseley, 1983]. Additionally, *D. radiodurans* is red-pigmented due to carotenoids incorporated in its cell wall [Brooks & Murray, 1981, Carbonneau et al., 1989], which can be regarded as a protective means. Carotenoids rather provide UV protection indirectly due to interaction with UV photons, formation of reactive oxygen species is facilitated and may result in the initiation of a reaction cascade damaging

[1] Whenever *D. radiodurans'* ionizing radiation resistance is meant, it can be abbreviated as *radio resistance* in this dissertation.

cell components. Carbonneau et al. (1989) assigned the carotenoids a role as biological antioxidants against reactive oxygen species and involvement in defense mechanisms as free radical scavengers than as a direct UV-protectant.

Lastly, returning to the point of departure: *D. radiodurans'* exceptional repair capacity. The latter reflects the incitement for this dissertation. This dissertation delineates the effort to distinguish elements involved in the complex UV-induced lesion recovery by studying the overall response to UV radiation of repair-deficient mutant strains of *D. radiodurans* in comparison to the wild-type strain and analyzing it with the help of lesion distribution profiles and stress-induced whole genome expression profiles.

1.1 *Deinococcus radiodurans* is affiliated to the family *Deinococcaceae*

The species of the genus *Deinococcus* represent a very diverse phylogenetic lineage within the domain Bacteria of which all are gram-positive, non-motile and non-spore formers. The methodical approach to ascertain *D. radiodurans'* affiliation included "16S rRNA gene sequence data that have been used to differentiate the species of the genus *Deinococcus* both from other taxa and from each other" [Rainey et al., 1997, Suresh et al., 2004, Rainey et al., 2005]. This chemotaxonomic approach revealed an apparently ancient derivation with a specific evolutionary relationship to the *Thermus* group [Hensel et al., 1986, Woese, 1987, Weisburg et al., 1989, Battista & Rainey, 2001, Griffiths & Gupta, 2004], which raises the question whether they had a thermophilic common ancestor [Makarova et al., 2001].

A distinct feature of the *Deinococcaceae* is their ability to withstand high fluences of ionizing and UV radiation that are lethal to virtually all other living organisms and to tolerate approximately 30-fold more DNA double strand breaks (dsb) than *E. coli* before surrendering to the genomic damage ([Cox & Battista, 2005] as well as references therein). There are twenty-five validly described species: *D. erythromyxa, D. proteolyticus, D. radiodurans, D.radiophilus, D. radiopugnans* [Brooks & Murray, 1981]; *D. geothermalis, D. murrayi* [Ferreira et al., 1997]; *D. grandis* [Rainey et al., 1997]; *D. frigens, D. marmoris, D. saxicola* [Hirsch et al., 2004]; *D. indicus* [Suresh et al., 2004]; *D. deserti* [de Groot et al., 2005]; *D. apachensis, D. hohokamensis, D. hopiensis, D. maricopensis, D. navajonensis, D. papagonensis, D. pimensis, D. sonorensis, D. yavapaiensis* [Rainey et al., 2005]; *D. ficus* [Lai et al., 2006]; *D. mumbaiensis* [Shashidhar & Bandekar, 2006] and *D. yunweiensis* [Zhang et al., 2007]. Twenty-one of these "tolerate what for most microorganisms is a sterilizing dose of ionizing radia-

tion, exhibiting detectable survival after exposure to 10 kGy γ-radiation" [Zimmerman & Battista, 2005]. The ionizing radiation resistance of the species *Deinococcus indicus* [Suresh et al., 2004], *Deinococcus frigens, Deinococcus saxicola* and *Deinococcus marmoris* [Hirsch et al., 2004] has not been conveyed yet. The latter being an exceptional group within the *Deinococci* in growing well in low-nutrient oligotrophic medium, preferring low temperatures ranging between 9 - 18$^{\circ}C$ and having been isolated from Continental Antarctica.

The mesophile species grow best in nutrient-rich media at temperatures between 30 and 37$^{\circ}C$, their doubling time ranging between 1.5 and 3 hours. However, *D. geothermalis* and *D. murrayi* are true thermophiles, with optimal growth temperatures of $45 - 55^{\circ}C$ as well as *D. maricopensis*, but growing at 40$^{\circ}C$. In general, the *Deinococci* are spherically shaped, exist as single, as pairs or as tetrads in liquid culture. Whereas *D. grandis, D. maricopensis, D. navajonensis, D. papagonensis, D. pimensis, D. yavapaiensis* are rod-shaped and *D. sonorensis* either forms spherical or short rod-shaped cells.

D. radiodurans is the type strain of the *Deinococcaceae* and received more attention by researchers than the other species. *D. radiodurans* features plasma and outer membranes and a multilayer cell envelope [Makarova et al., 2001]. The *D. radiodurans* genome is 3.28 Mb, with a GC content of 67% [Cox & Battista, 2005, Rainey et al., 2005]. The deinococcal genome is composed of a 2.64-Mb chromosome (chromosome I), a 0.41-Mb chromosome (chromosome II), a 0.18-Mb megaplasmid MP1 and a 0.045-Mb plasmid CP1 [Lin et al., 1999]. *D. radiodurans* has between 4 and 10 genome copies per cell that are dispersed into the diplo- or tetracoccal compartments, depending on the bacterial growth stage. During exponential growth 8 to 10 haploid genome copies are present in *D. radiodurans* and 4 genome copies during stationary phase [Hansen, 1978, Harsojo et al., 1981].

1.2 No unique DNA repair proteins presently known in *Deinococcus radiodurans*

Though *D. radiodurans'* genome was sequenced in 1999 [White et al., 1999] and many investigations were performed to elucidate its repair mechanisms [Moseley & Laser, 1965, Minton, 1994, Battista, 1997, Daly et al., 2004, Daly et al., 2007], up to now neither was able to fully explain its repair capacity. Recently roles of genes [Mattimore & Battista, 1996, Earl et al., 2002b, Earl et al., 2002a, Minsky et al., 2006] or revelation of *D. radiodurans'* rebuilding mechanism of its shattered genome [Zahradka et al., 2006] following $\gamma-$radiation could shed light on a few DNA repair components.

But, several studies have shown, that deinococcal proteins related to DNA damage repair exhibit unique features. Exemplified in deinococcal RecA ($DR2340$) which has been attributed not only a pivotal role in DNA repair but also essential housekeeping function [Cox, 2003]. Deinococcal RecA processes single-stranded DNA in the same manner as the prototypical *recA* protein of *E. coli* but preferably binds to double-stranded DNA, facilitating repair of double-strand DNA breaks [Kim et al., 2002]. Moreover, *D. radiodurans* seems to have developed an evolutionary strategy to multiply the domains of its canonical maintenance proteins resulting in acquiring novel functions [Haruta et al., 2003, Eggington et al., 2004, Lee et al., 2004, Wang & Julin, 2004, Leiros et al., 2005]. Especially proteins involved in homologous recombination repair (HR) have atypical protein structure arrangements, allowing a very efficient and rapid repair of double strand breaks (dsb). The HR-involved single-strand-binding protein (SSB–$DR099$ and $DR0100$) has two oligonucleotide/oligosaccharide-binding folds (responsible for forming DNA interactions) rather than one, that function as dimer rather than a tetramer and its concentration is $10x$ times higher than the normal *in vivo* level measured in *E. coli* [Bernstein et al., 2004, Eggington et al., 2004, Witte et al., 2005, Eggington et al., 2006]. Moreover, the *D. radiodurans* locus encodes the largest bacterial SSB polypeptide investigated so far.

A further example of this evolutionary strategy is the deinococcal *recQ* helicase that encodes three helicase and RNAse D C-terminal (HRDC) domains [Killoran & Keck, 2006]. To date the presence of single HRDC domain was found to be typical in prokaryotes. The results obtained by Killoran and Keck (2006) indicate that the multiple deinococcal RecQ HRDC domains can not be regarded as simple repetitive copies of the *E. coli recQ* HRDC domain.

Yet, it has become apparent that *D. radiodurans* is not equipped with a new or universal remedy but that it has been able to boost the ever-present typical DNA-repair pathways (excision repair, mismatch and recombinational repair) by employing specialized properties of existing active or passive systems. Together these seemingly minor enhancements with a modest contribution might convey such an exceptional skill to cope with radiation injury.

1.3 Effect of radiation

This section will briefly review what is known about *D. radiodurans'* physiology and enzymology as it relates to this species' response to radiation, slightly skewed by the fact that most studies focused only on $\gamma-$radiation-induced repair mechanisms.

Cox and Battista (2005) have summarized different strategies that may be used by *D. radiodurans* to protect its DNA from the effects of $\gamma-$rays. In comparison, little has been investigated concerning *D. radiodurans'* capability to repair UV-induced lesions including protein damage. However, UV-light induced protein damage occurs frequently since the absorption maximum of proteins is $\lambda = 280$ nm. At the DNA level, the primary target of UV radiation damage are DNA bases whereas ionizing radiation causes a broader range of damage, including single- (ssb) and double-strand breaks (dsb). As stated by Cox and Battista "the infrequent occurrence of ionizing-radiation resistance among distinct prokaryotic lineages indicates that this phenotype has arisen in unrelated species through horizontal gene transfer, or possibly convergent evolution. It is possible that these diverse prokaryotic cells adapted differently to a similar selective pressure and that there might be multiple mechanisms of radio resistance." The selective pressure was identified to be desiccation [Mattimore & Battista, 1996] leading to the interrelated phenomenon of desiccation-tolerance providing ionizing-radiation resistance to these species.

1.3.1 Ionizing radiation

Ionizing radiation is often labeled as high-energy radiation because it possesses enough energy to ionize molecules. In general, ionizing radiation is produced by the decay of radioactive elements. In particular, $X-$ and $\gamma-$radiation belong to the electromagnetic spectrum that includes visible light and radio waves. γ rays are photons that generate ions by several types of energy-absorption events and can penetrate deeply into a cell or tissue. Ion production is accompanied by the release of energetic electrons, generating multiple ions and electrons in one event. The dose absorbed by the cell, tissue or other matter, the so-called energy deposition, is measured in J/kg or in Gray (Gy) per unit mass (SI measurement; $1J/kg = 1Gy$). The radio resistance of microorganisms is compared by measurement of the D_{37} dose at which 37% of the cells survive. At the D_{37}, each cell on average has experienced one lethal event (the surviving fraction of cells is balanced by others that experienced two or more lethal events) [Daly & Minton, 1996].

Ionizing radiation causes multiple types and a broad range of DNA damage like modification of nucleobases, single strand and double-strand breaks as well as cross-links. Various strategies to prevent DNA from the effects of radiation have been considered to contribute to the ionizing-radiation resistance of *D. radiodurans*: protection of cellular targets, *recA*-dependent, *recA*-independent double-strand-break repair and base damage repair.

1.3.1.1 Protection of cellular targets

One of the central assertions in radiobiology is the declaration of DNA being the principal target of ionizing radiation. Therefore, measures playing a role in DNA protection were investigated first. Early studies [Hansen, 1980, Harsojo et al., 1981] revealed that *D. radiodurans* contains multiple genome copies, which provide highly redundant genetic information that could allow an alignment of homologous sequences between the genome copies to guide precise recombinational repair of dsbs. Yet, Zimmerman and Battista (2005) stated that the existence of such an alignment has not been established. Levin-Zaidman et al. (2003) were the first to educe that the specific toroidal nucleoid morphology detected in *D. radiodurans* [Eltsov & Dubochet, 2005] could protect the DNA fragments formed by dsbs from diffusing apart during repair [Minsky, 2003]. According to the authors, this mechanism requires two steps – first, maintenance of linear continuity of *D. radiodurans'* genome and second, fusion of the ring-like nucleoids in neighboring cells, subsequently undergoing homologous recombination.

Some of the authors' conclusions have been controversially discussed, stimulating subsequent studies [Minsky, 2003, Englander et al., 2004, Ghosal et al., 2005, Ohba et al., 2005, Frenkiel-Krispin & Minsky, 2006], among which Zimmerman and Battista's (2005) attempt to correlate specific nucleoid structure and radio resistance is the most remarkable one. The authors compared the genomic DNA of extremely radiation-resistant species of the genus *Deinococcus* and *Thermus* with the radiation-sensitive *E. coli*. The authors could not determine a relationship between the specific nucleoid structure and ionizing radiation resistance. Yet, the genome of the examined resistant species was shown to be more condensed relative to the sensitive ones, implying that this common feature could promote repair processes. Other assertions derived from the observation of Levin-Zaidman et al. (2003) concern the existence of non-homologous end joining within the proposed toroid-shaped nuclear matrix for *D. radiodurans* [Minsky, 2003, Englander et al., 2004, Minsky et al., 2006], and will be discussed in chapter 1.3.1.2.

As the ultrastructural basic approach to understand why bacteria as *D. radiodurans* are ionizing radiation resistant has been exhausted, new technologies were required to investigate the underlying molecular mechanisms. DNA microarrays following exposure to ionizing radiation have launched new possibilities for large-scale gene expression profiling. Tanaka et al. (2004) used this approach and identified five hypothetical novel genes implicated in the recovery from ionizing irradiation. These genes contribute notably to *recA*-dependent and *recA*-independent repair processes (cf. chapter 1.3.1.2).

Of these five novel genes, the DdrA protein was described first.

The DdrA protein protects the broken 3′ DNA ends to limit DNA degradation occurring post-irradiation and during desiccation [Harris et al., 2004]. As DNA strand breaks accumulate, nuclease action could disintegrate genomic DNA. Protection of DNA ends facilitates preserving genome integrity until environmental conditions become suitable to perform energetically unfavorable processes like cell proliferation and DNA repair.

It was recently hypothesized that the protection of alternative cellular targets may contribute to the high radio resistance in *D. radiodurans*. Daly and coworkers proposed ionizing radiation-induced protein oxidation rather than DNA injury to be crucial for radio resistance [Daly et al., 2004, Ghosal et al., 2005, Daly et al., 2007]. These recent studies "support the idea that the extreme-resistance phenotype of *D. radiodurans* and other bacteria with high intracellular Mn/Fe concentration ratios is dependent on the redox cycling of Mn(II) that protects proteins from oxidative damage during irradiation, with the result that enzyme systems involved in recovery survive and function with great efficiency." Mn(II) scavenges simple peroxyl radicals to provide immediate cytosolic protection and prevent lethal secondary oxidative modifications of proteins. Consistently the authors showed that resistant and sensitive bacteria are equally susceptible to a given dose of ionizing radiation-induced damage but that the amount of protein damage caused by that dose varied with intrinsic radio tolerance.

One additional mechanism was proposed by Cox and Battista (2005) who derived a joint strategy from the mechanisms described by Minsky's restricted diffusion (2003) and Daly's Mn(II) redox cycling [Daly et al., 2004, Daly et al., 2007], which they have named 'cryptic dsb' repair. The authors speculate that *D. radiodurans* has a mechanism that provides genome stabilization by avoiding dsbs induced by (secondary) oxidation. Assuming that such a protein-based or local DNA stabilization environment exists and is physically fostered by intracellular ionic composition that limit dsb dissociation, genomic continuity is preserved and repair of the cryptic dsbs would be error-free and *recA*-independent. If proteins are responsible for DNA stabilization, the authors assume that "they will be functionally analogous to the structural maintenance-of-chromosomes (SMC) proteins that are present in many eukaryotic and prokaryotic species," designated as cohesins and condensins ([Cox & Battista, 2005] and references therein). Remaining single-strand breaks could be further processed via single-strand annealing and/or homologous recombination (cf. chapter 1.3.1.2).

1.3.1.2 Repair of double strand breaks

Two general types of double-strand break (dsb) repair pathways exist that reconstitute a DNA helix [Friedberg, 2003]. Homologous recombination (HR) or DNA crossover requires information from a sister or homologous chromosome for accurate dsb repair. Whereas non-homologous end joining (NHEJ) allows joining of DNA termini even if there is no sequence similarity between the ends. Single-strand annealing (SSA) can be regarded as an aberrant homologous recombination since recombination occurs at non-homologous sites. NHEJ can be, and SSA is always, accompanied by a deletion event that spans one of the two homologous repeats or the intervening sequence.

The general process flow of dsb repair:

1. Detection of dsb
2. Recruitment of processing enzymes to cleave dsb sites (nuclease and polymerase)
3. DNA termini processing to create ligatable $5'-$phosphate or $3'-$OH nicks
4. Gap filling with remaining nicks
5. Nick sealing, ligation of the two strands by DNA ligase
6. Dissociation of repair proteins
7. Repaired DNA helix

The most recent model for HR is called synthesis-dependent strand annealing Figure 1.1B, a conservative DNA synthesis mechanism, differing from the semi-conservative replication occurring during normal chromosome duplication. The HR mechanism is distinguished from NHEJ in that it requires a *recA*-mediated strand invasion, strand isomerization (or branch migration) and subsequent loop digestion before reforming the DNA helix Figure 1.1.

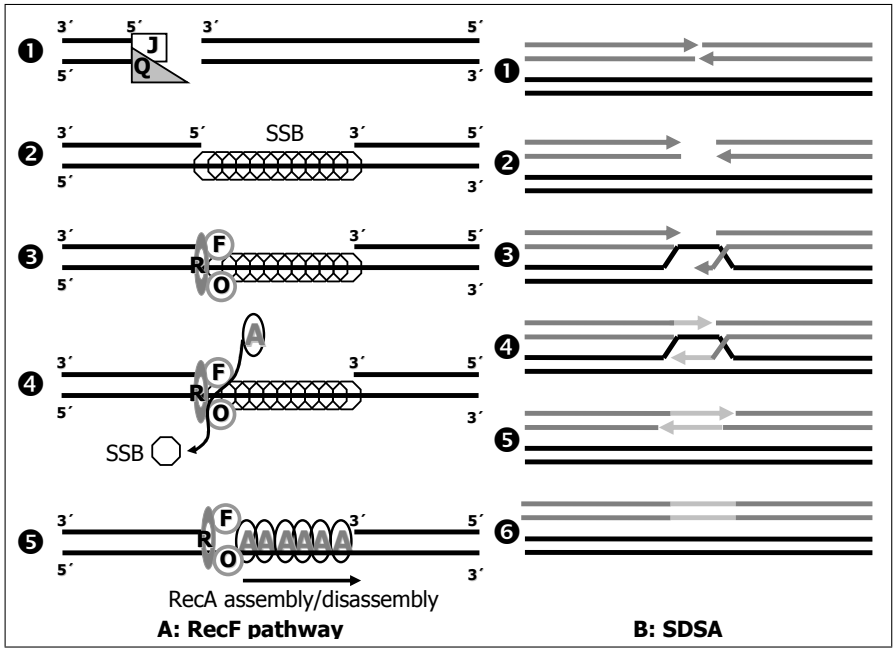

Fig. 1.1: To give a summary of dsb-repair pathways of *D. radiodurans*, synthesis-dependent strand annealing (SDSA) and the RecF-pathway are exemplified. **A:** RecF-pathway [Lee et al., 2004] – DNA is degraded by RecJ and RecQ at the dsb site (1). Single-strand binding protein (SSB) stabilizes the lesion site (2) so that RecF, RecO, and RecR can associate to limit the degradation by RecJ and RecQ (3). The RecFOR-complex promotes the loading of RecA (4), an ATP-dependent reaction in which SSB disassociates from the lesion site, and facilitates the RecA filament formation. **B:** SDSA – Breakage of the DNA helix (1) iniates this mechanism of error-free dsb repair by $5'$ to $3'$ resection from the $3'$ strand (2). One of the $3'$ strands invades a homologous region on an undamaged sister strand (3) preparing new DNA synthesis and creating a D-loop (4). By unwinding from the template, the newly synthesized DNA (light grey) can anneal and ligate (5), sealing the dsb (6).

Experiments on the HR mechanism in *E. coli* have shown that the heterotrimeric nuclease RecBCD complex is essential for *recA*-mediated recombination [Arnold & Kowalczykowski, 2000]. The RecBCD complex produces single-strand tails by its nuclease activity and promotes loading of RecA onto these tails. Comparison of genome sequences revealed that no such complex exists in *D. radiodurans* [Makarova et al., 2001, White et al., 1999] but that the deinococcal RecA is rather in favor of double-stranded than of single-stranded DNA [Kim & Cox, 2002, Haruta et al., 2003]. Further classical bacterial proteins involved in HR,

besides *recA*, that have been identified in *D. radiodurans* are single-strand-binding protein (SSB), recombinase D (RecD) [Wang & Julin, 2004]; DNA polymerase I (polA) [Zahradka et al., 2006], recombinase R (RecR) [Lee et al., 2004], recombinase O (RecO) [Leiros et al., 2005] and *recQ* helicase [Killoran & Keck, 2006]. Recent results obtained, seem to assign deinococcal *recD* protein rather a role in antioxidant pathway than in dsb HR repair [Wang & Julin, 2004, Servinsky & Julin, 2007].

Zahradka et al. (2006) assigned deinococcal DNA polymerase I a significant role in its recently revealed molecular mechanism for shattered chromosome reassembly that has been termed *extended synthesis-dependent strand annealing* (ESDSA), which requires HR as the final step to full-fledged circular chromosomes. The premises for high fidelity ESDSA are existence of at least two genome copies and random DNA fragmentation. Extensive synthesis of homologous single strands is achieved by utilizing information from overlapping complementary DNA fragments as primer (recipient strand) and as template (donor strand).

Deinococcal *recQ* consists of three HRDC domains, whereof each has distinct sequence characteristics and individually intervenes in the structure-specific DNA binding, DNA-dependent ATP hydrolysis and DNA unwinding activity of the RecQ protein. Killoran and Keck (2006) regard their data to agree with the proposed key role of RecQ in bacterial RecF-mediated recombination (a first working model for a deinococcal *recF* pathway was proposed by [Lee et al., 2004]; modified in Figure 1.1A). RecQ DNA helicase (*DR*1289) and RecJ $5' - 3'$ single strand (ss) DNA exonuclease have been proposed to process dsbs, whereas the RecF pathway proteins RecR (*DR*0198), along with RecF (*DR*1089) and RecO (*DR*0819), assist RecA (*DR*2340) loading onto ssDNA [Ivancic-Bace et al., 2003]. RecO is the only strand-annealing enzyme so far found in the *D. radiodurans* genome [Makharashvili et al., 2005].

The first suggestion to account for a temporal progression and interaction of more than one intrinsic repair mechanism in *D. radiodurans* was proposed by Daly and Minton in 1996. They presented evidence for a two-step repair chronology following ionizing radiation: a *recA*-independent reaction preponderates in the first 1.5 h post-irradiation recovery, maybe functioning as a preparatory phase, and a subsequent *recA*-dependent homologous recombination apparent between 5 and 9 h post-irradiation. The *recA*-independent reaction considered by the authors was hypothesized to be single-strand-annealing (SSA) whereas NHEJ was ruled out because of the exceptional resistance of *D. radiodurans* to killing and mutation induced by DNA-damaging agents.

Theoretical considerations and in vitro studies postulated a pre-existing reaction to account for an efficient sequence homology search to take place within a physiologically appropriate time slot [Daly & Minton, 1995, Minton & Daly, 1995, Minsky, 2003]. Though *recA*-mediated homologous recombination (HR) is the sole pathway to ensure high-fidelity repair of dsbs, it can be easily disabled as soon as a vast excess of fragments per genome is encountered. In this respect, the search for homologous DNA sites becomes futile because it takes more time for a nuclease to find repeats located further from a dsb and in the worst case, no intact template is left [Minsky, 2003, Englander et al., 2004, Minsky et al., 2006]. In order to counteract the need of homology search Minton and Daly (1995) proposed that dsb repair in *D. radiodurans* is promoted by a continuous chromosomal alignment that ensures accurate repair by always supplying a template in close proximity.

In contrast, non-homologous end joining (NHEJ) is usually referred to as an error-prone mechanism because it lacks sequence-specific processing enzymes that would deliver the dsbs to a homologous target site. However, if cohesion of shattered DNA fragments is ensured – either through nucleosome structure or mediated by proteins – an error-free rejoining can be performed [Frenkiel-Krispin et al., 2004, Minsky, 2003].

Levin-Zaidman et al. (2003) provided structural evidence of the significant contribution of chromosomal morphology in protecting and maintaining genome integrity. They demonstrated that DNA in *D. radiodurans* adopts an ordered and highly compact ring-like structure (toroid). The tightly packed shape of the DNA toroids act as rigid matrices, therefore, limiting molecular diffusion of the numerous irradiation-generated DNA breaks and arranging for close proximity between the fragments. Indicating that such an assembly enables an error-free and template-independent dsb repair, even following massive fragmentation [Levin-Zaidman et al., 2003].

Recent studies presented proteins (PolX and PprA) with predicted activities concurring to a deinococcal NHEJ system involved in dsb repair [Lecointe et al., 2004, Narumi et al., 2004]. The radiation-induced PprA binds to DNA termini, protects the strands from nuclease digestion and facilitates DNA end joining catalyzed by ATP- and NAD-dependent DNA ligases [Minsky et al., 2006, Ohba et al., 2005]. Irradiation induces the ATP-dependent ligase but down-regulates the NAD-dependent ligase, leading Ohba et al. (2005) to suggest that the small size ATP-dependent ligase might be involved in post-irradiation recovery. Especially its small size enables an unimpeded access to dsbs within the highly condensed DNA toroids. A topical review [Pitcher et al., 2007] concedes the case against a deinococcal NHEJ due to their attained premise that the prokaryotic NHEJ requires a Ku

protein and a multifunctional ATP-dependent DNA ligase (LigD). However, up to date no Ku homologs have been found in *D. radiodurans*.

1.3.2 Ultra-violet (UV) radiation

UV radiation comprises a wide wavelength spectrum and is subdivided into vacuum-UV (VUV), UVC, UVB and UVA ranging from >100 to 200 nm, 100 to 280 nm, 280 to 315 nm and 315 to 400 nm, respectively (definition of the spectral bands follows German norm DIN 5031-7). Due to the absorption of the short-wavelength portion of UV radiation by the stratospheric ozone layer existent on present Earth, all biological systems are protected from this energetically more damaging UV spectrum. Therefore, the total solar UV radiation flux on present Earth is composed of nearly 0% UVC, approx. 5% UVB and the remaining 95% attributes to the UVA fluence rates.

UV radiation causes formation of bipyrimidine photoproducts, the main photoproducts being cyclobutane pyrimidine dimers (CPD) and pyrimidine (6−4) pyrimidone photoproducts (6−4PPs) between two adjacent pyrimidine bases (cf. chapter 2.5.1).

1.3.2.1 Earth's UV radiation evolution

The existence of an ozone column provides Earth with a unique protection measure, but this feature was accumulated over time. In the Archean period (3.9 to 2.5 Ga ago), before the Earth experienced an ozone build-up, primordial colonizers of Earth's surface had to cope with a UV radiation environment consisting of higher UVB and UVC portions resulting in UV-fluences exhibiting a 1000 times higher biological effectiveness than those at present comprising $\lambda > 295$ nm [Cockell & Horneck, 2001, Rettberg et al., 1998, Horneck et al., 1998].

In contrast, the UV climate of Mars during the early geological time-scale was characterized rather by a steady increase of UV flux due to the increase in solar luminosity (a 25% less luminous Sun is assumed for early Earth and Mars; [Cockell et al., 2000]) and decrease of atmospheric pressure. Pressure decrease is associated with an increase of the DNA damaging UV fluence, because the incident UV radiation is skewed more towards shorter wavelengths, which exhibit a higher killing efficiency [Cockell & Andrady, 1999]. This corroborates calculations that on present-day Mars the biologically effective UV irradiance is approx. three orders-of-magnitude higher compared to today's Earth [Cockell et al., 2000], resulting from the low atmospheric pressure ranging at 7 hPa on average, a high concentration of carbon dioxide (CO_2) along with a much thinner atmosphere. Since CO_2 absorbs UV

radiation below 190 nm, the shorter spectral bands of UVC ($190-280$ nm) as well as UVB reach Mars surface un-attenuated, accounting for about 99.9% of the increase in biologically effective fluence for DNA compared to Earth [Cockell & Andrady, 1999]. The UVC fluence rate on the surface of equatorial Mars has been estimated to range between $8-10\%$ of the total UV flux ([Schuerger et al., 2006] and references therein).

Due to the lack of a protective ozone layer the incident solar UV radiation can only be attenuated by vapor droplets, water or CO_2-ice particles and dust in the martian atmosphere that foster absorption, reflection or scattering of UV radiation [Nicholson et al., 2005]. Additionally, a subsurface depth of just 1 to 2 mm would reduce the Mars surface UV flux to terrestrial levels under the shielding atmosphere of an ozone layer [Cockell & Andrady, 1999].

Despite these harsh present-day Mars conditions to terrestrial life, models predict that the spectral irradiances on present Mars are comparable to those of the Archean Earth [Ronto et al., 2003, Patel et al., 2003]. Hence, the biologically effective UV flux on present Earth is not the maximum radiation burden that some organisms can endure if assumed that organisms on Archean Earth developed repair processes for dealing with lesions induced by higher DNA damaging irradiances. Using terrestrial biology as baseline, the UV-induced damage accumulated during the present martian day might still be within the threshold of efficient repair processes acquired then and may not be a decisive constraint to life [Cockell, 2000, Cockell et al., 2000].

1.3.2.2 UV-induced damage repair

The predominant UV-induced lesions are cyclobutane pyrimidine dimers (CPD) and pyrimidine $(6-4)$ pyrimidone photoproducts $(6-4$ PPs) between two adjacent pyrimidine bases (thymine or cytosine - constellations of interest: TT, TC, CT and CC lesion cf. chapter 2.6.4, p. 37), whereas its distribution profile depends on the incident wavelength (chapter 2.5.1). UV damaged DNA causes torsional strain resulting in a distortion angle of $44°$ or $\sim 30°$ of the normal helical DNA structure due to formation of $6-4$ PPs or CPDs, respectively.

Bipyrimidine photoproducts are usually repaired by nucleotide excision repair (NER) or base excision repair (BER) and if these altered bases are regarded as mismatch, they could be repaired by the mismatch repair (MMR) mechanism as well. The fundamental difference between BER and NER is that BER can only be initiated when a specific enzyme, an appropriate DNA $N-$glycosylase, is capable of recognizing that specific altered base. Due to the limited number of DNA $N-$glycosylases, the more flexible NER mechanism evolved in cellular organisms. The NER mechanism detects damaged

DNA sites based on their abnormal structure (distorted double helix) and biochemistry, as indicated above. Several genes that are involved in either repair mechanism BER, NER or MMR have been identified in *D. radiodurans*. Mennecier and co-workers studied the MMR mechanism in *D. radiodurans* extensively and characterized it [Mennecier et al., 2004]. They could affirm *mutS1* (*DR*1039) and *mutS2* (*DR*1976), *mutL* (*DR*1696) and *mutU/uvrD* (*DR*1775) as core proteins of MMR. The functional deinoccal MMR process requires both MutS1 and MutL proteins together with the associated UvrD helicase, however, MutS2 was assigned a subordinate part. Mennecier et al. (2004) used MMR-deficient *D. radiodurans* cells to determine the function of this repair system in the overall genome-damage-prevention complex. The MMR-deficient strains remained resistant to $\gamma-$rays, mitomycin C (MMC) and UV radiation, indicating that the deinococcal MMR is not essential for genome reconstitution after DNA damage but "by its capacity to inhibit recombination between partially divergent sequences might contribute to the maintenance of genome stability."

Nucleotide excision repair (NER) system was the first to be examined, because the sequencing of the *D. radiodurans* R1 genome [White et al., 1999] revealed that gene orthologs of all components of the NER pathway of *E. coli* were present. Early studies proposed [Moseley & Evans, 1983, Evans & Moseley, 1983, Evans & Moseley, 1985] that *D. radiodurans* possesses two excision repair (ER) pathways, one mediated by UV endonuclease α, an *E. coli* homolog of the UvrABC endonuclease [Agostini et al., 1996, Narumi et al., 1997] and an optional excision repair involving UV endonuclease β [Earl et al., 2002b, Tanaka et al., 2005]. Both are equally contributing to *D. radiodurans'* UV resistance, because either is independently capable of restoring wild-type UV-resistance and to acquire UV-sensitivity, but both have to be inactivated to produce an excissionless phenotype [Minton, 1994]. This corresponds to the two mechanisms, one involving an endo- as well as an exonuclease and the excinuclease mechanism, proposed by Sancar for excision repair [Sancar, 1996, Sancar, 1999].

Excision repair can be scaled down to three formal steps [Sancar, 1996]:

1. Damage recognition
2. Dual incisions
3. Repair synthesis

Next to excision nuclease, ER requires the repair synthesis proteins *uvrD* (Helicase II) to release the protein complex or to create a gap by excising a

complete section of damaged DNA, Pol I (polymerase) to synthesize DNA, eventually, to fill-in the incurred gap, and DNA ligase (*dnlJ* $DR2069$) to repair the strands.

The UV endonuclease $\alpha-$mediated system corresponds to the excinuclease UvrABC mechanism. To recognize a damage site this mechanism needs a molecular matchmaker that "in an ATP-dependent reaction, brings two compatible yet solitary macromolecules together, promotes their association, and then dissociates to allow the matched protein complex to carry out its effector function" [Sancar, 1996]. The molecular matchmaker in *E. coli* as well as *D. radiodurans* is UvrA. The deinococcal UvrA protein ($DR1771$) is rather comprised of two subunits, UvrA1-UvrA2 (UvrA_2), as derived from experiments with corresponding mutants either UvrA1- or UvrA2-deficient [Agostini et al., 1996]. Due to the partial or full complementation of *uvrA*-deficient *D. radiodurans* strains by *E. coli* UvrA, Agostini et al. (1996) inferred that a hypothetical deinococcal UvrB protein ($DR2275$) exists that interacts with the *E. coli* UvrA to establish a UvrA_2B complex embedded in the UvrABC system ($DR1354$ subunit C of UvrABC). UV endonuclease α of *D. radiodurans* excises bulky adducts, interstrand cross links and bipyrimidine photoproducts of which the $(6-4)$ bipyrimidine adducts are mended preferably [Moseley & Copland, 1978, Moseley & Evans, 1983, Evans & Moseley, 1983, Minton, 1994, Agostini et al., 1996].

The UV endonuclease β-mediated system, however, corresponds to the endonuclease-exonuclease mechanism. UV endonuclease β ($DR1819$) recognizes pyrimidine dimers and catalyzes incision of the phosphodiester bond adjacent to the lesion [Evans & Moseley, 1988], enabling removal of the nicks. Such *UV-induced dimer endonucleases (UVDE* proteins were first detected in *Sacharomyces pombe* and *Neurospora crassa* [Sancar, 1996]. Suggesting that the endonuclease-exonuclease mechanism in *D. radiodurans* may process similarly and that UV endonuclease β may recognize a broad range of UV-induced lesions, including apurinic/apyrimidinic sites (AP sites[2]) and base mismatches next to the bipyrimidine photoproducts CPD and $6-4$ PP. This has been corroborated by [Earl et al., 2002b], who showed that deinococcal UV endonuclease β shares 30% amino acid sequence identity with the UVDE protein of *S. pombe*. Summarized, deinococcal UV endonuclease β recognizes the UV-induced damage, introduces a nick adjacent to the detected lesion, then an exonuclease digests the altered strand and finally, DNA synthesis takes place resulting in fill-in of the incurred gap.

[2] Apurinic/apyrimidinic or abasic sites (AP sites) are produced, when either a purine or pyrimidine base is forfeited.

Though various enzymes expected to function in the base excision repair route have been identified, e.g. DNA-AP lyase *mutM*, *DR*0493, Uracil-(*DR*0689) as well as a putative 3-methyladenine (*DR*2074) DNA glcosylase, its occurrence has not been verified yet [Minton, 1994].

One efficient mechanism identified in *E. coli* to remove UV-254 nm-induced lesions that lead to an arrest of replication is the RecF pathway. A simplified model outlining the function of RecF, RecO, and RecR during the recovery of replication after UV-induced DNA lesion is shown in Figure 1.2, slightly modified from [Chow & Courcelle, 2004].

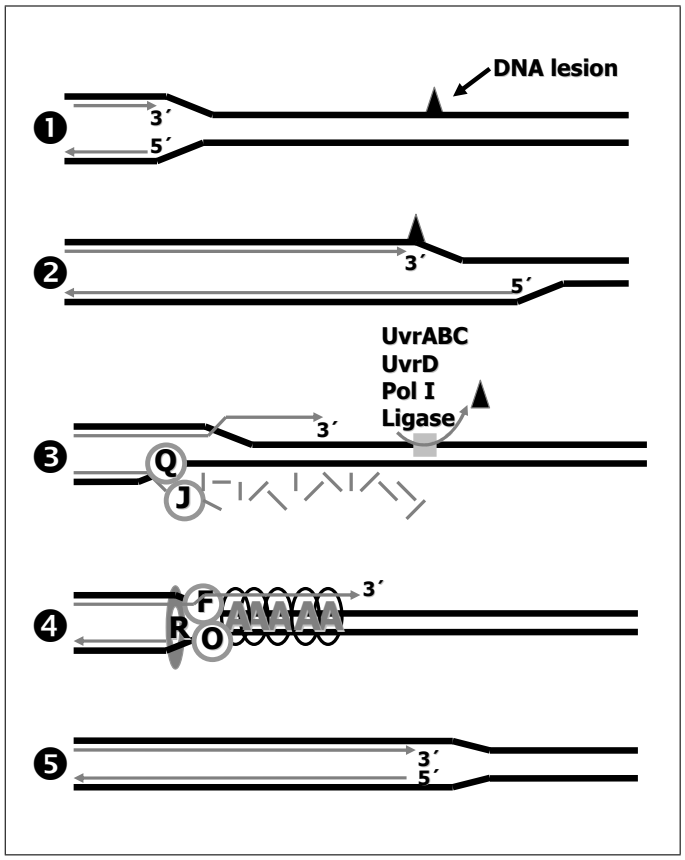

Fig. 1.2: UV-254 nm-induced lesions that lead to an arrest of replication are efficiently mended by the RecFOR complex. UV-induced DNA lesions block the replication process (1,2), following the arrest of replication the nascent DNA is partially degraded by RecJ and RecQ, so that NER proteins can repair the lesion (3). The RecFOR-complex promotes the filament formation of RecA at the DNA junction site (4), to maintain the integrity of the replication fork until replication can resume (5).

2. MATERIALS AND METHODS

Previous studies [Pogoda de la Vega et al., 2005] have shown that besides the well-known DNA mechanisms - nucleotide excision repair (NER) and homologous recombination repair (HR) - a yet undefined pathway must exist in *Deinococcus radiodurans*, which may be activated only when the previously mentioned pathways are inactivated. In order to investigate the involvement of either enzymatic DNA mechanism, two repair-deficient and UV-sensitive deinococcal strains as well as a mutant strain exhibiting similar ultraviolet (UV)-resistance as the wild-type strain were chosen. The UV-sensitive mutant strains either carry mutations in the *uvr*-gene complex [Moseley, 1983] or *recA*-gene [Gutman et al., 1994].

These strains were selected from the assortment of species supplied by A. Vasilenko and M. Daly, Uniformed Services University of the Health Sciences (USUHS), Bethesda, Maryland (MD), United States of America (USA). The genotype of the selected strains are assorted in Table 2.1.

2.1 Investigated strains of Deinococcus radiodurans

The wild-type strain investigated in this study is the strain that has been sequenced and deposited at The Institute for Genomic Research (TIGR) by White et al. (1999). The authors had erroneously reported that the sequenced strain was the *D. radiodurans* R1 type strain maintained at the ATCC under the designation 13939.

However, several studies revealed that the sequenced strain accumulated many mutations [Southworth & Perler, 2002], as suggested by the many base pair changes due to nucleotide deletions and insertions found between the ATCC 13939 strain and the sequenced strain [Eggington et al., 2004] and [Mennecier et al., 2004]. Instead a *D. radiodurans* R1 strain from the Minton laboratory collection, now maintained by M. Daly (USUHS), was sequenced [Correction & Clarifications, 2003]. It has been registered with the ATCC and is now catalogued as ATCC BAA-816.

The mutant strains 262 (*uvrA-2*) and UVs78 (*uvrA-1 uvsE*) were generated by the mutagenic effect of $N-$methyl$-N'-$nitro$-N-$nitrosoguanidine (MNNG), followed by scrutinizing for sensitivity to UV radiation, Mitomycin

C (MMC) or ionizing radiation [Minton, 1994, Moseley & Evans, 1983] and [Moseley & Copland, 1978]. The mutant strain 262 (*uvrA-2*) was obtained as an isolate exhibiting sensitivity to MMC, but not to UV radiation and "carries a 1,300-bp insertion sequence (IS) element, designated IS2621, that inserted 986 bp from the 3′ end of the *uvrA-1* gene" [Narumi et al., 1997]. Anecdotal reports even mention a slightly higher repair capacity of bipyrimidine dimers than compared to wild-type strain R1 [Earl, 2003].

The UV-sensitive strain UVs78 (*uvrA-1 uvsE*) was first described by Moseley and Copland (1978) and was produced by applying chemical mutagenesis as well. Though chemical mutagenesis seldom results in defined or targeted gene defects, the induced defects in UVs78 (*uvrA-1 uvsE*) could be attributed to both UV endonuclease- α and UV-endonuclease- β ([Minton, 1994] and [Evans & Moseley, 1983]), resulting in UV-sensitivity and inability to excise bipyrimidine dimers (genotype *uvrA-1 uvsE*, cf. Table 2.1). Further evidence for this genotype was provided by Earl [Earl et al., 2002b] who created a UV-sensitive mutant strain designated LSU1000 that duplicates the sensitivity pattern observed in UVs78 (*uvrA-1 uvsE*).

The *recA*-deficient strain was generated in the lab of M. Daly (cf. chapter 2). It was acquired by targeted insertional mutagenesis [Gutman et al., 1993, Gutman et al., 1994] coupled with the selective marker Chloramphenicol (Cm). By continuously testing the resistance to Cm, DNA damage-sensitive isolates could be selected, which confirmed that this feature is attributed solely to a defect in the *recA* gene [Gutman et al., 1994]. It was chosen because it exhibits the same phenotype as the mutant strain rec30, which is well described in the literature and has also been MNNG-generated and described by Moseley and Copland (1975). Because of rec30's extreme sensitivity to ionizing radiation, it has been used in the first studies to enlighten the repair mechanism of *D. radiodurans*.

2.1.1 General culturing of the D. radiodurans strains

All *D. radiodurans* strains were grown aerobically and maintained on TGY broth (0.5% Bacto Tryptone, 0.3% Bacto Yeast extract, both Bacto products have been purchased from BD Becton, Dickinson and Co, Difco Laboratories, Sparks, MD, USA, as well as 0.1% D(+)-Glucose-Monohydrate, Merck KGaA, Darmstadt, Germany) at their temperature optimum of $30°C$. In case of the mutant strain 1R1A (*recA*), the nutrient media was supplemented with Cm at a concentration 3 $\mu g/ml$. The cultures were generally grown for 40 h, then transferred into conical tubes and centrifuged at 5675 g (laboratory centrifuge 5810 R, Eppendorf AG, Hamburg, Germany) for 8 min for each wash step. The supernatant (TGY broth) was removed, and the

Tab. 2.1: List of *Deinococcus radiodurans* strains and their relevant genotypes.

Strain	Parental strain	Sensitivity to UV	γ	MMC	MMS	Mutated genotype	Repair features	References
R1	WT	R	R	R	R	none		Anderson et al. 1956
262	R1	R	R	S	R	*uvrA2*	high biP repair rate	Moseley & Copland 1978
1R1A	R1	S	S	S	R	*recA*	HR deficiency	Gutman et al. 1994
UVs78	302	S	R	S	R	*uvrA1 uvsE*	ER deficiency	Moseley & Evans 1983

γ – γ radiation, MMC – Mitomycin C, MMS – Methyl-methane-sulfonate; R – resistant, S – sensitive; biP – UV-induced bipyrimidine dimers, ER – Excision repair, HR – Homologous recombination repair

pellet was washed twice in ice-cold phosphate buffer solution (saline: 0.7% $Na_2HPO_4 \times 2H_2O$, 0.3% KH_2PO_4, 0.4% $NaCl$) and regained in sterile saline. After the first two washes, the sedimented cells were resuspended either in sterile saline or in defined synthetic minimal media (DMM as described in [Venkateswaran et al., 2000]). Resuspension of the culture in DMM was always performed when the cells were exposed to UV radiation and post-irradiation monitored photoproduct repair kinetics (chapters 2.5 and 2.5.2).

2.2 Transmission electron microscopy

Transmission electron microscopy (TEM) was applied to gain insight into the ultrastructure of the biological (living) organisms that have been investigated in this work (cf. also chapter 5). Prior to the TEM study the biological specimen had to undergo chemical fixation, dehydration, infiltration/embedding, followed by sectioning. The sectioning was performed at the University of Barcelona, Serveis Cientifico-Tecnics, Microscopia electronica, Campus Casanova, Barcelona, Spain and supervised by Dr. Nuria Cortadellas. The sections were cut with an ultramicrotome to a thickness of approx. 70 nm. Specimens were examined in a Zeiss 902 A transmission electron microscope (Carl Zeiss AG, Oberkochen, Germany) operated at an acceleration voltage of 80 kV throughout. TEM images were taken with a digital camera CCD iTem and analysed either with the analysis software SI Viewer (Olympus Soft Imaging Solutions GmbH, Muenster, Germany) or ImageJ Launcher (Image processing Analysis in Java, NIH, USA).

2.2.1 Fixation

For fine structural studies chemical fixation is necessary, first, to preserve cell organisation ideally as near as possible to the native state, and second, to protect the specimen against subsequent preparation steps with minimal deterioration of fine-structure. Glutaraldehyde has become the fixative of choice for routine electron microscopy, because it forms a network of cross-links mainly between amino groups, which stabilize the cells [Hajibagheri, 1999, Hayat, 1981, Slot et al., 1989]. One of the advantages of glutaraldehyde lies in its uncharged form providing a free passage through biological membranes. Fixation was employed in buffered 4% glutaraldehyde for 2 hours, followed by 4 wash steps of 15 min with 0.1 M Potassium-Sodium phosphate buffer. The final extent of glutaraldehyde cross-linking leads to a sol-gel-processing of the cytoplasm and rigidification of the cell compounds. After the pre-fixation *D. radiodurans* cells have then been embedded in 2% agarose, cooled and cut into blocks with an edge length of max. 1 - 1.5 mm. This step is followed by postfixation and staining with 1% buffered osmium tetroxide (OsO_4). The heavy metal OsO_4 enables contrasting cell structures, cross-linking proteins and binds lipids as well, especially membranes. Osmicated cells show a similar appearance in micrographs as in unfixed hydrated cryosections [Griffiths, 1996]. Additional wash steps, as indicated above, were performed to remove the unbound OsO_4. Glutaraldehyde fixation followed by OsO_4 acts rapidly, effectively and irreversibly.

2.2.2 Dehydration

Following fixation, two additional procedures are required for specimen preparation for conventional electron microscopy: dehydration and resin embedding. Since fine structural studies are performed under vacuum, the biological specimens have to be freed of water, which can be achieved by substituting the water present in cells by ethanol.

The stepwise dehydration is performed with an ethanol series as follows:

1. 30 min in 30% ethanol
2. 30 min in 50% ethanol
3. 30 min in 70% ethanol
4. replace with fresh 70% ethanol, leave overnight
5. 1 h in 80% ethanol

6. 1 h in 90% ethanol

7. 2 × 30 min in dried 100% ethanol (ethanol abs.)

2.2.3 Spurr resin embedding

The advantage of the Spurr procedure [Spurr, 1969] is the rapid infiltration of the specimen with the resin and the low viscosity of the embedding media. The applied embedding mixture "Spurr's Kit" (Electron Microscopy Sciences, Hatfield, Pennsylvania, USA) has been chosen for its low viscosity as well as penetration qualities, its complete compatibility with ethanol and because the resin hardness can be adjusted by changing the amount of the mixing ingredients. It has been found effective to alter the supplier's modifications for the resin constitution "hard" as shown in Table 2.2.

Tab. 2.2: Preparation of a hard Spurr's low viscosity embedding mixture.

Ingredients	ERL 4206	DER 736	NSA	DMAE S-1
Initial weight [g]	20.0	8.0	52.0	0.8

ERL 4206 — Vinyl cyclohexen dioxide is a cycloaliphatic diepoxide.

DER 736 — Diglycidyl ether of polypropylene glycol is a flexibilizer to control the hardness of the polymerized block.

NSA — Nonenyl succinic anhydride is a hardener with a relatively low viscosity.

DMAE S-1 — Dimethylaminoethanol (S-1) is an accelerator with low viscosity, rapid cure and the chosen concentration results in blocks with colour transparency.

The infiltration procedure was started by adding a 3 : 1 mixture of dehydrating fluid/embedding medium in the vial with the cell-containing agarose blocks (see chapter 2.2.1), swirled, and allowed to stand for 1 h. Then the mixture was replaced by a solution of embedding media/ethanol abs. (dehydrating fluid) (1 : 1), swirled and left to stand for another 1 h. After repeated drainage of the mixture, the 1 : 1 solution was replaced by a 1 : 3 ethanol abs./embedding medium, swirled and again left to rest 1 h. Next to last solely the embedding media was added, and after 2 h penetration, it was replaced by fresh embedding media left to stand overnight at room temperature. The infiltrated specimens were transferred into embedding moulds and fresh resin was added. Polymerisation was induced in an oven for 5 h at $40°C$ and overnight at $70°C$.

2.3 Test dependant sample preparation

Cultures destined to be exposed to low temperature (cold shock, chapter 2.8), to vacuum (chapter 2.7) and to the Mars-Environment-Simulation Studies (MESS, chapter 2.9) had to be desiccated prior to the test performance. Whereas the cultures assigned to UV-irradiation followed by profiling the repair of the UV-induced DNA photoproducts (chapters 2.5 and 2.5.2) have always been irradiated in suspension and were kept on ice.

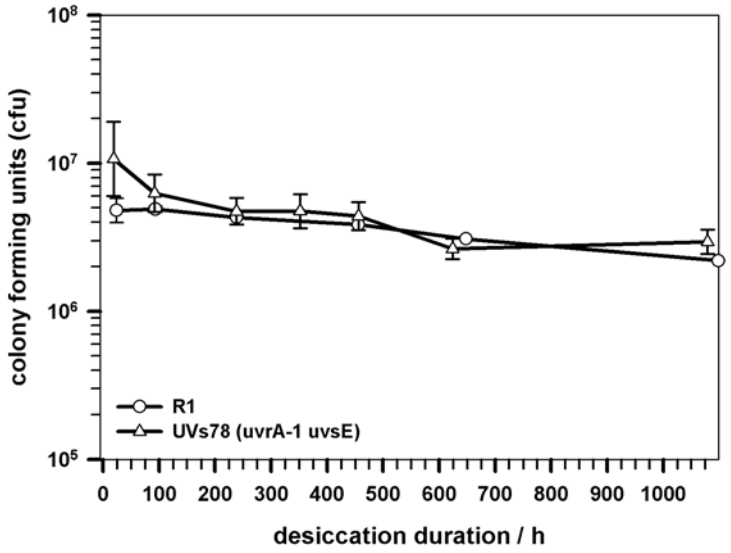

Fig. 2.1: The decisive 100 h desiccation period is exemplified [de la Vega, 2004] by a representative of each UV-susceptible class - R1 representing the UV-resistant and UVs78 the UV-sensitive class.

2.3.1 Preparation of desiccated layers of bacteria on quartz discs

If desiccated cells were required for the experimental setup, the cells were cultured, harvested and washed as described in chapter 2.1.1. Subsequently the washed cells were resuspended in ice-cold saline to attain about 1×10^8 cells per ml. 200 μl of the liquid culture was evenly spread on 25 $\times$ 25 mm glass slides and dried in an exsiccator over $CaSO_4$ (Kali-Chemie AG, Hanover, Germany) to achieve a relative humidity of max. 5%. The dried bacteria layer remained 100 h in the exsiccator. This desiccation period represents the critical value after which the desiccated cells do not show further inactivation related to the dehydration process (Figure 2.1 modified from

[de la Vega, 2004]). Therefore, the results obtained from the following exposure measures can truly be attributed to the applied experimental parameters.

2.4 Numerical and statistical analysis

All results gathered in this dissertation represent averages of the mean of nine measurements (3 independent experiments, 3 replicates per experiment) expressed with their standard errors and standard deviation, unless otherwise noted.

2.4.1 Numerical analysis

To determine the number of cells per milliliter, one frequently employed approach is to count the number of macro-colonies on nutrient agar plates that appear after the agar plates have been incubated at the bacteria's temperature optimum; *D. radiodurans'* optimum is $30°C$. The enumeration is expressed in colony forming units (cfu). Throughout this work, it is described as cfu per ml. In the case of the mutant strain 1R1A (*recA*) a 3 $\mu g/ml$ Cm-supplementation to the agar plates was required, followed by incubation at $30°C$ for up to 3 days, whereas the agar plates of the other investigated strains were solely incubated for 2 days, irrespective if treated or untreated cells had been spread on the plates.

2.4.2 Statistical analysis

The numbers of surviving bacteria (N) exposed to UV irradiation within the scope of the Mars-Environment-Simulation Studies (chapter 2.9) were divided by the numbers of surviving bacteria in control treatments (N_0) placed within the exposure unit but not exposed to UV-irradiation. Thus, the values N/N_0 represent the percentages of the initial bacterial populations surviving after both UV-exposure as well as exposure to Mars-typical conditions (pressure, diurnal temperature and humidity periods, and gas composition), see chapter 2.9.3 for further details.

Data in the experiment to measure the effects of vacuum (chapter 2.7) on bacterial survival were analyzed with student t-tests ($P \leq 0.05$) in which the experimental mean of surviving populations inside the pumping unit were individually tested against the laboratory control constant of $N/N_0 = 1$.

In general, raw microarray data (chapter 2.10) underlie technical and biological variability immanent to the experiment. Applying statistical tools for the data analysis allows to extract reliable information and to assess the

significance of differentially expressed genes. Before the statistical analysis can be performed, initial data analysis including normalization of the raw data, background correction and visualization of chip-to-chip variation is required [Knudsen et al., 2003]. Normalization is used to reduce unwanted technical artifacts across multiple DNA microarray chips. By correcting for overall chip brightness, amount and quality of target hybridization, amount of stain applied and labeling efficiencies of different sequences and other factors that influence the numerical value of expression intensity, the gene expression estimates between samples can be compared more confidently. There are several different methods for normalizing data [Grant et al., 2007].

For this experiment, the normalization method 'quantile' was selected. The goal of the quantile method is to make the distribution of probe intensities for each array in a set of arrays the same. The concept assumes that a quantile-quantile plot shows the same distribution of two data vectors if the plot is a straight diagonal line and not the same if it is other than a diagonal line [Bolstad et al., 2003]. The extracted data is defined by the applied experimental conditions in the sense that the conditions determine the necessary statistical tools. Comparison analysis helps to identify genes with large differences between individuals and small differences within individuals, and for this, it requires an adequate set of replicates. It uses the variability within the replicates to assign a confidence level as to whether the gene is differentially expressed. Furthermore, statistical inferences cannot be made with a sample size of one. Though it is better to have as many replicates as possible, three replicates have become common practice [Grant et al., 2007].

Cluster analysis identifies patterns of gene expression. Based on these patterns the genes are segregated into subsets. In this study, one time point and one treatment was applied to three individuals, i.e. the wild-type strain R1 and the two UV-sensitive mutants, resulting in three conditions (terms of condition are noted in chapter 2.10). For each UV-sensitive mutant three biological replicates and for the wild-type strain four biological replicates have been generated, which also represent the amount of hybridization experiments performed for each strain. Therefore, t-statistics was chosen for the comparison analysis. The software to analyze the micrarray data ArrayStar (Version 2.0.0 build 61, DNASTAR, Inc. Madison, Wisconsin, USA) uses an unpaired, two tailed, equal variance Student's Test [Draghici et al., 2003].

The P-value from a comparison test is the risk of discarding the null hypothesis, when it is actually valid. The null hypothesis (H_0) states that there is no significant difference in means of expression values between compared experimental conditions [Bolstad et al., 2003]. A threshold or error rate of 0.05 was defined. It represents a user-specified cut-off below which the results are classified as statistically significant. The list of genes with

significant differential expression is output and log fold changes calculated. In this dissertation, the fold change is the same as the ratio of the means of the normalized intensities measured (cf. chapter 2.10.1).

2.5 UV irradiation

First, it was necessary to generate a profile of the repair capacity of each strain of the UV-induced DNA photoproducts (chapter 4.1, p. 64). For this reason, the cultures were subjected to UV radiation exposure of different wavelength ranges, followed by post-irradiation monitored photoproduct repair kinetics (chapter 4.2, p. 66). The selected wavelength ranges comprise the simulated UV radiation environment (λ >200 nm) of the early Earth (before the built-up of the ozone layer) or of the planet Mars as well as selected spectral ranges of the environmental UV (λ >315 nm) climate on present Earth (cf. chapter 1.3.2.1, p. 20). In order to compare the results with literature data, the effects of monochromatic UV radiation at 254 nm were analyzed as well.

2.5.1 Applied UV ranges

Environmental UV is of polychromatic nature, i.e. it corresponds to broadband UV light and causes various chemical interactions depending on the applied wavelength. These photochemical reactions include photo-induced reversion of cyclobutane pyrimidine dimers (CPD) at shorter wavelengths (λ <254 nm), photoisomerization [Ravanat et al., 2001] of the bipyrimidine $(6-4)$ adducts into their Dewar valence isomers at longer wavelengths (λ >320nm), or, in case of photoreactivation, photoenzymatic reversion of CPD at longer wavelengths (λ >380 nm) [Bockrath & Li, 1997]. The solar simulator SOL2 (Dr. Hönle AG, UV-Technologie, Munich, Germany) emitting a spectrum of $\lambda = 200-400$ nm was chosen as polychromatic UV source. To obtain the spectral ranges of the environmental UV on present Earth, cut-off filter WG 335, 3 mm (Schott, Mainz, Germany) in combination with the band pass filter UG11 (transmission range $240-400$ nm, cut-off of infrared wavelengths to avoid temperature increase during irradiation), were used to obtain the desired UV range of $\lambda = 315-400$ nm.

Next to polychromatic UV, monochromatic UV from a germicidal low-pressure lamp (Model NN 8/15, Heraeus, Berlin, Germany) was applied to allow comparison of the acquired results with literature data. The spectral irradiance of the mercury low-pressure lamp with a major emission line at 253,65 nm was measured with a double monochromator (Bentham model DM 300). The fluence rate was determined by using a UV-X radiometer (UVP

Ultra-Violet Products, Cambridge, United Kingdom). The fluence rates of the different UV ranges are shown in Table 2.3.

Tab. 2.3: Fluence rates of the simulated UV radiation environment of the early Earth or Mars (λ >200 nm), of environmental UV on present Earth (λ >315 nm) and of UVC (λ =254 nm) as measured by the UV-X radiometer.

UV-range/nm	Fluence rate/Wcm^{-2}
>200	13.2
254	0.7
>315	0.9

2.5.2 Liquid holding recovery

The goal of liquid holding recovery (LHR) is to provide a well-defined experimental set up, that allows determining the unaltered repair capability of each investigated strain. Hence, a medium was required that was truly minimal, highly characterized and suitable for testing the metabolic capabilities of *D. radiodurans*. The synthetic minimal medium developed by Venkateswaran et al. (2000) consists of a metabolizable carbon source, exogenous sulfur-rich amino acids and nicotinic acid (as vitamin source) dissolved in phosphate buffer. The authors could also show that the levels of radiation resistance of *D. radiodurans* were similar irrespective of the growth medium or recovery substrate, which is why it was chosen as irradiation and recovery medium in this work.

The exposed cultures were prepared, washed and resuspended in 200 ml defined minimal medium (DMM) as described in chapter 2.1.1. The bacteria suspensions were irradiated on ice to inhibit repair processes. Furthermore continuous magnetic stirring during irradiation ensured homogeneous exposure of the cells. For each irradiation step 60 ml of the solution was transferred into a glass petri dish (13.3 cm in diameter) and exposed to UV radiation of different wavelengths (see Table 2.4 for the applied fluence of each wavelength). This results in a calculated fraction of non-shielded cells ranging at 96.37% [Pogoda de la Vega et al., 2005].

Following UV irradiation the bacteria suspension was transferred into a 500 ml Erlenmeyer flask, kept on ice until returned to a 30°C shaker to monitor the repair kinetics. During a time course of 2 h, measures were taken at 30 min-intervals. At each measure point, a 25 ml-sample was taken from the

agitated flask, transferred into a chilled conical tube, and finally centrifuged at 5675 g at 4°C for 30 min. The cell pellets were then stored at −80°C until further application of either bipyrimidine photoproduct quantitation (cf. chapters 2.6.1 and 2.6.4) or microarray analysis (cf. chapters 2.6.2 and 2.10) were performed.

Tab. 2.4: Applied fluence of the investigated wavelength ranges pertaining to the biological effect of the chosen fluence.

UV-range/nm	Fluence / kJm^{-2}	Biological effect
>200	0.79	F_{90} of UVs78
254	0.21	F_{90} of R1
>315	3.31	F_{100} of all strains

To assert that the biological effect of the applied fluence was as expected Table 2.4, cell survival of the irradiated microorganisms was determined by their ability to form macroscopic visible colonies on nutrient agar plates after incubation (cf. chapter 2.4.1).

2.6 Post-UV-irradiation treatment

Bipyrimidine photoproduct quantitation (chapter 2.6.4) entails DNA extraction (chapter 2.6.1) of all obtained time points 0.5, 1, 1.5 and 2 h post irradiation, whereas microarray analysis requires RNA extraction (chapter 2.6.2). Irradiation expression profiling (chapter 2.10) was solely carried out with recovery time point 0.5 h post-irradiation of the UV-sensitive mutants UVs78 (*uvrA-1 uvsE*) and 1R1A (*recA*) compared to wild-type strain R1.

2.6.1 DNA Extraction

The DNA was extracted by using the commercially available Wizard Genomic DNA Purification Kit from Promega Corp. (Madison, USA) and applying the modifications noted in [de la Vega, 2004]. Briefly, the cell pellets were thawed, washed twice in 1.5 ml ice-cold saline and centrifuged at 5675 g for 10 min. Then the washed cells were transferred to RNAse-free microcentrifuge tubes and pelleted again by centrifugation at 14243 g for 4 min — the centrifuge was constantly kept at 4°C. The first part of cell wall disruption was performed by regaining each pellet in 1 ml ethanol absolute (Merck KGaA, Darmstadt, Germany) and left to rest for 5 min on the bench.

The second part of cell wall lysis consisted of adding first 480 μl Tris-EDTA buffer (Sigma Aldrich Chemie GmbH, Steinheim, Germany) to the mixture, followed by 120 μl of 50 mg/ml Lysozyme stock solution (see chapter 2.6.2) and incubated at 37°C for 1 h. The sample mixture was then centrifuged at 14243 g for 4 min. Nuclei lysis and protein precipitation required to obtain the genomic DNA followed manufacturer's instruction. The DNA enzymatic hydrolysis prior to the quantitation of the bipyrimidine photoproducts (see chapter 2.6.4) was performed as described eslewhere [Douki et al., 2000].

2.6.2 RNA Extraction

The commercially available QIAGEN RNeasy Mini Kit (QIAGEN GmbH, Hilden, Germany) was used to extract RNA from the *D. radiodurans* wild-type R1, as well as from the mutant strains UVs78 (*uvrA-1 uvsE*) and 1R1A (*recA*). Total RNA was extracted from 25 ml irradiated culture from each strain.

In addition to those chemicals that were supplied with the kit Lysozyme (50.000 U/mg), ethanol absolute, extra pure (both purchased from Merck KGaA, Darmstadt, Germany), $\beta-$ Mercaptoethanol and 100× concentrate Tris-EDTA (TE) buffer, pH approx. 8.0 (both purchased from Sigma Aldrich Chemie GmbH, Steinheim, Germany) had to be provided. A 50 mg/ml stock solution of Lysozyme was prepared and stored in single-use aliquots at $-20°C$, whereas the other chemicals were set up before use. The on-column extraction procedure was followed according to the manufacturer's recommendations in "The RNeasy Mini protocol for isolation of total RNA from bacteria" and was slightly modified. Bacterial pellets of the post-0.5 h UV-irradiation recovery measures were gained from the liquid holding recovery experiment (chapter 2.5.2) and the first cell wall disruption was performed as described in chapter 2.6.1 before storage at $-80°C$. The pellets were slightly thawed and prepared for a second cell wall lysis (3 mg/ml Lysozyme in TE buffer). In order to improve the RNA yield additional homogenization was performed with QIAshredder homogenizers (QIAGEN GmbH, Hilden, Germany) as indicated in the manufacturer's protocol. The QIAGEN RNase-Free DNase Set (QIAGEN GmbH, Hilden, Germany) was used for the digestion of trace genomic DNA in the crude total RNA. Solid DNase I (1500 Kunitz units) was dissolved in 550 μl of RNase-free water and stored in single-use aliquots at -20°C. 10 μl of DNase I stock solution was added to the sample mixture and incubated at $20 - 30°C$ for 15 min on the bench top. Following DNA digestion, two buffer wash steps were carried out and finally, 30 μl of RNase-free water was applied to elute the RNA from the membrane of the column that had been placed into a collection tube. The

RNA yield achieved for 10^9 cells of R1 and UVs78 (*uvrA-1 uvsE*) averaged out 65 μg and 45 μg, respectively, whereas 2×10^8 cells of 1R1A (*recA*) yielded approximately 43 μg. The RNA amount is in good agreement to typical yields listed by the manufacturer from the same initial starting amount of *Bacillus subtilis* and *E. coli* cells of 55 μg and 33 μg total RNA, respectively. The extracted total RNA was stored at $-80°C$ until initial quality control prior to preparation for microarray hybridization (chapter 2.10.1).

2.6.3 Quality assessment of RNA

The amount of the total isolated RNA was measured via UV spectroscopy at a wavelength of 260 nm (Genequant, Amersham Biosciences, Freiburg, Germany). In general, RNA probes showing an E_{260} to E_{280} ratio ranging between 1.7 and 2.1 were further utilized. A quick and efficient qualitative and quantitative biochemical analysis was assessed with the Agilent BioAnalyzer (Agilent, Palo Alto, California, USA). The micro-fluidic *Lab-on-a-Chip* technology utilized by the BioAnalyzer instrument is based on the manipulation of tiny volumes of liquid in miniaturized systems. To run the assay a mixture of gel matrix and dye concentrate (provided by the manufacturer) as well as 1 μl of each samples was loaded onto the RNA 6000 Nano LabChip. Electro-kinetic forces push dye labeled RNA through selected pathways in a controlled manner. In parallel a RNA ladder (RNA 6000 Ladder; Ambion, Huntingdon, United Kingdom) is run to quantify the measured RNA. The quality of the extracted total RNA is graded by an implemented proprietary RNA integrity number (RIN) software. By assigning a numerical measure, one can intuitively judge the degradation condition of each sample; fully degraded RNA is termed RIN 1, whereas intact RNA receives RIN 10. In this analysis total RNA with at least RIN 7.0 were further processed.

2.6.4 Photoproduct assay

The level of bipyrimidine photoproducts in enzymatically digested DNA was measured by an accurate and highly specific assay that involves the association of high performance liquid chromatography (HPLC) with tandem mass spectrometry detection (HPLC-MS/MS). The main advantages of the HPLC-MS/MS-technique with respect to other DNA damage assays are as follows:

1. No radioactive labeling of the DNA is required.

2. For a given type of photoproduct, the four bipyrimidine derivatives are quantified separately.

3. All twelve possible bipyrimidine photoproducts can be quantified in one analysis.

4. The fully automated HPLC analysis allows a relatively high throughput.

The separations of digested DNA were performed on an Uptisphere ODB (particle size 3 $\mu m, 150 \times 2$ mm I.D) octadecylsilyl silica gel column (Interchim, Montlucon, France) connected to a Series 1100 Agilent apparatus. The oven temperature was $28°C$. A gradient of acetonitrile (maximum proportion 20%), in 2 mM triethylammonium aqueous solution, was used at a flow rate of 200 $\mu l min^{-1}$. A UV spectrometer set at 275 nm placed at the outlet of the column was used for the quantification of normal nucleosides. Then, the eluent was mixed on-line with methanol (100 $\mu l min^{-1}$) and further directed toward the inlet of an API 3000 tandem mass spectrometer (SCIEX/Perkin Elmer, Toronto, Canada). Bipyrimidine photoproducts including *cis-syn* cyclobutane pyrimidine dimers (CPD), $(6-4)$ photoproducts and Dewar valence isomers of TT, TC, CT and CT dinucleoside monophosphates were quantified in the multiple reaction-monitoring mode. For this purpose, specific transitions reported elsewhere were used [Douki et al., 2000, Douki & Cadet, 2001, Douki & Cadet, 2003]. Calibration of the response of the mass spectrometer was achieved by injection of a mixture containing a known amount of each of the photoproducts.

2.7 Desiccation/Vacuum

In the case of desiccation experiments, the fact that vacuum resembles an extreme mode of dehydration was turned to account. Hence, the cells were exposed to vacuum to reduce the exposure duration but profiting of the fact that the encountered biological effect is comparable. This facilitated the assessment of the biological effective range of extreme desiccation on *D. radiodurans*; the desiccated cells (description of specimen preparation in chapter 2.3.1) were suspended to short-term and long-term vacuum exposure. Short-term exposure periods range from 24 h up to 3 weeks (investigated time courses: 1d, 2d, 7d and 21d), whereas long-term exposure periods comprise the time courses 2 months and 1 year. Depending on the exposure period either of two vacuum chambers set up in the Planetary and Space Simulation Facilities (PSI) at DLR, Cologne, Germany, were used. Short-term vacuum exposure was operated in chamber $\Psi 6$ and long-term exposure in $\Psi 8$ (specification details are listed in Table 2.5).

Tab. 2.5: Pumping unit specifications.

	PSI 6	PSI 8
Inner compartment:		
D×H [cm]	15×30	25×40
Windows material:	vitreous silica (Herasil)	Quartz (Suprasil)
D [cm]	13	10
Overall P-range [Pa]	$\geq 10^{-5}$	$\geq 10^{-7}$
Experiment P [Pa]	3.6×10^{-5}	2.7×10^{-6}

D – Maximal diameter, H – Heigth, P – Pressure

The vacuum chambers utilized at PSI consist of different pump tubes in series that allow either to reach high vacuum (defined pressure range: $10^{-1} - 10^{-7}\ Pa$) or ultrahigh vacuum (UHV with a defined pressure range of $> 10^{-7}\ Pa$). A booster pump provides the required starting pressure, which has to be lower than atmospheric pressure to approach the ultimate pressure[1] of each vacuum chamber. It is very important that the vacuum inside the pumping unit be as perfect as possible. Any residual free gas molecules might be ionized at operating voltages leading to faulty operation of the system. Therefore, remaining gas is either directly conveyed into the surrounding atmosphere or it is captured inside the pumping unit via condensation, adsorption or chemical transformation [Vogel, 1995].

The Ψ6 vacuum chamber is appropriate for high vacuum exposure experiments whereas Ψ8 reaches UHV due to the ion getter pumping mechanism. The latter mechanism principally employs chemical transformation to free its system from remaining gas molecules. The gas is chemically combined to solid compounds having very low vapor pressures. Followed by an ionization step that drives the atoms or molecules at extremely high velocities under the influence of electromagnetic forces towards a solid surface. The ions are adsorbed by the solid surface, a process denoted as *gettering* [Hablanian, 1997].

2.8 Cold shock

Cells exposed to low temperatures were prepared as described in chapter 2.3.1 with slight modifications. The washed cells were regained in sterile saline and 20 μl of the stock solution, corresponding to 1×10^7 cells, were spread on a small 7 mm disc, placed into the exsiccator and remained there for

[1] The best vaccum that this type of pump can achieve under ideal conditions.

100 h. The desiccated discs were separated into control group and treated group. The control group remained at constant $4°C$, whereas the treated group was cold shocked at either $-80°C$ or $-20°C$. A measure was taken every 24 h during a time course of 4 days. Each sample was coated with 30 μl PVA (10 % polyvinyl alcohol buffered stock solution) and left to polymerize approx. 3 h. Cell removal from the disc with the help of the PVA-layer lead to a retention rate close to 100%. The suspensions were dilution plated in triplicate on the appropriate solid medium and the cell's survival was determined by enumerating the visible macroscopic colonies (cfu) that form after incubation (chapter 2.4.1).

2.9 Mars-Environment-Simulation Studies

UV radiation is a parameter, which influences every solar body and is the most deleterious component - biologically spoken - of the space radiation environment. This chapter deals with an austere UV radiation environment characterized by aride conditions, high solar radiation flux, anoxic atmosphere and extreme temperature ranges which is typical for planet Mars – an aptitude test to appraise how the *D. radiodurans* species resist the lethal effects in order to maximize their survival.

The realistic simulation of a complete Martian surface environment is a considerable technical challenge Table 2.6. It is especially difficult to reproduce the Martian UV-climate realistically. The key point is that the thermo-physical conditions on the surface of present Mars have not been adequately simulated in one single experiment. However, it is indispensable to investigate the biological effects of combined environmental parameters, because they might not necessarily be additive, but can be synergistic or antagonistic.

A realistic simulation should include diurnal cycles of temperature, humidity and UV radiation in a simulated Martian atmosphere and at Martian pressure, with Martian soil analogues, dust particles, and ionizing radiation. The Mars-Environment-Simulation Studies were conducted to assess the effects of diurnal temperature and humidity cycle variations in a Martian atmosphere and at Martian pressure alone as well as in combination with Mars solar radiation on the survival of *D. radiodurans* [Pogoda de la Vega et al., 2007].

Due to literature, reporting an attenuating effect of UV-radiation and enhancing survival of bacterial spores by a minimal amount of shielding [Horneck et al., 2001, Schuerger et al., 2003, Rettberg et al., 2004], the protective role of dust coatings on bacterial survival was surveyed as well (details are described in chapter 2.9.3).

Tab. 2.6: Martian environmental parameters and the limits for survival and growth of terrestrial organisms. The environmental limits shown are modified from [Horneck, 2006].

Parameter	Mars	Growth	Survival
Temperature / $°C$	-123 – $+25$	-20 – $+113$	-262 – $+150$
Pressure / Pa	560	10^5 – 10^8	10^{-7} – $> 10^8$
Ionizing radiation	0.2 Gy / a	$\sim$ 50 Gy	$\geq$ 5000 Gy
UV radiation	$\geq$ 200 nm	$\geq$ 290 nm	$\geq$ 290 nm
Water activity / gcm^{-3}	7×10^{-4}	$\geq$ 0.7	0 – 1.0
Salinity	regional high	$\leq$ 30 %	salt crystals
pH	unknown	1 – 11	0 – 12.5
Nutrients	unknown	high metabolic variability and starvation tolerance	not necessary
Gas composition	95.32% CO_2 2.70% N_2 1.60% Ar 0.13% O_2	diverse needs	better without O_2

CO_2 - Carbon dioxide, N_2 - Nitrogen, Ar - Argon, O_2 - Oxygen

2.9.1 Experimental implementation

In order to derive the necessary premises required to design the Mars simulation chamber at the Planetary and Space Simulation Facilities (PSI) localization had to be agreed upon in such a way as to determine the regional and seasonal Martian environmental terms, thus, providing specifications for a close-to-realistic simulation. The southern hemisphere on Mars was chosen because it exhibits polygonal patterned ground similar to those found on Earth, that inhabit microbial communities [Wagner et al., 2003]. Thermophysical conditions that are present during the southern summer at latitude of 60° on Mars were employed for the Mars-Environment-Simulation Studies.

Simulation of the Martian surface environment include the unique atmospheric composition (predominately CO_2) and a mean surface pressure of about 7 hPa. The first requirement was met by ordering a specifically designed Mars-like gas (Linde AG, Wiesbaden, Germany); its composition is shown in Table 2.7.

Tab. 2.7: Composition of the Mars-like gas.

Element	Volume%
CO_2	95.55
N_2	2.70
Ar	1.60
O_2	0.15
Manufacturing tolerance	± 5%
Analysis specificity	± 2%
Water moiety	ca. 370 ppm

The last premise was achieved by using the Mars-like gas to attain the anticipated pressure of 7 hPa in the vacuum chamber at a constant rate. In addition, the environmental stresses temperature, humidity and UV radiation have been introduced.

2.9.2 Environmental specifications

The diurnal cycles of temperature have been derived from [Carr, 1981] with slight modifications. The temperature profile was generated with an Ultra-Kryomat RUL80 (Lauda Dr. R. Wobser GmbH & Co. KG, Lauda-Königshofen, Germany). A 100 h-time slot profile of the diurnal temperature cycles and the resulting water activity, expressed as a_w-value, are presented in Figure 2.2.

The physical definition of water stress activity (a_w) is the increase of water vapor saturation with decreasing temperature (see Figure 2.2).

A Wolfram halide lamp (Solar sun simulator, Dr. Hönle AG, UV-Technologie, Munich, Germany) was chosen as UV source. The spectral irradiance of the solar simulator lies in the range of $200-400$ nm as has been modeled for the surface of equatorial Mars by several research teams [Cockell et al., 2000, Patel et al., 2003, Schuerger et al., 2003]. The Mars simulation chamber is equipped with a UV grade fused silica window (10 mm thickness), which on one hand slightly attenuates the passing UV as to simulate the thin Martian atmosphere and secondly, directs the light beam onto the microbial targets. Considering the theoretical surface flux model as described in [Patel et al., 2003] the UV flux in summer at the destined latitude of 60° lies around $38 Wm^{-2}$. The working distance of the UV source was fit to match this UV flux.

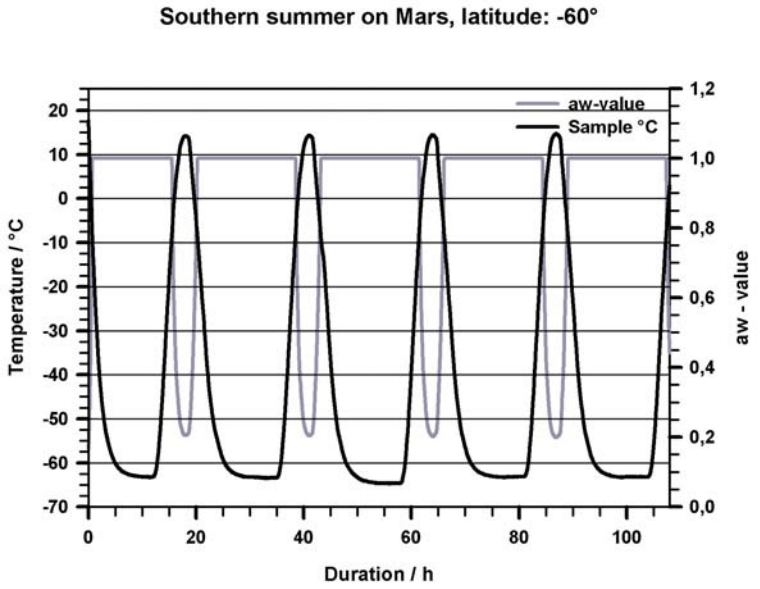

Fig. 2.2: Diurnal profile of the Mars-like temperature and water activity cycles during exposure.

2.9.3 Exposure conditions

Because of the innate low penetrating power of UV radiation, its lethal effects can be successfully prevented by a minimal amount of shielding. Next to assessing the viability rates of the unshielded cells, the investigated *D. radiodurans* strains R1, mutant strain 262 (*uvrA-2*) and the UV-sensitive strain UVs78 (*uvrA-1 uvsE*) were mixed with Mars-like minerals of different grain size. Two Mars soil analogues with the following properties were used: "Goldenrod iron oxide" B-6090 (MPSI, Mineral and Pigment Solutions, Inc., South Plainfield, USA) with a grain size of 300 nm, and a nano-crystalline iron (III) oxide (Alfa Aesar, A Johnson Matthey Company, Karlsruhe, Germany) of 8-10 nm grain size. "Goldenrod iron oxide" is the name for a commercial mineral pigment produced by blending red hematite ($\alpha - Fe_2O_3$) and yellow goethite ($\alpha - FeOOH$) pigments [Morris & Golden, 1998]. The nano-crystalline iron (III) oxide is a synthetically produced hematite. The Mars soil analogues were pre-sterilized at $130°C$ for 24 h and cooled to ambient temperature. For the experiments 10 mg of pre-sterilized soil analogue material was mixed with 1.5×10^7 cells per 1 ml before desiccation (cf. chapter 2.3.1, p. 30) to achieve a contiguous layer of dust. Controls were conducted to guarantee that the treatment was sterile and that the experiment could be performed without contaminating either the Mars soil analogue or the bacterial monolayers.

RTV-2 silicone rubber (RTV-S 691, Wacker-Silicones, Munich, Germany) was used to fix samples into accommodation hardware that was placed into the vacuum chamber for these simulation experiments. The advantage of the dual-part addition curing silicone rubber is that vulcanization takes place at room temperature.

2.10 Gene expression profiling

The gene expression profiling using DNA microarrays was applied to identify genes differentially expressed post-UV-irradiation and to recognize and classify common expression patterns by groups of genes. The basic principle is the following: For a given sequence spotted on the array, if one sample contains more of the corresponding mRNA transcript, then the signal intensity for the dye used to label that sample should be higher than for the other dye.

The following hybridizations were conducted and analyzed:

1. UVC-irradiated R1 0.5 h post-irradiation recovery
2. UVC-irradiated UVs78 (*uvrA-1 uvsE*) 0.5 h post-irradiation recovery
3. UVC-irradiated 1R1A (*recA*) 0.5 h post-irradiation recovery

Each probe was repeated with at least three independent and randomly selected biological replicates, and in the case of R1, four replicates were assessed. Biological replicates to assess biological variability are essential to infer that the mean expression of a gene differs in two populations.

2.10.1 Workflow of gene expression analysis

Preparatory steps prior to the gene expression analysis comprise 1. RNA isolation of the samples (chapter 2.6.2), 2. a quality check via an E_{260} to E_{280} ratio and 3. a visual inspection (see chapter 2.6.3). After that, the samples were transferred into bar-coded tubes and sent on dry ice to RZPD–German Resource Center for Genome Research in Berlin, Germany. RZPD and NimbleGen Systems (Madison, USA; Reykjavik, Iceland) have carried out the following steps from initial quality control to sample labeling as well as data extraction.

To ensure that the quality needs are fulfilled and no degradation is present in the sent *D. radiodurans* RNA, the samples were re-analyzed with the Agilent 2100 Bioanalyzer (cf. chapter 2.6.3) and the RNA was again quantified by spectrometry. The prokaryotic RNA was labeled via first strand cDNA

synthesis, subsequent partial digestion and finally a terminal transferase reaction using biotinylated nucleotides was applied. Quality and quantity control of the created cDNA is performed as mentioned above. The biotin-labeled samples are then further transferred to NimbleGen, where hybridization to the microarray chip was achieved on a proprietary automated system. Before hybridization, the biotinylated samples are labeled with the fluorescent stain Cy3-Streptavidin. The intensity of the fluorescence signal was measured, scanned and the provided microarray data was extracted from the scanned image.

3. ENVIRONMENTAL STRESS SCENARIO

Of all environmental stresses organisms have to encounter on Earth, sunlight is an essential, omnipresent and life-limiting factor not only on Earth but also on every solar body. Sunlight adheres not only positive effects like photosynthesis and vitamin D synthesis, amongst others, but represents the primary biocidal parameter resulting from its inherent complex mixture of mutagenic and protein damaging wavelengths. As stated in chapter 1.3.2 (p. 20), solar UV radiation comprises a wide wavelength spectrum. Due to atmospheric absorption, the incident UV radiation flux on present Earth is largely composed of UVB and of UVA ($\lambda = 280 - 400$ nm).

Consistently, most recent terrestrial biological systems are equipped with diverse repair mechanisms and UV protecting compounds to meet the lesions induced by these wavelengths. UVA ($315 - 400$ nm) generates mainly indirect effects via photosensitizers that produce reactive oxygen species (ROS) which, in turn, induce cellular response to oxidative stress. Whereas UVB ($280 - 315$ nm) and UVC account for direct effects, especially DNA damage reflected in the formation of bipyrimidine photoproducts (cf. chapter 2.5.1, p. 33), one of the key ramifications of UV radiation (chapter 1.3.2.2).

Chemotaxonomic characterization of the radiation-tolerant genus *Deinococcus* have not only revealed an apparently ancient derivation but also a specific evolutionary relationship to the *Thermus* group ([Woese, 1987] and [Griffiths & Gupta, 2004]). Woese (1987) generated an evolutionary distance matrix from the eubacterial phylogenetic tree, which is based upon 16S rRNA sequence comparison, placing the genus *Deinococcus* close to the root of the eubacterial tree and proposing the existence of a putative thermophilic common ancestor [Makarova et al., 2001]. Suggesting that the biologically effective UV flux on present Earth is not the maximum radiation burden that *D. radiodurans* can endure if it is considered to be a progeny of primordial colonizers. Particularly, if assumed that organisms on Archean Earth developed repair processes for dealing with lesions induced by higher DNA damaging irradiances (chapter 1.3.2).

Next to its broadband UV-resistance ([Pogoda de la Vega et al., 2005] and [de la Vega, 2004]) *D. radiodurans* is exceptionally resistant to ionizing radiation, as Mattimore and Battista (1996) established – a spin-off resulting

from *D. radiodurans'* desiccation tolerance.

Based on this perception, experiments were conducted to investigate the biological consequences of high UV radiation flux alone and as part of a harsh environment scenario. Model predictions have anticipated that the spectral irradiances of the Archean Earth are comparable to those on present Mars [Ronto et al., 2003]. As calculated for Archean Earth, present Mars UV irradiance shows a three-orders of magnitude greater biologically effective flux, a consequence of its thin atmosphere and a high concentration of carbon dioxide (CO_2) [Cockell et al., 2000]. Thus, the prevailing thermo-physical conditions on the surface of present Mars served as template to design the extreme environmental scenario detailed in chapters 2.9 till 2.9.2.

Before exposing *D. radiodurans* cells to the load of stressors of the harsh environment scenario MESS [Pogoda de la Vega et al., 2007], the individual biological consequence of each thermo-physical parameter had to be deduced in advance. The results obtained of the single stress parameters as well as of the MESS are detailed in the following subchapters.

3.1 Effect of single parameter

The survival limits of *D. radiodurans* were deduced from the primary hostile parameters of Martian and space environments: the biologically effective short-wavelength portions of the UV-spectrum (VUV and UVC, wavelength ranges listed in chapter 1.3.2), low atmospheric pressure (vacuum) causing extreme desiccating circumstances, low temperatures, oxidizing conditions in atmospheric dust and regolith, as well as the presence of galactic cosmic rays [Nicholson et al., 2005].

Galactic cosmic rays (GCR) are characterized as the most complicated mixture of radiation known, and are composed of 98% protons and heavier ions and 2% electrons. Iron ions belong to the major component of GCR (cf. chapter 3.1.4, p. 53), featured by its higher biological efficiency and its high abundance compared to other particles of the GCR spectrum [Berger, 2003].

To determine the stress response range of the genus *Deinococcus*, mutant strains of *D. radiodurans* were carried along. The mutant strains were investigated in parallel to the wild-type strain (regarded as reference strain). Depending on the applied stressors the chosen competitor sample was either a UV-sensitive mutant or a mutant showing wild-type-like UV resistance, but disrupted in a protein involved in the UvrABC repair system (cf. chapter 1.3.2.2, p. 21), playing a seemingly minor role in UV resistance, thus, potentially relevant in other stress-response systems [Tanaka et al., 2005].

3.1.1 UV irradiation

The establishment of a UV characterization along with a wavelength-specific DNA damage profile following UV irradiation of *D. radiodurans* (chapter 4) was central if the biological consequences, in terms of phenotypic and molecular-based effects, of high UV radiation flux were to be determined. As pointed out in the previous section, mutant strains differing in their DNA repair capacity compared to the *D. radiodurans* wild-type strain were carried along. The investigated strains differ in their radiation susceptibility, resulting in the classification of a UV-sensitive (UVs78 and 1R1A) and a UV-resistant class (wild type strain R1 and 262) [de la Vega, 2004], [Pogoda de la Vega et al., 2005].

Tab. 3.1: Characteristics of the survival curves published in [Pogoda de la Vega et al., 2005] (slightly modified).

UV range	Strain	F_t/kJm^{-2}	F_{37}/kJm^{-2}	EC/m^2kJ^{-1}	R^2
254 nm	R1	0.350	0.640 ± 0.148	1.563	0.977
	262	0.380	0.630 ± 0.310	1.587	0.964
	UVs78	0.005	0.021 ± 0.097	47.619	0.963
	1R1A	0.004	0.035 ± 0.136	28.571	0.989
>200 nm	R1	8.600	15.400 ± 0.151	0.065	0.931
	262	12.300	22.200 ± 0.049	0.045	0.996
	UVs78*	1.400	2.100 ± 0.032	0.476	0.970
>280 nm	R1	67.000	132.400 ± 0.049	0.008	0.968
	UVs78*	0.300	35.200 ± 0.187	0.028	0.901
>315 nm	R1	187.500	244.800 ± 0.065	0.004	0.978
	UVs78	100.500	191.600 ± 0.009	0.005	0.976
	1R1A	183.700	221.500 ± 0.018	0.005	0.991

F_t/Jm^{-2}: Threshold fluence, corresponds to the extrapolate of portion at which the percent survival remains 100%, F_{37}/Jm^{-2}: Fluence, which causes a survival fraction of 37%; EC: efficiency coefficient, predicts the wavelengths efficiency and is the reciprocal value of F_{37}; R^2: correlation coefficient of regression through the exponential part of the curve. The correlation coefficient is a quantity that gives the quality of a least squares fitting to the original data.

*Data calculated from the lower fluence portion ($< 4kJm^{-2}$) of the survival curve

The selected polychromatic UV wavelength ranges comprise the simulated UV radiation environment (>200 nm) of the Archean Earth (before the built-up of the ozone layer) or of the planet Mars as well as selected spectral ranges of the environmental UV (>315 nm) climate on present Earth. The main cellular target of UV radiation is DNA, which leads to alteration of the DNA

bases resulting in formation of bipyrimidine dimers (details are outlined in chapter 2.5.1).

Succinctly, with increasing UV wavelengths ($UVC \triangleright UVB \triangleright UVA$) the UV sensitivity of the UV resistant class of *D. radiodurans* strains (R1 and 262 (*uvrA-2*)) decreases and becomes similar to the UV sensitive class (UVs78 (*uvrA-1 uvsE*) and 1R1A (*recA*); cf. Table 3.1.1). The type and amount of photoproducts are identical in UV-resistant and UV-sensitive strains and a specific photoproduct lesion pattern for each applied wavelength range could be distinguished (details can be retrieved from [de la Vega, 2004]). However, mediating only the distribution pattern of UV-induced bipyrimidine dimers of DNA repair-defective *D. radiodurans* mutants compared to the wild-type strain R1, the obtained results lead to the a priori statement that *D. radiodurans* encodes a yet undefined repair pathway [Pogoda de la Vega et al., 2005]. It is apparent only when the DNA repair pathways nucleotide excision and homologous recombination are inactivated (chapter 1.3.2.2, p. 21).

3.1.2 Desiccation/Vacuum

D. radiodurans is highly resistant to desiccation [Mattimore & Battista, 1996], indicating that it should tolerate vacuum exposure as well since the effects resulting from long-term desiccation are similar to vacuum infliction [Bucker et al., 1972]. Dose and co-workers ([Bieger-Dose et al., 1992] and [Dose et al., 1992]) proved that desiccated bacterial cells suffer of extensive DNA double strand breaks, single strand breaks as well as of DNA crosslinks. This damage profile is comparable to that detected after exposure to ionizing radiation [Ward, 1975]. The requirement of desiccated bacterial cell layers on quartz discs and determining *D. radiodurans'* critical value of desiccation to assess the biological consequences of low temperature and vacuum as well as combined environmental conditions on Mars surface have been outlined in chapter 2.3.1.

Vacuum and desiccation exposure were performed in parallel, with the samples denoted "Dry" in Table 3.2 representing the lab control of the vacuum-exposed cells ("Vac" in Table 3.2). The average survival ratio indicates the additional inactivation percentage of each strain if desiccated at room temperature.

Astonishingly, the *recA*-deficient strain 1R1A was already inactivated by five orders of magnitude during the preparatory step of the vacuum and temperature experiments, i.e. desiccation in the exsiccator. Therefore, this strain was excluded from the following experiments.

Tab. 3.2: The percentage of the survival fraction following vacuum (Vac) and desiccation (Dry) exposure at room temperature. The presented data have been calculated from three independent trials (except for the 1-year exposure data, which have been derived from 2 trials). The data of the vacuum exposure are the same as depicted in Figure 3.1. The survival ratio represents the ratio of the survival percentage of the listed desiccation and vacuum effect.

R1 (WT)			
Time course	Vac%	Dry%	Survival ratio
1 week	71	73.2±1.5	1.0
3 weeks	100	100.0±0.1	1.0
8 weeks	62	4.1±0.3	0.1
1 year	100	63.8±9.3	0.6
Average survival ratio			0.7
262 (*uvrA-2*)			
Time course	Vac%	Dry%	Survival ratio
1 week	88	79.4±9.7	0.9
3 weeks	100	9.7±1.0	0.1
8 weeks	65	5.8±1.4	0.1
1 year	100	66.8±12.9	0.7
Average survival ratio			0.4
UVs78 (*uvrA-1 uvsE*)			
Time course	Vac%	Dry%	Survival ratio
1 week	52	36.2±2.6	0.70
3 weeks	100	0.8±0.2	0.01
8 weeks	82	17.2±1.2	0.21
1 year	100	68.4±14.8	0.68
Average survival ratio			0.4

It has been noticed that the mutant strains share the common feature of lacking a component of the UvrABC system (cf. chapter 1.3.2.2, p. 21), indicating an additional function of these components in preserving genome integrity from desiccation effects.

The main difference in vacuum and desiccation exposure in this study is the parameter humidity. To achieve low-pressure ranges of 10^{-6} to $10^{-7} Pa$ humidity has to be excluded and the vacuum chamber is equipped with limited measures to reduce humidity remnants. Exposures in these instruments truly simulate arid environments, which may explain the differences in survival as observed in the exposed *D. radiodurans* strain. The results in Table 3.2 indicate that *D. radiodurans* is vulnerable to humidity shifts but if this environmental stressor is largely diminished, enhances its capability to tolerate desiccation.

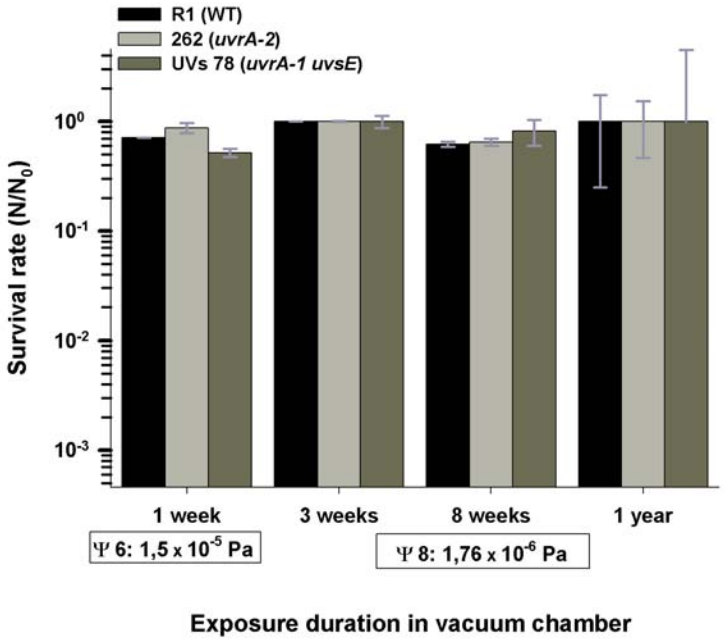

Fig. 3.1: Due to the fact that the *recA*-deficient strain 1R1A is severely affected by desiccation, this strain was excluded from the vacuum exposure series. The investigated *D. radiodurans* strains, R1 (WT) as well as mutant strains 262 (*uvrA-2*) and UVs78 (*uvrA-1 uvsE*), show slight but not significant differences in their survival potential to this stressor. The error bars have been calculated from the average error and standard deviation of at least three independent trials and six parallel samples ($n = 18$). With the exception of data obtained for the time courses 8 weeks and 1 year, which comprise data from two trials of each indicated pressure.

The differences in surviving fractions of the varying temporal vacuum exposures may result from the two different vacuum chambers that have been used in this study (vacuum chamber characteristics are noted in chapter 2.7, p. 38). The vacuum chamber Ψ6 was entirely used for the short-term exposure of 1 week, because chamber Ψ8 is appropriate for long-term exposure only and can obtain lower pressure than Ψ6. Though the utmost pressure of about $1 \times 10^{-5} Pa$ achievable in Ψ6 was obtained, this challenge lead to an inactivation rate of 30% for the UV-resistant strains R1 and 262 (*uvrA-2*), corresponding to a survival of approx. 70%, as well as the inactivation of 50% of the UV-sensitive strain UVs78 (*uvrA-1 uvsE*). In contrast lower pressure ranges of an average of $1,76 \times 10^{-6} Pa$ lead to no inactivation Figure 3.1.

As pointed out earlier a premise to achieve the utmost low pressure in a vacuum chamber is the least possible humidity. Due to the varying humidity in the facility, varying amounts can creep into the vacuum chamber during sample accommodation. Therefore, this experimental series had to be repeatedly performed to account for reproducible conditions. Amongst others two runs in vacuum chamber Ψ8 (time course: 8 weeks) obtained a pressure of approx. $8 \times 10^{-7} Pa$, which resulted in an inactivation of two orders of magnitude relative to the cell number before the challenge (cf. Figure 3.1). Airo et al. (2004) provided evidence that slight temperature shifts are sufficient to obtain a wide range of survival responses of *D. radiodurans* to heat- and cold-shock ($42°C$ had a survival rate of 90%, whereas $40°C$ and $52°C$ resulted in 60% and 40% survival, respectively). Their overall goal was to educe the optimal heat- and cold-shock temperature for *D. radiodurans* to acquire thermo- and cryotolerance. Accordingly, it is concluded that $1 \times 10^{-6} Pa$ is the threshold vacuum pressure for *D. radiodurans* to acquire vacuum tolerance under the described experimental conditions because the survival percentage remains 100%.

3.1.3 Cold shock

Desiccated *D. radiodurans* cells were prepared as described in chapter 2.3.1 and exposed to either $-20°C$ or $-80°C$ for 24 h, 48 h, 72 h and 96 h to determine the cold shock response and to assay the survival rate by CFU counts (chapter 2.4.1, p. 31).

Since the UV-sensitive strains were affected severely by cold shock in the absence of a cryo-protectant like glycerin, solely the designated UV-resistant strains R1 (WT) and 262 (*uvrA-2*) were tested. Except for the typical biological fluctuations (variable titre, measuring and slight handling differences), the cold shock did not affect the two *D. radiodurans* strains as depicted in Figure 3.2. The chosen exposure duration remained above the

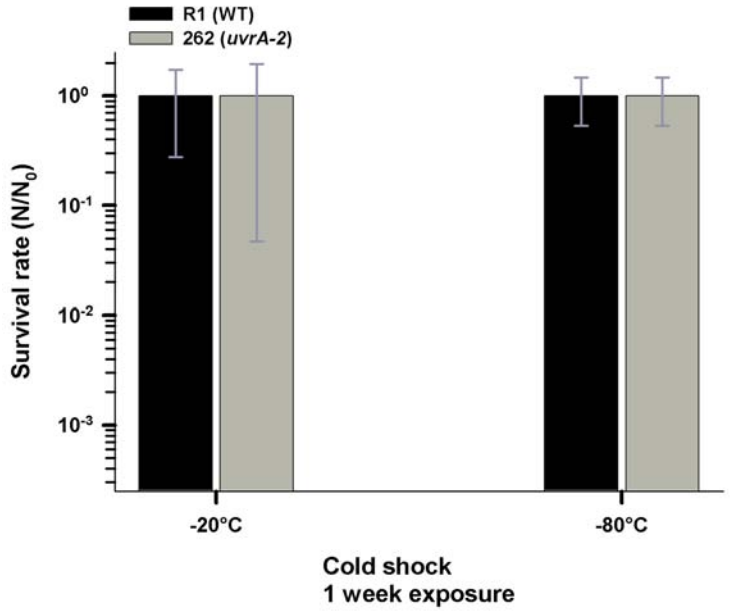

Fig. 3.2: The UV-resistant strains R1 (black) and mutant strain 262 (*uvrA-2*) (grey) were exposed to a cumulated time-line of 96 h. No significant variations were observed. Therefore solely the survival rate of the total exposure duration is represented in the plot. Error bars have been calculated from the standard deviation of at least three independent trials and four parallel samples ($n = 12$).

critical time line for this stress parameter.

Because the applied temperature of $-80°C$ is utilized to store microbial cultures, it is assumed that the temporal limit is almost infinite. It was not the aim of this study to determine the life limiting low temperature of *D. radiodurans*. Instead $-80°C$ was chosen to ascertain, that the lowest boarder temperature of the anticipated temperature range for the simulation of the harsh environment (cf. Figure 2.2 in chapter 2.9.2, p. 42) does not intrinsically inactivate the exposed cells.

3.1.4 Survival limits of wild-type strain R1

The overall goal of this chapter was to educe the survival limits of a terrestrial microorganism to the harsh environment, as it may have existed on Archean Earth. Due to its ancient derivation and early evolutionary presence ([Woese, 1987]; [Makarova et al., 2001]), the genus *Deinococcus* was predestined as investigation object to evaluate this. On the basis of the fact that Archean Earth was featured by UV fluence with a three orders of magnitude

greater biological effectiveness than at present [Cockell & Horneck, 2001], UV radiation represented the primary biocidal selective pressure at that time. Therefore, the survival data of the wild-type strain *D. radiodurans* R1, which is equipped with an intact repair system, was comprised in Figure 3.3 as tolerance baseline for terrestrial biology.

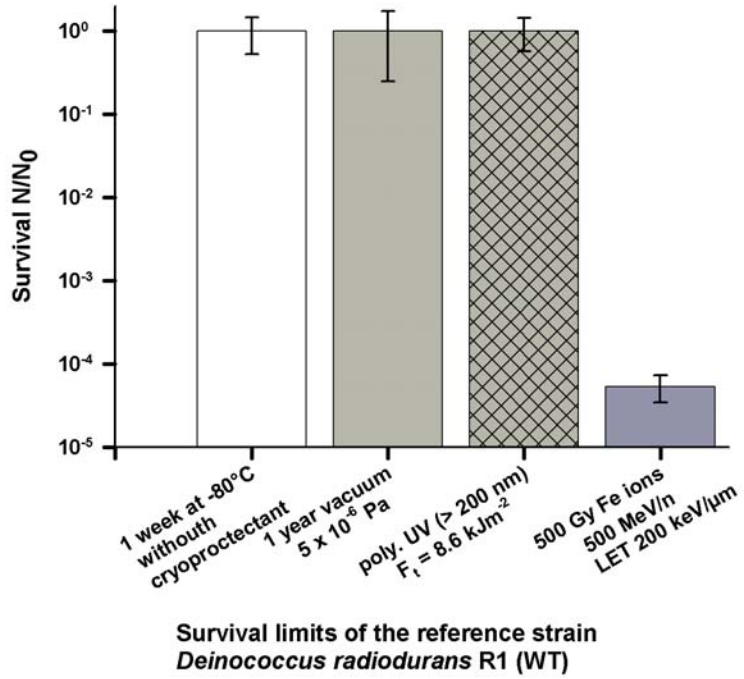

Fig. 3.3: With the exception of Fe-ion bombardment (at HIMAC of the National Institute for Radiological Sciences (NIRS) in Chiba, Japan), the data shown represent critical values of the indicated stress parameters at which the survival rate of R1 remained 100%. Averages and standard errors of the mean were determined from 3 replications (does not apply to the irradiation with heavy ions).

Next to surviving low temperatures up to $-80°C$ and 1-year vacuum exposure at $1,76 \times 10^{-6} Pa$, *D. radiodurans* survived 0.5 kGy Fe-ion bombardment, which was chosen as a representative of heavy ions that are part of the GCR (galactic cosmic rays) environment. The opportunity to investigate the effect of this remaining parameter was provided by Ralf Moeller, whose research project 17B463 "Gene activation of heavy ion treated *Bacillus subtilis* 168 endospores during germination involved DNA-repair" was accepted by the National Institute for Radiological Sciences (NIRS) in Chiba,

Japan. The experiments were performed at NIRS Heavy Ion Medical Accelerator (HIMAC). The obtained results reflect rather a heavy ion-tolerance tendency due to the limited amount of exposed wild-type *D. radiodurans* samples, which varied depending on the remaining sample capacity of R. Moeller (experimental set up is described in [Moeller, 2007]).

With the exception of UV radiation, none of the applied single stressors put a strain on *D. radiodurans'* survival capability. Thus, the experimental series of the single parameter effects corroborated *D. radiodurans'* exceptional and broad stress tolerance (Figure 3.3). Nonetheless, the question left to be answered is whether *D. radiodurans* is capable to survive exposure to first, a combination of two single parameters and second, the daily exposure to a simulated harsh environment. These objectives are addressed in the following chapters 3.2 and 3.2.1.

3.2 Effect of combined parameters

According to studies by [Airo et al., 2004], *D. radiodurans* is susceptible to temperature shifts. Therefore, an experimental series was performed to identify the role of this stressor to the overall tolerance response of *D. radiodurans* as well. The results will aid subsequently in determining the contribution of each applied single and complex component of the simulated harsh environment.

As previously noted, mutant strain 1R1A (*recA*) was excluded from the complete experimental series due to its severe desiccation sensitivity, therefore, no sufficient basis is warranted for additional stress exposure. Though UVs78 (*uvrA-1 uvsE*) exhibits desiccation and vacuum tolerance, its sensitivity to low temperature restricted the exertion to this series.

Exposure to the stressor combination vacuum and temperature shift lead to an overall survival rate of 56% and 57% for the reference strain R1 (WT) and the mutant strain 262 (*uvrA-2*), respectively. As educed from the effect of single parameters, on average at least 30% can be attributed to the vacuum as indicated in Table 3.2. According to [Airo et al., 2004] temperature shifts under their experimental conditions resulted in a survival rate of $20 - 40\%$. From these data, it is concluded that the stressors vacuum and temperature shift exert rather an additive than a synergistic effect on the survival rate. In contrast to UV radiation, which exerts a synergistic effect on *D. radiodurans'* viability as is clearly visible in Figure 3.4, neither strain survived when UV radiation was inserted to the scenario. The applied UV flux conformed to Earth's orbit UV radiation. Cockell and Horneck (2001) averred that

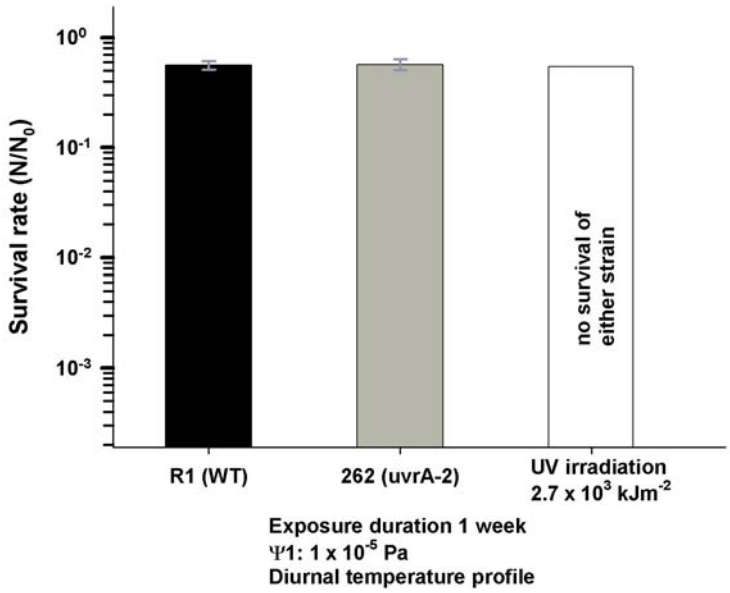

Fig. 3.4: Parameter combination of vacuum and the diurnal temperature profile as shown in Figure 2.2 (chapter 2.9.2). Exposure for one week lead to a survival of approx. 50% for both *D. radiodurans* strains (wild-type R1 and mutant 262 (*uvrA-2*)). Addition of UV radiation had a devastating effect on the viability of the cells. The error bars represent the standard deviation from the mean of four independent experiments.

Earth's orbit UV flux could be employed to investigate the possible effects of UV radiation on Archean Earth before ozone amelioration, because it is uninhibited by Earth's atmosphere.

3.2.1 Mars-Environment-Simulation Study (MESS)

The objective of this study [Pogoda de la Vega et al., 2007] was to test the viability of *D. radiodurans* strains, with different inherent UV susceptibility, to the cumulative environmental stresses encountered on the surface of present Mars. The existent thermo-physical Mars surface conditions are characterized by its aridity, high UV flux and low temperatures. The Mars-Environment-Simulation Study (MESS) is the first set up so far that conducts a close-to realistic simulation of the Martian UV environment. Particularly, because several environmental parameters could be simulated in one single experiment: vacuum/low pressure, anoxic atmosphere and diurnal cycles in temperature and relative humidity, energy-rich UV radiation as

well as shielding by different Martian soil analogue materials (details of the thermo-physical conditions in chapters 2.9 till 2.9.2).

This was one of the greatest technical challenges encountered in the course of this dissertation. The experimental implementation acquired a coordinated assembly of diverse instruments to assure on-line monitoring as well as a reliable, autonomous operational sequence of the diurnal temperature cycles for at least 7 days (cf. chapter 2.9).

The investigated strains comprise the reference strain R1, mutant strains 262 (*uvrA-2*) and UVs78 (*uvrA-1 uvsE*). To ascertain the expected protective measure of Mars soil analogues, the mutant strain UVs78 (*uvrA-1 uvsE*) was carried along with its UV-sensitivity being the essential provision and taking into account that its temperature sensitivity will attribute extensively to its survival rate.

The desiccated samples of each independent experiment run were split and subjected to the following treatments (preparation details specified in chapter 2.3.1) and are addressed in Figure 3.2.1 as itemized below:

1. *Non-treated* corresponds to the lab control of each *D. radiodurans* strain and represents the initial viable cell count before exposure.

2. *Mars* refers to the samples exposed to the diurnal temperature and humidity cycle (Figure 2.2 in chapter 2.9.2) and Martian atmosphere set at 7 hPa in the Mars simulation chamber.

3. *Earth* refers to the samples remaining in the lab, which are subject to slight daily temperature cycles ($\pm 5°C$) at 1013 hPa (or 1 atm).

4. *Mars+UV* denote the samples encountering the Mars conditions (see item 2) and exposed to Mars-like solar radiation.

5. *Earth+UV* denote the sample treatment as described in item 3 but encountering additional exposure to Mars-like solar radiation.

The experimental set up permitted to suspend all three *D. radiodurans* strains in parallel and to investigate the effect of the combined environmental parameters with and without UV radiation in one run. To determine the long-term effect of the Martian UV radiation environment, the cells were exposed for 1 week and a cumulated fluence was applied that is equivalent to 7 d on the Martian surface. The constant parameters of the experimental setup are the Martian atmosphere (cf. Table 2.7, chapter 2.9.1) and the Martian pressure set at 7 hPa. The results of this study have been published in [Pogoda de la Vega et al., 2007].

Effect of the diurnal temperature and humidity cycles without UV

The temperature and humidity cycles (cf. Figure 2.2 in chapter 2.9.2, p. 42) lead to an inactivation of approx. 50%, 80% and 60% of the reference strain R1, the UV-sensitive strain UVs78 (*uvrA-1 uvsE*) and mutant strain 262 (*uvrA-2*), respectively (Tables 3.3 and 3.4 state the survival percentage). The *Earth* samples of the reference strain R1 showed a similar survival rate, but those of the mutant strains exhibited an additional viability decrease of about 10%. Depending on the type of hematite used to mix the *Mars* and *Earth* samples an inhomogeneous biological effect was observed. Adding the nano-crystalline hematite (NCH) leads to a viability rate of 66% and 35% of the *Mars* samples of the mutant strains UVs78 (*uvrA-1 uvsE*) and 262 (*uvrA-2*), respectively, but those of the reference strain remained unaffected Table 3.3. However, adding Goldenrod B-6090 in the chosen concentration had no effect on either strain. The survival rate of all *Earth* samples of strain 262 (*uvrA-2*) are similar to their matching *Mars* samples. The same is true for the data of the *Earth* samples without hematite of the reference and UV-sensitive strain compared to their matching *Mars* samples. Differences in viability have been observed for the *Earth* sample of the reference strain R1 mixed with NCH and the UVs78 (*uvrA-1 uvsE*) mixture with Goldenrod B-6090 reducing their viability by ca. 30% compared to their matching *Mars* samples Table 3.3.

Tab. 3.3: Comparison of mean survival percentage of the *Mars* and *Earth* treated *D. radiodurans* strains after exposure to the simulated Martian environment without UV radiation at the PSI facilities (temperature and humidity cycles, predominately CO_2, 7 hPa).

	Mars			*Earth*		
Strain	no hematite	NCH†	Goldenrod‡	no hematite	NCH†	Goldenrod‡
R1	51.3%	>100%	>100.0%	54.0%	66.7%	>100.0%
262	20.7%	65.5%	>100.0%	37.4%	71.2%	>100.0%
UVs78	36.2 %	35.0 %	>100.0%	47.2%	30.0%	73.7%

†Bacteria suspension mixed with $10mg/1.5 \times 10^7$cfu/sample of nano-crystalline hematite (NCH), grain size: 8-10 nm

‡Bacteria suspension mixed with $10mg/1.5 \times 10^7$cfu/sample of Goldenrod B-6090, grain size: 300 nm

Only Goldenrod B-6090, the hematite of larger grain size, indicated a positive effect on the viability rates of the *Mars* treated cells. One reason might be that water molecules may be enclosed in the porous hematite, therefore antagonizing the desiccation effect that is associated with the temperature and humidity cycles.

The contribution of the stated antagonizing effect is particularly expressed by the unexpected increased survival rate of UVs78 (*uvrA-1 uvsE*). These findings support the assumption of [Diaz & Schulze-Makuch, 2006], who regard water as "safeguard" from external stress.

Effect of Mars-like solar radiation

As expected UV radiation was very efficient in reducing the microbial populations under the investigated surface conditions, especially when lacking screening measures by physical substrates (Figure 3.2.1A).

Screening of UV radiation by nano-crystalline hematite (NCH) of grain size 8-10 nm was not sufficient and neither strain survived UV exposure (see Table 3.4).

Tab. 3.4: Comparison of mean survival percentage of the *Mars+UV* and *Earth+UV* treated *D. radiodurans* strains after exposure to Mars-like solar radiation at PSI facilities (UV radiation, temperature and humidity cycles, predominately CO_2, 7 hPa). In total an added up dose of $145 kJm^{-2}$ was applied.

	Mars+UV			*Earth+UV*		
Strain	no hematite	NCH†	Goldenrod‡	no hematite	NCH†	Goldenrod‡
R1	⋆n.s.	⋆n.s.	97.5%	⋆n.s.	⋆n.s	87.5%
262	⋆n.s.	⋆n.s.	40.7%	⋆n.s.	⋆n.s.	18.6%
UVs78	⋆n.s.	⋆n.s.	17.0%	⋆n.s.	⋆n.s.	24.8%

†Bacteria suspension mixed with $10mg/1.5 \times 10^7$cfu/sample of nano-crystalline hematite (NCH), grain size: 8-10 nm

‡Bacteria suspension mixed with $10mg/1.5 \times 10^7$cfu/sample of Goldenrod B-6090, grain size: 300 nm

⋆n.s.: no survival

Viability rates were only measured when Goldenrod B-6090 was added to the bacteria (Figure 3.2.1B). As expected the *Mars+UV* samples of mutant strain 262 (*uvrA-2*), which has been affiliated to the UV-resistant strains in Pogoda de la Vega et al. (2005), and the reference strain show higher survival rates than the UV-sensitive strain UVs78 (*uvrA-1 uvsE*) Table 3.4.

Surprisingly the surviving fraction of the *Earth+UV* samples of strain 262 (*uvrA-2*) is reduced by additional 50% compared to the *Mars+UV* samples (cf. Table 3.4), while it remained more or less constant for the reference strain and UV-sensitive strain UVs78 (*uvrA-1 uvsE*).

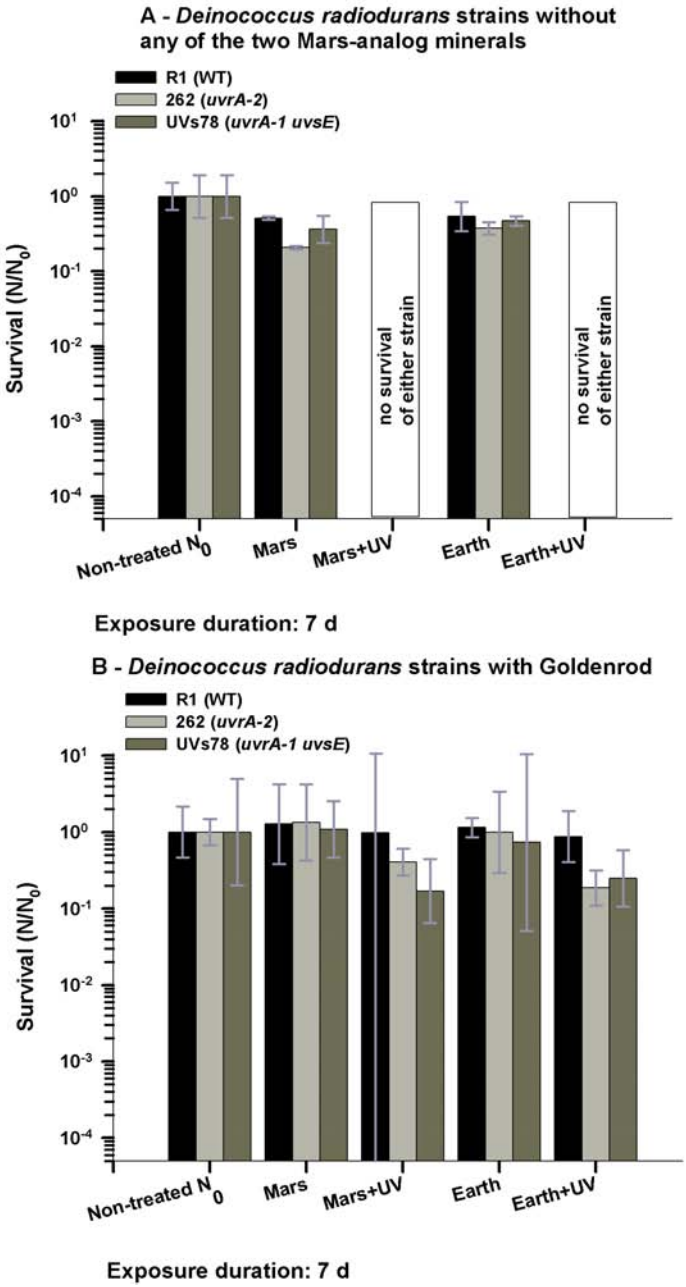

Fig. 3.5: Three *D. radiodurans* strains R1 (WT), 262 (*uvrA-2*) and UVs78 (*uvrA-1 uvsE*) were exposed to the simulated Martian UV climate conditions. The survival is given by the quotient N/N_0 (cf. chapter 2.4.2). The samples encountered the average dose of 145 kJm^{-2}. Averages and standard errors are the mean of 9 measurements (3 experiments, 3 replicates per experiment). **A:** Devoid of hematite, the plot of the survival rate confirms that the environmental factor UV radiation is the most deleterious one because no strain survived. **B:** The Goldenrod B-6090 hematite of grain size 300 nm confers better shielding towards UV radiation on all exposed strains.

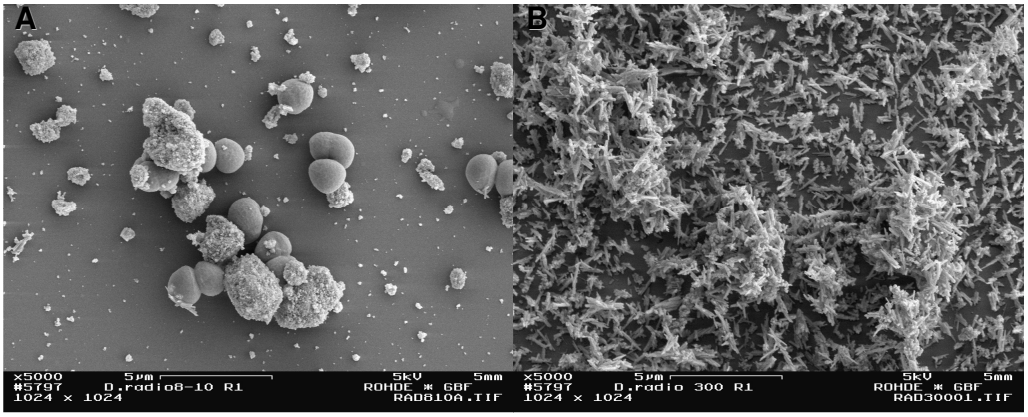

Fig. 3.6: SEM-images of the wild-type strain R1 suspension mixed with $10mg/1.5 \times 10^7 cfu$ of A: nano-crystalline hematite (NCH), grain size 8-10 nm and B: Goldenrod B-6090, grain size 300 nm. Compared to the suspension mixture with NCH no single cell is distinct from the overall surrounding of the Goldenrod grains, covering the cells like a blanket.

Since low-temperature phases prevail in the course of the diurnal temperature cycles (cf. Figure 2.2 in chapter 2.9.2), ice layers may remain and therefore overlay liquid brines, which could function as a filter and protect the samples from UV radiation. Despite the fact that the viability of the *Earth+UV* samples of the mutant strain 262 (*uvrA-2*) is lower compared to the *Earth+UV* probes of the UV-sensitive strain, one should take into account that the values presented in Table 3.4 are the mean of this experimental series. Considering the error bars in Figure 3.2.1 it can be stated, that the *Earth+UV* treated cells of both mutant strains show a similar inactivation rate of approx. 80%.

Preliminary microscopic studies Figure 3.6B illustrate a tight clustering of the Goldenrod B-6090 particles, which appear to cover the entire bacterial layer. Such a 'coat' supplies a homogeneous and effective shielding of UV radiation. If water remains available in the pores of the hematite, an additional and synergistic effect can derive, so that the dehydration stress may be less severe. Thus, the surviving fraction of microbes may well have made use of UV-resistant responses and water molecules and soil as protection.

3.3 Discussion

In this chapter, the viability of *D. radiodurans* strains to single and cumulative stressors encountered in an inhospitable environment was tested. The thermo-physical conditions on the surface of Mars functioned as model for simulating environmental conditions that may have existed on Archean Earth. The biological consequence of each selected stressor and its individual contribution were educed first.

The lowest boarder temperature of the anticipated temperature cycle for the simulation of the harsh environment (cf. Figure 2.2 in chapter 2.9.2) had no effect on the exposed cells. Though it has been postulated that the effects of long-term desiccation are similar to vacuum infliction, our findings suggest, that this comparison is restricted by inherent endowments. The investigated *D. radiodurans* strains exhibited different tolerance rates. Desiccation in reference strain R1 (WT) resulted in a viability decrease of 30% on average, whereas the mutant strains 262 (*uvrA-2*) and UVs78 (*uvrA-1 uvsE*) are inactivated up to 60%. Since both mutant strains bear a deficient component of the UvrABC repair system, it is assumed that UvrA-1 and UvrA-2 are complementary in providing desiccation tolerance. The greatest impact was observed in the *recA*-deficient strain 1R1A having an inactivation rate of five orders of magnitude, excluding this strain for further studies concerning the harsh environment scenario. This observation provided evidence that the *recA*-mediated salvage pathways are essential to attain desiccation tolerance.

In contrast, the biological consequence of vacuum depended on the applied low-pressure. In the course of the vacuum series $1 \times 10^{-6} Pa$ was identified to be the threshold vacuum pressure for *D. radiodurans* strains to retain 100% survival.

Previous studies, [de la Vega, 2004] and [Pogoda de la Vega et al., 2005], have corroborated UV radiation to be the primary biocidal factor. The results obtained in this dissertation provide evidence that UV radiation engenders synergistic effects in combination with other stressors like temperature, humidity and desiccation (vacuum, respectively). Together with its inherent biocidal activity UV radiation potentiates the biological effectiveness of the associated parameters. Whereas low temperature and vacuum represent additive factors, when introduced into a well-defined environment (laboratory experiments), their life-limiting potentials accumulate.

Lastly, the selected stressors were combined to simulate an inhospitable UV environment. In general, desiccated *D. radiodurans* cells survived 7 d Mars-like cycles of temperature and water activity without UV radiation. However, introducing UV radiation (equivalent to 7 d on the surface) had a devastating effect on microbial viability rates in all investigated strains.

Chances of survival for the *D. radiodurans* strains are enlarged, if shielded by dust particles or covered by soil, suggesting that residing in microhabitats below the surface was most probable for *D. radiodurans'* ancestors on Archean Earth or present Mars. But recent calculations by [Dartnell et al., 2007] revealed that *D. radiodurans'* survival depends on the surface characteristics (surface models: dry regolith, water ice and regolith with layered permafrost), especially in the context of accumulated subsurface radiation over time. Subsurface radiation is composed of ionizing radiation fluxes, solar energetic particles and galactic cosmic ray particles. Within this scope, it would be interesting to establish a survival profile of *D. radiodurans* recovering from heavy ions like iron. This subsurface radiation flux can be further enhanced by radionuclide dacay, leading Dartnell and coworkers [Dartnell et al., 2007] to propose that viable cells would predominate in frozen crater lakes or polar caps owing to the near-zero radionuclide content of pure water ice.

By using Mars analogue soils, the simulated harsh environment exerted an additional selective pressure — the oxidative potential of hematite in the presence of water molecules. Experiments of Moehlmann, [Moehlmann, 2004] and [Moehlmann, 2005], showed that dissolved iron leads to UV-radiation-induced hydroxyl formation in the presence of adsorbed water at an oxidative surface ('Photo-Fenton reaction'), eventually influencing the surface chemistry [Spacek et al., 1995].

Therefore, ongoing investigations should place emphasis on the induction of oxidative stress response mechanisms that result from UV-radiation-induced hydroxyl formation in the presence of dissolved iron.

4. REPAIR KINETICS OF UV RADIATION-INDUCED DNA DAMAGES

The characterization of a specific UV-induced bipyrimidine photoproduct lesion pattern for each applied wavelength range established for four *D. radiodurans* strains differing in their UV-susceptibility, already succeeded in hypothesizing that *D. radiodurans* encodes an as yet undefined repair pathway [Pogoda de la Vega et al., 2005]. It is apparent only when the DNA repair pathways nucleotide excision and homologous recombination (HR) are inactivated. Summarized, with increasing UV wavelengths ($UVC \triangleright UVB \triangleright UVA$) the UV sensitivity of the UV resistant class of *D. radiodurans* strains (R1 and 262) decreases and becomes similar to the UV sensitive class (UVs78 and 1R1A). The type and amount of photoproducts are identical in UV-resistant and UV-sensitive strains [Pogoda de la Vega et al., 2005].

Having determined *D. radiodurans'* UV-wavelength dependent photobiological response, this chapter describes further characterization of the repair rate of wavelength-specific UV-induced bipyrimidine dimers and the interrelated UV irradiation recovery of the mentioned above *D. radiodurans* strains. Establishing that a post-irradiation recovery period of 0.5 h is sufficient for *D. radiodurans* wild-type strain to repair on average 80 % of the total UV-induced photolesions. The repair capacity is closely related to the genetic equipment[1] of *D. radiodurans*. If crucial genes are inactivated or an entire repair pathway disrupted, the rate of lesion removal is dramatically reduced resulting in amendment of max. 10% of the total induced bipyrimidine dimers.

4.1 Wavelength-dependent bipyrimidine pattern

Stationary phase cells of *D. radiodurans* strains R1 (wild-type), 1R1A (*recA*), UVs78 (*uvrA-1 uvsE*) and 262 (*uvrA-2*) were irradiated in defined minimal media (DMM, chapter 2.5.2, p. 34) to final fluences of 210 (λ = 254 nm), 791 (λ > 200 nm) and 3312 Jm^{-2} (λ > 315 nm) of UV radiation. The bipyrimidine distribution pattern for each measured wavelength-range was

[1] Gene loci (*recA*) are verbalized and written in italics, whereas their gene products (RecA) are not emphasized and are written as substantives.

determined using HPLC (high performance liquid chromatography) coupled with tandem mass spectrometry (HPLC-MS/MS, chapter 2.6.4, p. 37).

Due to the fact that the UVC-irradiated samples were destined for determining the differential gene expression, this series was carried out in quintuplicate. The HPLC-MS/MS measures of the polychromatic UV-irradiated samples were performed in triplicate and gave an error range of 10–15% before normalization. On account of the varying DNA yield between 10 and 30 μg gained after extraction (chapter 2.6.1), the measured bipyrimidine photoproducts were normalized to correspond to 1 μg DNA.

Surviving fractions were determined by dividing the number of survivors from each fluence by the titer of the non-irradiated culture (Table 4.1-1) to confirm that the applied fluence is consistent with the anticipated biological effect (chapter 2.5.2, p. 34).

Tab. 4.1: Surviving fraction of the irradiated *D. radiodurans* cultures as calculated from N/N_0 (chapter 2.4.2, p. 31).

	Wavelenght spectrum		
	>200 nm	254 nm	>315 nm
Strain	average ± SER	average ± SER	average ± SER
R1	9.86×10^{-1} ± 0,09	9.86×10^{-1} ± 0.11	1.00 ± 0.23
262	9.56×10^{-1} ± 0.20	8.99×10^{-1} ± 0.15	1.00 ± 0.33
1R1A	3.41×10^{-1} ± 0.23	6.79×10^{-2} ± 0.17	1.00 ± 0.50
UVs78	7.89×10^{-1} ± 0.23	4.97×10^{-3} ± 0.07	1.00 ± 0.11

Cyclobutane pyrimidine dimers (CPDs) and pyrimidine $(6-4)$ pyrimidone photoproducts $(6-4$ PPs) are the prevalent photo-induced DNA lesions while strand breaks and DNA-protein-cross links are only produced in minor moieties. Generally UV radiation induces the formation of 90% CPD and 10% $6-4$ PP, with the thymine-containing CPDs predominating irrespective of the applied UV-wavelength [Cadet et al., 2005]. Boling and Setlow predicted that at a fluence of 500 Jm^{-2} 1% of the thymine in the genome exists as a CPD [Boling & Setlow, 1966].

As expected, the bipyrimidine patterns of the differing UV-susceptible strains are similar but vary depending on the applied UV-wavelength-range, Table 4.3. The prevalent UV-induced CPD throughout the applied wavelength spectra is TC CPD. In contrast to the photo-induced CPD distribution pattern of DNA of rodent and human cells that showed a predominance of TT CPD and small amounts of TC CPD as well as CT CPD (reviewed in [Cadet et al., 2005]). Though, considering *D. radiodurans'* GC content this shift towards Cytosine-containing CPD is very likely.

Tab. 4.2: Average yield of UV-wavelength dependent DNA photoproduct formation of the analyzed bipyrimidine dimers (expressed in lesions/ 10^6 bases per 1 Jm^{-2}). In order to achieve uniform integers, the calculated values were multiplied by 10^4.

Bipyrimidine dimer	Wavelength		
	254 nm	>200 nm	>315 nm
TT CPD	231.0	21.8	1.8
TC CPD	476.3	31.5	3.5
CT CPD	187.4	28.6	2.3
CC CPD	206.6	26.7	2.8
$6-4$ TC	151.2	10.7	1.0
$6-4$ TT	16.4	1.6	0.1
TC Dewar	0.0	0.0	0.3
TT Dewar	0.0	0.0	0.0

Comparing the amount of lesions per 1 Jm^{-2} Table 4.2 induced after sublethal fluences of monochromatic (254 nm) or polychromatic UV radiation reveals a continuous decrease of approx. one order of magnitude irrespective of the photolesion type. Polychromatic UV radiation at longer wavelengths ($\lambda > 315$ nm) displays the lowest biological effect on the vitality of the differing UV-susceptible *D. radiodurans* strains and induces two orders of magnitude less photolesions in total. The appearance of TC and TT Dewar valence isomers at longer wavelengths can be fully attributed to the efficient isomerization of initially generated $6-4$ PPs at TC and TT sites which is induced by $\lambda = 320$ nm.

4.2 Wavelength-dependent photoproduct repair kinetics

Different post-irradiation incubation time points (0.5, 1, 1.5 and 2 h) were analyzed by HPLC-MS/MS (chapter 2.6.4, p. 37) to determine the post-irradiation repair kinetics of the UV-induced photoproducts of the selected *D. radiodurans* strains.

Tab. 4.3: Total amount of UV-induced DNA bipyrimidine photoproduct. The values listed are the starting point of the calculated repair rate and correspond to 100% of each measured bipyrimidine dimer.

254 nm				
Bipyrimidine dimer	Strain			
	R1	262	1R1A	UVs78
TT CPD±SER	7.43±1.79	8.23±1.89	12.77±4.04	9.02±0.09
TC CPD±SER	2.28±0.54	4.90±1.02	5.39±1.83	4.27±0.78
CT CPD±SER	3.88±0.88	5.77±1.28	3.96±1.00	2.08±0.28
CC CPD±SER	5.51±2.21	5.26±0.82	4.68±1.68	3.08±0.55
6 – 4 TC±SER	0.27±0.09	3.28±1.26	3.15±1.45	3.10±1.62
6 – 4 TT±SER	0.19±0.04	0.37±0.09	0.44±0.15	0.22±0.09
TC Dewar±SER	0.00	0.00	0.00	0.00
TT Dewar±SER	0.00	0.00	0.00	0.00

> 200 nm				
Bipyrimidine dimer	Strain			
	R1	262	1R1A	UVs78
TT CPD±SER	1.86±1.41	2.36±1.56	3.57±0.75	2.18±0.25
TC CPD±SER	1.50±1.28	1.75±0.31	2.37±0.28	1.29±0.19
CT CPD±SER	1.91±1.23	2.55±0.19	3.20±0.06	1.39±0.22
CC CPD±SER	1.69±0.88	2.57±0.02	2.99±0.42	1.19±0.20
6 – 4 TC±SER	0.50±0.43	0.74±0.74	1.17±0.16	0.99±0.18
6 – 4 TT±SER	0.07±0.04	0.12±0.03	0.21±0.02	0.10±0.01
TC Dewar±SER	0.00	0.00	0.00	0.00
TT Dewar±SER	0.00	0.00	0.00	0.00

> 315 nm				
Bipyrimidine dimer	Strain			
	R1	262	1R1A	UVs78
TT CPD±SER	0.88±0.10	1.00±0.60	0.84±0.27	1.87±0.85
TC CPD±SER	0.35±0.09	0.58±0.46	0.43±0.24	1.03±0.42
CT CPD±SER	0.53±0.17	0.73±0.39	0.63±0.15	1.19±0.58
CC CPD±SER	0.80±0.28	0.66±0.38	0.94±0.06	1.34±0.91
6 – 4 TC±SER	0.04±0.00	0.09±0.04	0.35±0.27	0.90±0.12
6 – 4 TT ±SER	$1.99 \cdot 10^{-2}$ $\pm 1.48 \cdot 10^{-2}$	$1.01 \cdot 10^{-2}$ $\pm 1.54 \cdot 10^{-3}$	$3.39 \cdot 10^{-2}$ $\pm 2.10 \cdot 10^{-2}$	$42.85 \cdot 10^{-2}$ $\pm 1.94 \cdot 10^{-3}$
TC Dewar±SER	0.09±0.09	0.13±0.11	0.03±0.03	0.16±0.07
TT Dewar ±SER	$8.60 \cdot 10^{-3}$ $\pm 2.82 \cdot 10^{-3}$	$2.12 \cdot 10^{-3}$ $\pm 9.72 \cdot 10^{-6}$	$6.54 \cdot 10^{-3}$ $\pm 5.11 \cdot 10^{-3}$	$3.20 \cdot 10^{-2}$ $\pm 2.45 \cdot 10^{-2}$

Listed in Table 4.3 is the absolute number of each UV-induced bipyrimidine dimer, which represents the basis for calculating the repair rate of each photolesion type at the various time points and different wavelength spectrum. Though CPDs are the prevalent observed lesions in *D. radiodurans*, this bipyrimidine dimer is mended very efficiently by *D. radiodurans'* repair system.

Astonishingly, a recovery time of 0.5 h was sufficient for the wild-type strain R1 to repair round about 75% TT $(6-4)$ adduct and CPDs at the TT and CC sites Table 4.4 induced by UV-(254 nm)-radiation. The greatest repair efficiency of *D. radiodurans* R1 was observed for the removal of 90% TC and CT CPD. In contrast, an undistinguished repair efficiency of nearly 40% post-0.5 h irradiation was observed for mutant strains 262 (*uvrA-2*) and 1R1A (*recA*) irrespective of the bipyrimidine dimer type.

Differences in repair rate between the two mutant strains 262 (*uvrA-2*) and 1R1A (*recA*) start 1 h post-irradiation and culminate in the final measured time point of 2 h (Figure 4.2B and C). Recovery post-2 h-irradiation result in removal of up to 70% of either photoproduct type in the case of mutant 262 (*uvrA-2*). 262 (*uvrA-2*) repairs $6-4$ PP more efficiently than does 1R1A (*recA*), whereas the CPD is repaired equally well considering an average error range of $\pm 10\%$. As expected the UV-sensitive double mutant UVs78 (*uvrA-1 uvsE*) displayed no measurable repair, unchanging up to 2 h post-irradiation recovery (Table 4.4, 254 nm and Figure 4.2). The obtained results are in clear contrast to repair kinetics data from a Δ*uvrA-1 uvsE*-mutant strain described in [Tanaka et al., 2005], who reported that 70% and 60% CPDs and $6-4$ PPs, respectively, remained after post-2 h-radiation recovery. The described mutant strain was created by insertional mutagenesis and the photoproduct repair rate was determined by enzyme-linked immunosorbent assays (ELISA). But ELISA technique can only measure DNA photoproduct classes [Cadet et al., 2005].

The polychromatic UV wavelength-ranges (>200 nm and >315 nm) induced in total less DNA photoproducts in either strain than UV-(λ =254 nm) radiation (Table 4.3, Figures 4.2 and 4.2). Accordingly, the wild-type equipment of *D. radiodurans* R1 achieves greater repair efficiency for the polychromatic wavelength spectra compared to its repair rate following UVC radiation, with the exception of $6-4$ PPs, which show similar repair rates as for the UVC-induced $6-4$ PPs Table 4.4.

Wavelength-dependent differences in repair efficiency are solely observed in the mutant strains 262 (*uvrA-2*) and 1R1A (*recA*), but UVs78 (*uvrA-1 uvsE*) was incapable to repair the UV-(> 200 nm)-induced lesions Table 4.4.

The UV-resistant mutant 262 (*uvrA-2*) increased its repair efficiency following UV-(>200 nm) irradiation Figure 4.2B.

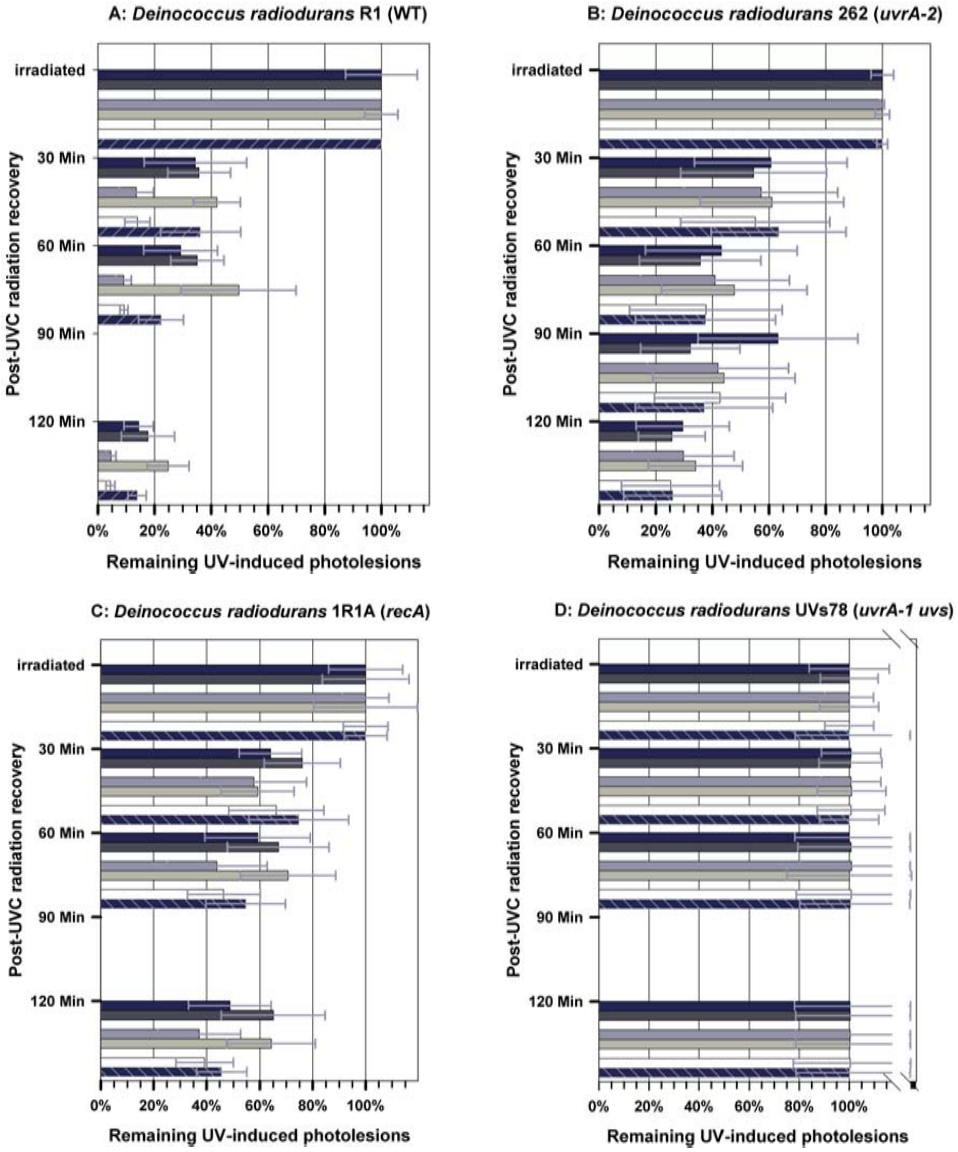

Fig. 4.1: UV-(254 nm)-induced photoproduct repair kinetics. A: wild-type strain R1, B: UV-resistant mutant strain 262 (*uvrA-2*), C: HR-deficient strain 1R1A and D: UV-sensitive double mutant UVs78. Each data point represents the average standard deviation (error bar) of at least three independent experiments.

Tab. 4.4: Time dependent repair rates of the DNA photoproducts induced by the different UV radiation qualities.

% photoproduct remnants post- 0.5/2 h radiation recovery								
Strain	CPD				$6-4$ PP		Dewar	
	TC	TT	CT	CC	TC	TT	TC	TT
254 nm								
R1	11/5	22/12	10/4	30/11	31/20	27/17	0	0
262	57/30	61/30	55/25	63/26	61/34	55/26	0	0
1R1A	58/37	64/49	66/39	75/46	59/64	76/65	0	0
UVs78	no repair							
>200 nm								
R1	11/9	8/9	10/7	11/12	10/10	18/14	0	0
262	47/20	34/28	31/33	58/37	54/20	25/17	0	0
1R1A	72/47	78/53	81/35	80/31	76/45	96/61	0	0
UVs78	no repair							
>315 nm								
R1	3/2	5/6	4/3	3/2	27/18	3/2	9/6	3/1
262	39/2	80/3	22/2	40/3	100/8	100/0	86/15	100/16
1R1A	27/5	35/7	28/1	26/32	41/36	35/15	35/35	14/9
UVs78	100/28	100/31	100/24	100/19	100/39	92/29	100/32	100/22

The first recovery time point of 0.5 h was sufficient to remove nearly 60% CPD with the exception of CC CPD, which shows a similar repair rate as post-254 nm-irradiation. A significant difference post-0.5 h-radiation recovery in 262 (*uvrA-2*) has been observed for the repair of $6-4TT$, but the increased efficiency levels off to meet the yield of remnant lesions post-2 h-irradiation as measured when irradiated with UV-(254 nm) radiation.

Surprisingly, irradiation of the 1R1A (*recA*) strain with UV-(>200 nm) seemed to defer repair initiation reflected in the low repair rate of averagely 20% of CPD as well as $6-4$ PPs post-0.5 h recovery. As for 262 (*uvrA-2*) the remnant photolesions post-2 h recovery of 1R1A (*recA*) meets the yield following monochromatic UV radiation, except for the effective removal of $6-4TC$.

A major increase of repair efficiency resulted from irradiation of *D. radiodurans* strains with polychromatic UV radiation of longer wavelength portions. UV-(>315 nm)-induced photoproducts where almost entirely removed from the genome of the designated UV-resistant class (R1 and mutant 262 (*uvrA-2*)), which is true for 1R1A (*recA*) as well, with the exception of the

6 − 4 PP lesions and CC CPD Figure 4.2.

However, Dewar valence isomers even if generated at low yields have been repaired less effectively by way of comparison. Moreover, the strains carrying a mutation in the ER-system, namely 262 (*uvrA-2*) and UVs78 (*uvrA-1 uvsE*), exhibit off-grade repair ability compared to the other *D. radiodurans* strains.

The prevalent result of the obtained photoproduct repair kinetics is the unexpected repair capability of UVs78 (*uvrA-1 uvsE*) at longer polychromatic UV-wavelengths culminating in roughly 70% remnant photoproducts at 2 h post-irradiation recovery (Table 4.4 and Figure 4.2).

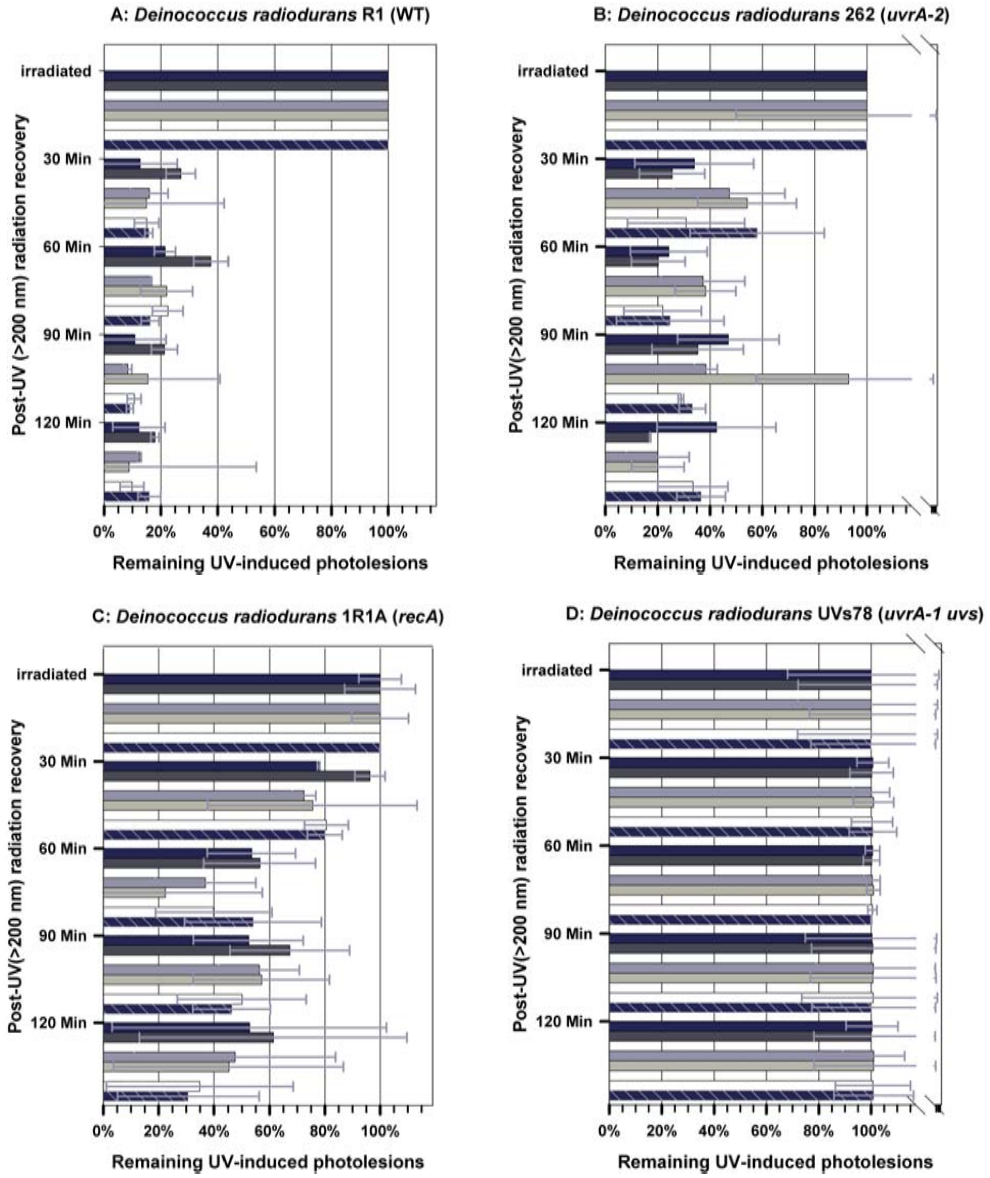

Fig. 4.2: UV-(>200 nm)-induced photoproduct repair kinetics. A: wild-type strain R1, B: UV-resistant mutant strain 262 (*uvrA-2*), C: HR-deficient strain 1R1A and D: UV-sensitive double mutant UVs78. Each data point represents the average standard deviation (error bar) of at least three independent experiments.

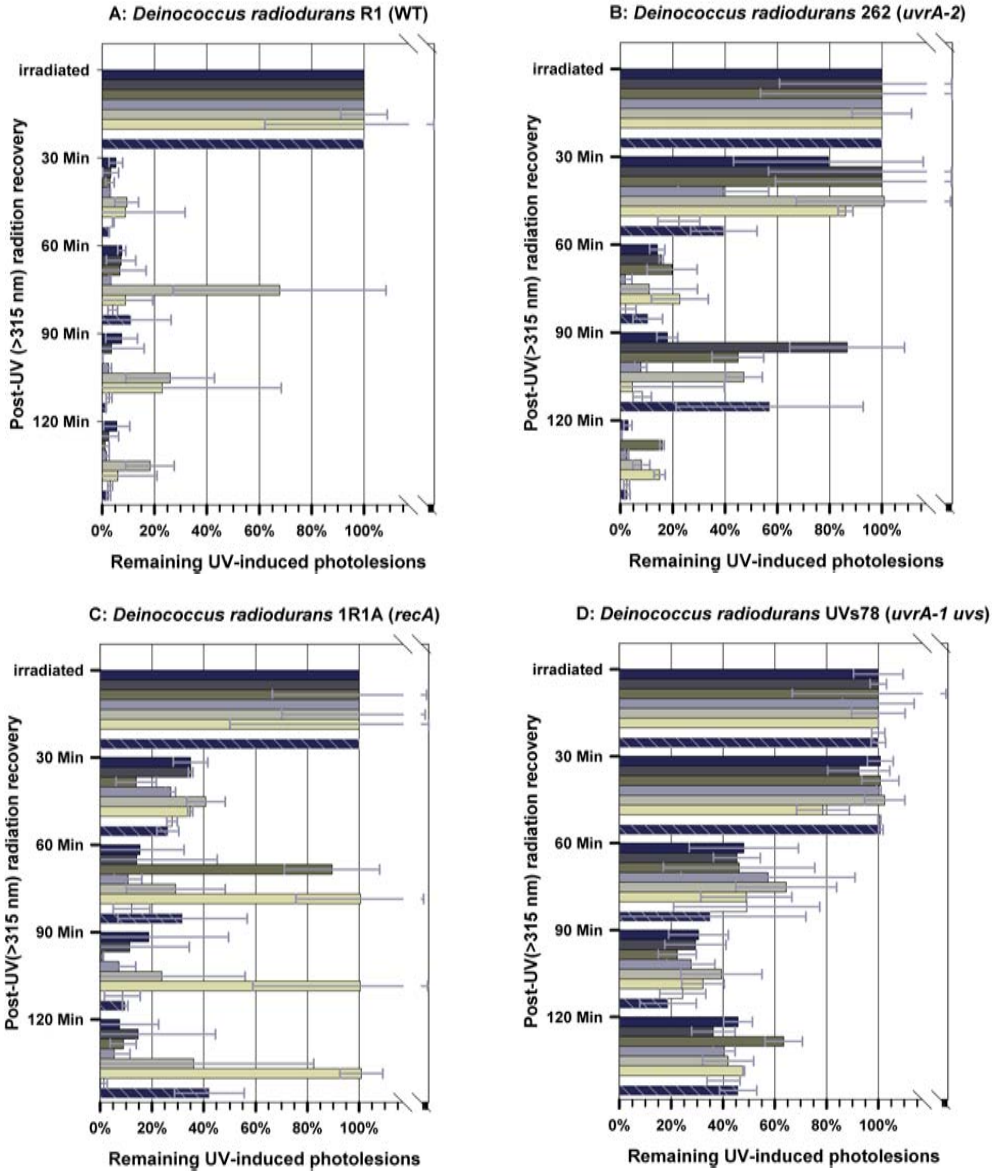

Fig. 4.3: UV-(>315 nm)-induced photoproduct repair kinetics. A: wild-type strain R1, B: UV-resistant mutant strain 262 (*uvrA-2*), C: HR-deficient strain 1R1A and D: UV-sensitive double mutant UVs78. Each data point represents the average standard deviation (error bar) of at least three independent experiments.

4.3 Discussion

The data of the post-0.5 h-irradiation repair rate of the UV-(>315 nm)-induced photolesions Table 4.4 of UVs78 (*uvrA-1 uvsE*) corroborate previous studies that observed a burst of genomic DNA degradation after exposure to a sublethal fluence of UV radiation [Moseley & Laser, 1965]. From the detailed photoproduct repair kinetics of UV-(>315 nm) irradiated UVs78 (*uvrA-1 uvsE*) cells, it can be derived that the DNA degradation takes place in the first hour post-UV-irradiation and subsequent repair reflected in recovery time point 2 h (Table 4.5 and Figure 4.2D).

This distinctive physiological change has only been observed in UVs78 (*uvrA-1 uvsE*). As confirmed by Earl [Earl et al., 2002b] the UV-sensitivity pattern of their created LSU1000 mutant resembles the sensitivity pattern of mutant UVs78 (*uvrA-1 uvsE*), leading to the genetic characteristics of eliminated excision repair (ER) by the UvrABC complex as well as the alternative ER-pathway via UV damage endonuclease β (UVDE, see chapter 1.3.2.2, p. 21). Further studies on UvrABC-deficient strains [Tanaka et al., 2005] provided evidence, that loss of the gene loci *uvrA-1, uvrA-2* or *uvsE* had a marginal effect on *D. radiodurans'* survival. In addition the repair kinetics of these mutants showed that deletion of UV damage endonuclease β resulted in a lower repair efficiency compared to the loss of UvrA-1. Taking into account the results of this study leads to a tentative assumption that rather UV endonuclease β than the gene product of UvrA-1 might be involved in the regulation of genomic DNA degradation and subsequent nucleotide export from the cell.

Tab. 4.5: Repair kinetics of the UV-sensitive mutant strain UVs78 (*uvrA-1 uvsE*).

>315nm	% remnant photoproducts		
Bipyrimidine dimer	Recovery time		
	30 min	60 min	120 min
TC CPD	≥100	57	28
TT CPD	≥100	48	31
CT CPD	≥100	49	24
CC CPD	≥100	35	19
TC 6 – 4	≥100	64	39
TT 6 – 4	92	45	29
TC Dewar	79	49	32
TT Dewar	≥100	46	22

Not only genetic equipment but also the applied wavelengths seem to influence *D. radiodurans'* repair efficiency, especially polychromatic UV radiation enables the UV-sensitive class to repair the UV-induced lesions and retain their vitality. As pointed out in previous chapters (chapter 1.3.2, p. 20 and chapter 3, p. 46) *D. radiodurans* belongs to a family with ancient derivation which might have existed on Archean Earth, an environment exhibiting higher DNA damaging irradiances. Consistently, the *Deinococcaceae* should be equipped with repair mechanisms to meet the lesions induced not only by these wavelengths (λ >200 nm) but also by those at present Earth (λ >295 nm). This may provide a possible explanatory approach for the observed increase in repair efficiency following polychromatic UV irradiation and suggests that the wavelength range $\lambda = 315 - 400$ nm activates a photosensitive gene or gene cluster that is involved in UV-induced damage repair.

On account of the efficient repair of CC CPD, the obtained results also provide evidence that HR pathway contributes to the phenomenon that *D. radiodurans* cells lack UV radiation-induced mutation. The characteristic UV-induced tandem mutation $CC \rightarrow TT$ results from the high mutagenic potential of CC photoproducts [Cadet et al., 2005]. Though 1R1A (*recA*) is able to repair this photolesion, its utmost repair rate never exceeds 70%.

Summarized, the photoproduct repair kinetics of the differing UV-susceptible *D. radiodurans* strains have provided first clues to the UV-repair process flow: The ER efficiently removes both CPDs and $6-4$ PPs. HR assists removal of CPD from UV-irradiated DNA, but plays a minor role in removal of $6-4$ adducts.

Though the ER is not existent in the ER-deficient mutant, up to 70% of both bipyrimidine photoproduct types were equally repaired post-UV (>315 nm)-irradiation. If the repair ability were due to the existent HR-pathway, a minimum repair of at least CPD should be measurable following UV-254 nm- and UV-(>200 nm)-radiation. Hence, an additional pathway must be available that allows repair of both photoproduct classes and its efficiency is noticeable if longer polychromatic UV-wavelengths are present.

5. WHOLE GENOME EXPRESSION ANALYSIS OF R1 AND UV-SENSITIVE MUTANT STRAINS FOLLOWING UVC RADIATION RECOVERY

Sunlight is a naturally occurring so-called exogenous source for DNA damage, whereas reactive oxygen species (ROS) formed during cellular metabolism are referred to as endogenous factor. The effect of such damages are reflected numerously as base loss, base dimerization, base alkylation, base deamination, and base oxidation but also as single- or double-strand breaks resulting in lasting modifications of the information encoded by the DNA. Moreover, replication and recombination may lead to alterations in base sequences as well. Hence, genome maintenance is given top priority to ensure that the information encoded by DNA remains largely unaltered. To ensure genome integrity numerous DNA repair mechanisms have evolved including direct damage repair, nucleotide excision repair, mismatch repair, base excision repair, and recombinational repair. Each system has specialized to repair certain types of lesions (cf. chapter 1.3.2.2, p. 21).

Studies investigating *D. radiodurans'* UV-resistance identified excision repair and recombinational repair systems as the major UV-induced DNA damage repair pathways [Minton, 1994]. However, having established the response and recovery profile of *D. radiodurans* R1 and of two UV-sensitive mutant strains to a broad UV-spectrum substantiated solely that the pathways are essential to mend short wavelength UV-induced lesions in *D. radiodurans*. The selected mutant strains show moderate UV repair capabilities following UV radiation of longer wavelength portions, notably the UV spectrum that is not absorbed by Earth's ozone column. Which is why the existence of a further bypass or alternative repair system has been hypothesized to be activated if either classical repair system is not available [Pogoda de la Vega et al., 2005].

The impetus for studying the repair-defective mutant strains 1R1A (*recA*) and UVs78 (*uvrA-1 uvsE*) (UV damage endonuclease-deficient) was to make use of their inherent loss of essential UV-related repair and stress response proteins for profiling their transcriptional response by applying DNA microarray technology. Especially the fact that both mutant strains exhibited

enhanced UV-sensitivity similar to designated radiation sensitive bacteria like *E. coli* (F_{37} values 21, 35 and 30 Jm^{-2} for UVs78, 1R1A and *E. coli*, respectively) was a decisive factor.

The microarray technique was utilized to examine the genome-wide effect of UV-(254 nm) radiation on wild-type and the two UV-sensitive and repair-deficient strains as a crucial component to understand the mechanism of this phenomenon. Monochromatic UV radiation, λ =254 nm, was chosen because this wavelength range induces direct damage and therefore, the repair mechanism of DNA photoproducts is not obscured by indirectly induced repair pathways. Especially longer UV-wavelength portions tend to induce indirect effects like oxidative damage, initiated by the formation of reactive oxygen species (ROS) leading amongst others to single- or double-strand breaks.

All genes are identified as described in the published genome sequence [White et al., 1999] available at The Institute for Genomic Research (TIGR). The gene designations are based on those used in TIGR Comprehensive Microbial Resource (CMR). The prefix represents the abbreviation of the organism (*D. radiodurans DR*) and loci are chronologically numbered, whereas *A* preceding the numeric characters denotes protein encoding genes (PEG) on chromosome II of *D. radiodurans*, *B* denotes PEG on the megaplasmid MP1, *C* denotes PEG on the plasmid CP1 and designations without a preceding letter are located on chromosome I. The primary annotation summary assigns *D. radiodurans* a total of 3246 genes, of which 91.18% represent 3187 PEG and up to now only 1696 genes have been assigned a role category (53.12%). But its genome still exhibits approximately 1000 hypothetical genes.

To determine the differential gene expression of the different UV susceptible strains a single fluence was selected proven to be able to generate sufficient biological impacts in the cell (chapter 2.5.2 and chapter 4). The DNA microarray chips have been commercially purchased from NimbleGen Systems (Madison, USA; Reykjavik, Iceland) and service has been provided by RZPD, German Resource Center for Genome Research (Berlin). Due to research budget constraints 10 microarray hybridizations were feasible. In total four biological replicates of the wild-type strain *D. radiodurans* R1 and three replicates of each UV-sensitive strain UVs78 (*uvrA-1 uvsE*) and 1R1A (*recA*) have been processed by RZPD (details cf. chapter 2.10.1, p. 44).

The aim of this microarray study was to make use of the differing UV-susceptibility and UV-damage repair capability of the investigated strains. Thus, to faciliate the selection of genes of interest by comparing the whole genome expression of the irradiated strains and to provide a qualitative tool to detect unidentified players of the UV damage repair system.

5.1 Differential UVC-induced gene expression of R1 and UV-sensitive strains

The microarray data analysis was performed with the software ArrayStar (Version 2.0.0, DNAstar Inc., Madison, Wisconsin, USA) and the applied statistics were selected as described in chapter 2.4.2 (p. 31). In accordance to the settings, the P value and the absolute fold change values were generated by the software. Throughout the analysis the fold change is the same as the ratio of the means of the normalized fluorescence intensities measured on the array (3187 open reading frames).

A first approach of sorting the gained microarray results determined the 50 highest signal intensities of each investigated strain. High signal intensities of protein encoding genes (PEG) where considered if an elevated signal was present in three out of four replicates in the case of R1, and in the case of the UV-sensitive mutant strains, an elevated signal in two out of three replicates was required. Following this, the 50 highest fluorescence signal intensities of each group of replicates per strain where aligned and had to be present either in wild-type strain and one mutant or in either mutant strain, which resulted in a total of 92 genes of interest. Of these solely 6 PEG show an elevated signal in all three investigated strains.

Cross comparison of the microarray data of irradiated wild-type strain R1 and irradiated UVs78 (*uvrA-1 uvsE*) resulted in calculated P values of 1.0, which point out that these genes cannot be statistically differentiated (visualized as scatter plot in Figure 5.1). Therefore, the focus was solely laid on the differentially expressed genes of 1R1A (*recA*) compared to wild-type strain. The applied fluence induced 2346 genes at 2-fold change, 1075 genes at 4-fold and 195 genes at 8-fold change in the case of the 1R1A (*recA*) mutant compared to wild-type strain R1.

Interpretation of the obtained microarray data were performed by utilizing two public archives providing gene annotations: Kyoto Encyclopedia of Genes and Genomes (KEGG) (Kyoto, Japan) and National Center for Biotechnology Information (NCBI) [Barrett et al., 2007] supported and maintained by the National Library of Medicine (NLM) and the National Institute of Health (NIH) (Bethesda, MD, USA). Moreover, KEGG provides metabolic pathway maps of sequenced genomes. Additionally the annotation/analysis tool SEED was used for comparative genome analysis. The SEED platform is provided and maintained by the Fellowship for Interpretation of Genomes (FIG) (University of Chicago, USA).

Specific databases on information on proteins are available too. For this microarray data analysis the catalog of the Integrated resource of protein

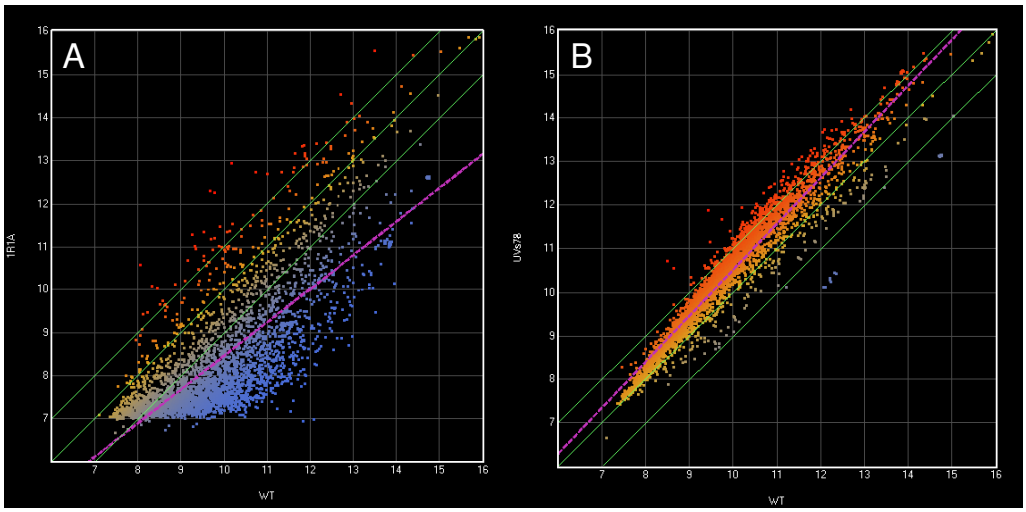

Fig. 5.1: Scatter plot of the UV-(254 nm) radiation-induced genes in R1 compared to the UV-sensitive strains UVs78 (*uvrA-1 uvsE*) and 1R1A (*recA*). The parameters were set in such a way, that R1 was chosen as control replica group and either mutant strains was defined as the experimental replica set. **A**: Scatter plot of the genes induced in 1R1A (*recA*) following treatment. **B**: Scatter plot of the genes induced in UVs78 (*uvrA-1 uvsE*) following treatment. Both axis show log_2-values. The threshold lines are colored green. The middle green line is the identity line, or the $x = y$ line. Data points on this line represent genes that are expressed at the same level in both datasets. The other two lines delineate genes with at least a two-fold change in intensity value in one of the datasets. The dashed purple line on the scatter plot is the linear regression or best-fit line, a line that passes as near to as many data points as possible.

families, domains and functional sites (InterPro) and UniProt (Universal Protein Resource) were deployed to derive the biological function of the selected PEG [Mulder et al., 2007]. UniProt is a central repository of protein sequence and function accessing information comprised in Swiss-Prot, TrEMBL, and PIR. It is maintained by the European Bioinformatics Institute (EBI, an outstation of European Molecular Biology Laboratory EMBL), Swiss Institute of Bioinformatics (Swiss-Prot) and Protein Information Resource (PIR), Georgetown University Medical Center, Washington, USA. The UniProt Knowledgebase (UniProtKB) is a public access point for extensive curated protein information, including function, classification, and cross-reference [Gasteiger et al., 2001].

5.1.1 92 genes of interest

The selected 92 genes with elevated signal intensities represent a broad spectrum of biological processes related to DNA damage repair, translation/transcription, protein fate, cell cycle, cell wall biogenesis and central intermediary metabolism. The prevalent group of these selected PEG is denoted as transposase, which have been generally classified as "other replication, recombination and repair proteins".

Transposases belong to the prokaryotic mobile genetic elements (MGE), which are central players in mobilizing genes, both in a given genome or between bacterial cells. Due to the fact that many chimerical elements have been identified recently that reveal strong similarities with elements of diverse families, the public database ACLAME (A CLAssification of Mobile genetic Elements) has been generated, which is dedicated to the collection, classification, organization and eventual correction of MGE from various sources (phage genomes, plasmids, transposons and other genomic islands) [Leplae et al., 2004]. This was utilized to classify the abundant class of transposases (transposases are listed in Table 5.3 including the assigned classification of the ACLAME database).

The classification of the functional modules of MGE at the protein, gene, and higher levels is generated in a semi-automatic way. At present, proteins annotated on complete phage and plasmid DNA sequences are automatically classified using the graph theory based Markov clustering algorithm MCL [van Dongen, 2000] to produce families.

Classification of the tranposase listed in Table 5.3 revealed mainly the affiliation to the IS[1]4-family, the so called RNAse H-clan. Members of this clan include enzymes involved in an Archaea-typical repair system suggested by [Makarova et al., 2002] on behalf of bioinformatic-based whole genome screening. Other enzyme members are amongst others integrase (role in the biological process of DNA integration), exonucleases X-T and $3' - 5'$ exonuclease, the latter two exhibit proofreading activity as determined for *E. coli* DNA polymerase I, which catalyses the hydrolysis of unpaired or mismatched nucleotides. The remaining group belongs to the IS630-family, which has rather been obtained via horizontal gene transfer and includes insertion sequences of *Synechocystis sp.* PC 6803 [Hickman et al., 2000].

[1] **I**nsertion **S**equence

Tab. 5.1: The cross comparison of the microarray data yielded 92 genes with elevated signal intensities. For the sake of completeness the corrected, normalized signal intensities are shown for all investigated strains. The input given to ArrayStar is based on the gene expression summaries of normalized data and have been produced using the RMA (Robust Multi-chip Average) algorithm [Grant et al., 2007]. The PEG have been sorted by their designated functional groups as derived from NCBI (cf. chapter 5.1). The prevalent group are the transposase comprising ca. 38%, followed by the group of hypothetical proteins representing ca. 23% and the PEG involved in DNA repair in the broadest sense add up to 11%.

		f-value	Signal intensity values			f-value
	Biological process	1R1A	WT	UVs78	1R1A	UVs78
Gene	DNA damage repair/stress response proteins (ca. 11%)					
*DR*0099	ssb, single-stranded DNA-binding protein	1.12	15.46	15.33	15.62	-1.09
*DR*0100	ssb, authentic frameshift	-1.02	15.85	15.74	15.82	-1.07
*DRA*0254	resolvase, putative	-8.18	13.42	14.50	10.39	2.11
*DR*1760	resolvase	-7.64	13.38	14.44	10.45	2.09
*DR*2128	DNA-directed RNA polymerase (rpoA), α-subunit [EC: 2.7.7.6]	1.85	13.16	12.71	14.05	-1.36
*DR*2415	DNA-binding response regulator	2.58	12.97	12.23	14.34	-1.68
*DR*1279	superoxide dismutase (sodA), Fe-Mn family [EC: 1.15.1.1]	-6.96	14.35	15.49	11.55	2.21
*DR*0326	hypothetical protein – ddrD§	1.68	12.83	12.42	13.58	-1.33
*DR*2340	recA protein	-1.10	13.02	12.43	12.88	-1.51
*DR*0070	hypothetical protein – ddrB§	1.04	13.49	12.90	13.55	-1.51
Gene	Transposase (ca. 38%)					
*DR*0255	putative transposase	-1.04	15.92	15.93	15.86	1.00
*DRC*0004	putative transposase	1.12	15.69	15.49	15.86	-1.14
*DRC*0029	putative transposas	-6.69	13.83	15.05	11.09	2.33
*DRB*0020	putative transposase	-6.85	13.84	15.05	11.06	2.32
*DR*2425	hypothetical; putative transposase	-5.63	14.41	15.37	11.91	1.95
*DR*1196	putative transposas	-6.83	13.87	15.08	11.10	2.31

Tab. 5.1b (continued): 92 genes of interest

		f-value	Signal intensity values			f-value
	Biological process	1R1A	WT	UVs78	1R1A	UVs78
Gene	Transposase (ca. 38%)					
*DRB*0055	transposase, pseudogene	-10.71	13.46	14.71	10.04	2.38
*DRB*0057	transposase, putative	-7.14	13.83	15.03	11.00	2.30
*DRB*0134	transposase, putative	-6.95	13.85	15.05	11.06	2.29
*DR*0144	transposase, putative	-7.02	13.87	15.09	11.06	2.32
*DRB*0102	transposase, putative	-7.15	13.85	15.04	11.01	2.29
*DRB*0005	transposase, putative	-6.70	13.86	15.06	11.12	2.29
*DRB*0117	transposase, putative	-6.85	13.89	15.08	11.12	2.28
*DRB*0120*m*	putative transposase	-5.56	14.36	15.33	11.89	1.95
*DRB*0056	putative transposase	-14.17	13.97	14.91	10.14	1.92
*DRC*0019	transposase-related	-3.27	12.68	14.21	10.97	2.88
*DRA*0253	putative transposase	-6.12	13.80	14.82	11.18	2.04
*DR*0010	putative transposase	-6.06	13.74	14.80	11.14	2.08
*DRB*0058	putative transposase	-6.08	13.75	14.83	11.14	2.12
*DRB*0113	putative transposase	-6.24	13.80	14.80	11.16	2.00
*DRB*0018	putative transposase	-6.07	13.80	14.79	11.19	2.00
*DRB*0103	putative transposase	-6.23	13.72	14.76	11.08	2.05
*DRB*0132	transposase, putative	-6.30	13.74	14.79	11.09	2.07
*DR*1762	putative transposase	-6.18	13.76	14.85	11.13	2.14
*DR*2324	transposase, putative	-4.38	14.76	13.16	12.63	-3.04
*DR*1593	transposase, putative	-4.40	14.75	13.15	12.62	-3.04
*DR*1933	transposase, putative	-4.54	14.77	13.14	12.59	-3.10
*DR*0978	transposase, putative	-4.45	14.75	13.15	12.60	-3.03
*DR*1651	transposase, putative	-4.30	14.74	13.17	12.63	-2.96
*DR*0666	transposase, putative	-4.25	14.70	13.15	12.61	-2.93
*DR*1381	transposase, putative	-4.37	14.72	13.13	12.60	-3.02
*DR*1618	transposase, putative	-5.80	13.58	14.43	11.04	1.81
*DR*0870	transposase, putative	-5.88	13.52	14.35	10.96	1.78
*DRB*0059	transposase, putative –*Sig1R*	-5.67	13.65	14.44	11.15	1.73
*DR*2222	transposase, putative	-5.71	13.52	14.35	11.01	1.78

Tab. 5.1c (continued): 92 genes of interest

		f-value	Signal intensity values			f-value
	Biological process	1R1A	WT	UVs78	1R1A	UVs78
Gene	Protein Fate (ca. 7.5%)					
*DR*1314	hypothetical, heat shock-protective gene –*Sig1R*	1.76	12.47	13.93	13.29	2.74
*DR*0227	hypothetical protein – ddrG§	2.19	11.61	12.53	12.74	1.90
*DR*1473	phage shock protein A (pap) –*Sig1R*	2.07	12.36	12.93	13.41	1.49
*DR*1459	serine protease, subtilase family	2.91	11.80	11.49	13.35	-1.24
*DR*1891	tetratricopeptide repeat family protein (binds nucleic acids)	2.68	11.33	11.65	12.75	1.25
*DR*0129	molecular chaperone DnaK –*Sig1R*	1.83	12.47	12.73	13.34	1.19
*DR*0907	cold shock protein (CspA)	3.54	12.71	14.01	14.53	2.46
Gene	Transcription and transcriptional regulators					
*DR*2574	transcriptional regulator, helix-turn-helix motif – ddrO§	2.41	12.14	12.18	13.41	1.03
*DR*0309	elongation factor (EF) TU, an endogenous promoter [EC: 3.6.5.3]	1.07	12.98	13.49	13.07	1.43
*DR*2050	EF-Tu [EC: 3.6.5.3]	1.08	13.00	13.50	13.11	1.41
*DRB*0109	ribonucleoside-diphosphate reductase (nrdF), β-chain [EC: 1.17.4.1]; purine/pyrimidine metabolism	-9.31	12.93	13.73	9.71	1.74
*DR*2123	translation initiation factor IF-1 (infA)	-1.27	14.02	14.65	13.67	1.56

Tab. 5.1d (continued): 92 genes of interest

		f-value	Signal intensity values			f-value
	Biological process	1R1A	WT	UVs78	1R1A	UVs78
Gene	Nucleotide transport and ABC transport membrane protein genes					
*DR*2588	iron complex ABC transport system substrate-binding protein; high Fe-ion affinity	1.49	13.33	14.13	13.90	1.74
Gene	Protein synthesis (6.5%)					
*DR*0098	30S ribosomal protein S6 (rpsF); small subunit	1.53	14.12	15.17	14.73	2.07
*DR*0101	30S ribosomal protein S18 (rpsR); small subunit	1.41	15.04	14.06	15.53	-1.97
*DR*1294	30S ribosomal protein S16 (rpsP); small subunit	2.05	12.86	13.34	13.89	1.40
*DR*2124	50S ribosomal protein L36; large subunit	-1.55	14.33	14.83	13.69	1.42
*DR*2005	50S ribosomal protein L35 (rpmI); large subunit	1.18	14.33	14.31	14.56	-1.01
*DR*0102	50S ribosomal protein L9 (rplI); large subunit	1.23	13.45	12.43	13.75	-2.03
Gene	Energy acquisition					
*DRC*0036	oxidative cyclase, putative (Fe-S oxidoreductase)	-3.49	13.00	14.04	11.19	2.05
Gene	Central intermediary metabolism					
*DR*1519	ketol-acid reductoisomerase (ilvC) [EC: 1.1.1.86]; valine/leucine synthesis	-4.16	14.36	13.99	12.31	-1.29

Tab. 5.1e (continued): 92 genes of interest

		f-value	Signal intensity values			f-value
	Biological process	1R1A	WT	UVs78	1R1A	UVs78
Gene	Outer structures (ca. 5%)					
*DR*2070	membrane lipoprotein (tmbC)	1.61	12.27	13.00	12.96	1.66
*DR*1115	S-layer-like array-related protein	6.92	10.17	10.18	12.96	1.01
*DR*2508	hexagonally packed intermediate-layer surface protein	-1.07	13.91	13.52	13.81	-1.31
*DR*0383	S-layer-like array-related protein	4.17	13.50	12.67	15.56	-1.77
*DR*1185	S-layer-like array-related protein –*Sig1R*	2.08	14.41	13.99	15.46	-1.34
Gene	Hypotheticals (ca. 23%)					
*DR*2344	hypothetical protein	-1.37	14.97	15.47	14.52	1.42
*DR*1697	hypothetical protein	-2.25	14.56	14.52	13.39	-1.03
*DR*1951	hypothetical protein	-11.51	12.93	13.94	9.41	2.02
*DR*0481	hypothetical protein	1.58	13.05	12.85	13.72	-1.15
*DR*1926	hypothetical protein	2.04	11.83	12.02	12.86	1.13
*DR*2489	hypothetical protein	5.57	9.79	9.87	12.26	1.06
*DR*1370	hypothetical protein	2.91	11.64	11.68	13.18	1.03
*DR*2441	hypothetical protein	1.14	13.95	14.31	14.13	1.29
*DR*0138	hypothetical protein	2.86	11.84	12.10	13.36	1.20
*DR*0025	hypothetical protein	4.04	10.72	11.09	12.74	1.29
*DR*1919	hypothetical protein	1.95	13.02	12.58	13.98	-1.36
*DR*0852	hypothetical protein	-2.45	11.38	11.94	10.09	1.47
*DRC*0039	hypothetical protein	-2.67	13.32	14.11	11.90	1.73
*DR*2559	hypothetical protein	-9.36	12.77	13.85	9.54	2.12
*DR*0661	hypothetical protein	-1.69	13.76	14.79	13.01	2.04
*DR*2180	hypothetical protein associated with GTPase	-3.59	13.88	14.69	12.04	1.75
*DRA*0278	hypothetical protein	-3.39	13.98	15.06	12.22	2.12
*DR*1197	hypothetical protein	-5.98	13.85	15.08	11.27	2.35
*DR*1715	hypothetical protein	1.71	12.15	11.82	12.92	-1.26
*DR*2414	hypothetical protein	-1.02	13.96	13.86	13.93	-1.08
*DR*0331	hypothetical protein	-5.03	14.11	14.81	11.78	1.62

WT – Wild-type strain R1; f-value – Calculated fold change value

Sig1R indicates that this PEG has been identified to belong to the Sig1-regulon [Schmid et al., 2005a] of sigma factor Sig1, outlined in detail in chapter 5.2.1 (p. 100)

§[Tanaka et al., 2004] – DNA damage response proteins (*ddr*)

Due to the fact that the ACLAME database cannot assign any function to the transposases *DR*2324 and *DR*1593 it can be assumed that these have been acquired as well via horizontal gene transfer, since the best hit identified the cyanobacteria *Nostoc sp.* PCC 7120 (former *Anabaena sp.*) with 52% similarity. Furthermore, it should be noted that comparing the sequences of these two deinococcal transposase are identical except in one amino acid (data not shown). Even comparative genomic analysis did not reveal a functional role of *DR*0255 and *DRC*0004, which were among the six PEG with elevated signal intensities in all strains, because neither PEG produced alignable regions in close genomes. Therefore this microarray analysis supported by function-determination with the ACLAME database could not determine whether the transposases are essential key players of or activate the UV-induced damage repair systems in *D. radiodurans*.

Tab. 5.2: The transposase assigned to the IS4-family by ACLAME show primarily homology to other deinococcal transposase but not to any other group of MGE. Therefore a detailed list of the E-values and the grade of homology is shown in the appendix D.1 (p. 148).

IS4-family		
*DR*0010	*DR*0144	*DR*1196
*DR*1618	*DR*1762	*DRA*0253
*DRB*0018	*DRB*0020	*DRB*0055
*DRB*0057	*DRB*0058	*DRB*0102
*DRB*0103	*DRB*0113	*DRB*0132
*DRB*0134	*DRC*0019	*DRC*0029

The abundance of IS4-family affiliated transposases prompted scrutinizing of the induced genes whether further members of the RNAse H-clan may be present and be related to the conserved core of the Archaea-typical repair system. The putative DNA repair system largely specific to thermophiles consists of a conserved core array of 5 genes: a predicted DNA helicase, a RecB family exonuclease and 3 uncharacterized genes, of which one might encode a nuclease of a novel family [Makarova et al., 2002]. A distinct feature of this core array determined that these five core genes are not only conserved but are often found in the same order in the majority of the investigated thermophiles. To a lesser extent, two additional genes could be detected in the gene neighborhood, which may facilitate the repair progress of this gene set but rather seem to be an optional expansion of the conserved core [Makarova et al., 2002].

In this respect, it is interesting to note that PEG $DR2180$ was among the 92 genes with elevated signal intensities, that has been obtained by *D. radiodurans* via gene exchange by thermophiles with the best homolog protein found in *Aquifex aeolicus* (NCBI gene identification number: 2984130) [Makarova et al., 2001]. Based on bioinformatics this uncharacterized family is conserved in bacteria and archaea, $DR2180$ (GTPase associated protein) and $DR2181$ (small GTPase of Ras/Rab[2] family), belong to the unusual predicted operons found in *D. radiodurans*. The orthologous GTPase in *Myxococcus sp.* suggests that this operon might play a role in cellular signalling.

Screening of the listed transposase did not reveal any core genes related to this thermophile-specific repair system, but rather other members of the RNAse H-clan affiliated to the helicase II-family could be detected ($DR1572$ and $DR2444$). Indeed genes in close neighborhood of the designated helicase II were induced as well. Comparative genomic analysis could not determine further functional homologs in the gene neighborhood of $DR1572$ that fulfill the above mentioned functional premises. In contrast the induced gene neighborhood of $DR2444$ revealed very promising core genes, but will be discussed in further detail in chapter 5.2.1 (p. 100) because this PEG is not among the 92 genes with elevated signals described here.

As mentioned previously, only six PEG showed an elevated signal intensity and overlapped in all three investigated strains, thus, destined to be major contributors to confer UV-resistance to *D. radiodurans*. Of these $DR0255$ and $DRC0004$ are denoted as transposase, whereas $DR2344$ and $DR1697$ have been annotated as hypothetical proteins. The remaining PEG encode the HR-involved single-strand-binding protein (SSB–$DR099$ and $DR0100$), which has two oligonucleotide/oligosaccharide-binding folds and functions as dimer [Bernstein et al., 2004, Witte et al., 2005, Eggington et al., 2006]. To determine solely PEG with a significant contribution to the UV damage repair system, genes encoding proteins involved in the central intermediary metabolism have been expelled and the remaining PEG have been further scrutinized by examining the gene loci in close proximity.

[2] The Ras superfamily of small GTPases are important regulators of cellular biology with roles in growth, survival, differentiation, etc. Members of this family are amongst others Rho and Rab.

Tab. 5.3: Transposase and their assigned classification to a distinct ACLAME family*. All the proteins encoded by a group of MGE (phages, plasmids, etc.) are compared between each other using the BLAST program provided by NCBI (chapter 5.1). The resulting list of sequence pairs is transformed into a scoring matrix with the E-value (expected value) as distance. The matrix is given as input to the MCL algorithm to produce a list of clustered proteins (clustering, cf. chapter 2.4.2).

Function unknown			
Aligne index	E-value	ID%	Organism
*DR*2324			
	1.e-107	52	*Nostoc sp.* PCC 7120
*DR*1593			
	1.e-107	52	*Nostoc sp.* PCC 7120
IS630-family			
Aligne index	E-value	ID%	Organism
*DR*0255			
214	1.e-56	63	*DRB*0120*m*
0	9.e-51	57	*Sinorhizobium meliloti* 1021
*DRC*0004			
77	2.e-15	57	*DRB*0120*m*
65	7.e-12	50	*DRB*0056
*DRB*0120*m*			
167	3.e-42	51	*DRB*0056
44	3.e-05	53	*Ralstonia solanacearum* GMI1000
*DR*2425			
77	1.e-14	57	*DRC*0004
*DRB*0056			
65	4.e-11	50	*DRC*0004

*An ACLAME family is defined as a set of similar sequences sharing one or more functions.

Tab. 5.4: List of the 31 PEG with elevated signal intensities. The gene expression summaries of the normalized data are listed as well (details cf. Table 5.1). The six genes with an elevated signal intensity that overlap in all three investigated *D. radiodurans* strains are marked PEG*.

		f-value	Signal intensity values			f-value
	Biological process	1R1A	WT	UVs78	1R1A	UVs78
Gene	DNA damage repair/stress response proteins (ca. 11%)					
*DR*0099*	ssb, single-stranded DNA-binding protein	1.12	15.46	15.33	15.62	-1.09
*DR*0100*	ssb, authentic frame-shift	-1.02	15.85	15.74	15.82	-1.07
*DRA*0254	resolvase, putative	-8.18	13.42	14.50	10.39	2.11
*DR*1760	resolvase	-7.64	13.38	14.44	10.45	2.09
*DR*2128	DNA-directed RNA polymerase (rpoA), α-subunit [EC: 2.7.7.6]	1.85	13.16	12.71	14.05	-1.36
*DR*2415	DNA-binding response regulator	2.58	12.97	12.23	14.34	-1.68
*DR*2340	recA protein	-1.10	13.02	12.43	12.88	-1.51
Gene	Transposase					
*DR*0255*	putative transposase	-1.04	15.92	15.93	15.86	1.00
*DRC*0004*	putative transposase	1.12	15.69	15.49	15.86	-1.14
*DRB*0134	transposase, putative	-6.95	13.85	15.05	11.06	2.29
*DRB*0005	transposase, putative	-6.70	13.86	15.06	11.12	2.29
*DRC*0019	transposase-related	-3.27	12.68	14.21	10.97	2.88
*DRA*0253	transposase, putative	-6.12	13.80	14.82	11.18	2.04
*DR*0010	transposase, putative	-6.06	13.74	14.80	11.14	2.08
*DRB*0103	transposase, putative	-6.23	13.72	14.76	11.08	2.05
*DRB*0132	transposase, putative	-6.30	13.74	14.79	11.09	2.07
*DR*1762	putative transposase	-6.18	13.76	14.85	11.13	2.14
*DR*2324	transposase, putative	-4.38	14.76	13.16	12.63	-3.04
*DR*1381	transposase, putative	-4.37	14.72	13.13	12.60	-3.02

Tab. 5.4b (continued): 31 putative genes linked to UV tolerance

		f-value	Signal intensity values			f-value
	Biological process	1R1A	WT	UVs78	1R1A	UVs78
Gene	Protein Fate					
*DR*1891	tetratricopeptide repeat family protein (binds nucleic acids)	2.68	11.33	11.65	12.75	1.25
Gene	Transcription and transcriptional regulators					
*DRB*0109	ribonucleoside-diphosphate reductase (nrdF), β-chain [EC: 1.17.4.1]; purine/pyrimidine metabolism	-9.31	12.93	13.73	9.71	1.74
Gene	Outer structures					
*DR*2508	hexagonally packed intermediate-layer surface protein	-1.07	13.91	13.52	13.81	-1.31
*DR*0383	S-layer-like array-related protein	4.17	13.50	12.67	15.56	-1.77
*DR*1185	S-layer-like array-related protein	2.08	14.41	13.99	15.46	-1.34
Gene	Hypotheticals					
*DR*2344*	hypothetical protein	-1.37	14.97	15.47	14.52	1.42
*DR*1697*	hypothetical protein	-2.25	14.56	14.52	13.39	-1.03
*DR*1951	hypothetical protein	-11.51	12.93	13.94	9.41	2.02
*DR*0481	hypothetical protein	1.58	13.05	12.85	13.72	-1.15
*DR*1919	hypothetical protein	1.95	13.02	12.58	13.98	-1.36
*DRC*0039	hypothetical protein	-2.67	13.32	14.11	11.90	1.73

Tab. 5.5: The decisive gene loci rendering the putative PEG linked to UV radiation tolerance as listed in Table 5.4. Here only the fold-change values of 1R1A (*recA*) compared to the wild-type strain R1 are listed.

Gene	Biological process DNA damage repair/stress response	f-value 1R1A
*DRC*0005	resolvase	-1.79
*DRC*0006	hypothetical protein (Mg-dependent DNAse)	-4.30
*DRC*0018	integrase/recombinase XerD, putative	-1.56
*DRB*0104	integrase/recombinase XerD, putative	-7.93
*DRB*0135	RNA helicase, putative	-5.19
*DRB*0136	ATP-dependent helicase HepA	-6.85
*DR*1184	MutT/nudix family protein (oxidative damage repair enzymes)	-1.62
*DR*1696	DNA mismatch repair protein MutL	-1.28
*DR*1916	DNA helicase RecG	-2.03
*DR*1921	exonuclease SbcD, putative	-6.94
*DR*1922	exonuclease SbcC (ATPase, DNA repair)	-2.62
*DR*1949	ribonuclease HII (RnhB), RNAse H clan	-1.79
*DR*2416	sensor histidine kinase	3.06
*DR*2418	DNA-binding response regulator	-1.86
*DR*2439	hypothetical protein (similar to *Bacillus subtilis* DinB family)	-1.14
*DR*2509	hypothetical protein (predicted endonuclease involved in recombination)	-3.10

Tab. 5.5b (continued): Gene neighbors of the putative 31 PEG

Gene	Biological process Protein Fate	f-value 1R1A
*DR*0382	gcp O-sialoglycoprotein endopeptidase, putative (possible chaperone activity)	6.16
*DR*0482	B-cell receptor associated protein-related protein (membrane protease)	1.43
*DR*2322	serine protease, subtilase family, C-terminal fragment	-4.22
*DRC*0020	Adenine-specific DNA methylase	-5.62
Regulatory proteins		
*DRA*0252	transcriptional regulator, MerR family	-2.14
*DRB*0110	thioredoxin-related response regulator	-6.06
*DR*1379	transcriptional repressor, TetR family (AcrR)	-5.72
*DR*1894	transcriptional regulator, AsnC family	-5.18
*DR*1761	hypothetical protein (transposase-like)	-4.41
Cell cycle control		
*DR*0013	chromosome partitioning ATPase Soj	-3.36
*DR*0480	hypothetical protein (predicted ATPase implicated in cell cycle control)	-1.13
*DRB*0001	chromosome partitioning ATPase, putative, ParA family	-9.95

This analysis resulted in 25 PEG to be further analyzed and adding up to 31 potential key players including the 6 overlapping PEG Table 5.4. The decisive gene loci in close proximity of the 31 potential key players are listed in Table 5.5. Notably all potential key players exhibit neighboring PEG linked to DNA damage repair.

5.2 Transcription profile of 1R1A *(recA)*

UV-(254 nm) radiation induced a vast majority of PEG, therefore a first approach was aimed at reducing the induced genes by applying a selective cut-off at 10-fold change. 81 genes fulfilled this threshold and were further examined. Corroborating that *recA* is a key protein contributing to *D. radiodurans'* exceptional radiation resistance [Daly et al., 1994, Sheng et al., 2005, Zimmerman & Battista, 2005], but the most highly induced genes in 1R1A (*recA*) were entirely down regulated. In general those genes repressed in

1R1A (*recA*) are up regulated in UVs78 (*uvrA-1 uvsE*), with the exception of six PEG. Of these overlapping repressed genes, two are denoted as hypothetical proteins, two belong to the general ABC transport systems, one PEG is related to eukaryotic diacylglycerol kinase (cellular signal transduction) and one PEG is a guanine-nucleotide binding protein predicted to regulate modules in processing and cytoskeleton assembly (marked with an asterisk in Table 5.6).

The overlapping repressed genes were further scrutinized by comparative genomic analysis. $DR1560, DR1429$ and $DR2061$ showed no alignable regions in close genomes, but these three PEG show interesting genes in close proximity: $DR1558$ – a DNA binding response regulator; $DR2063$ – Polyribonucleotide nucleotidyltransferase (EC[3] 2.7.7.8 involved in purine and pyrimidine metabolism) and $DR1431$ – Phosphoribosylamine-glycine ligase (EC 6.3.4.13 involved in purine metabolism).

As indicated in Table 5.6 all members of the predicted unusual operon, designated Pilin IV cluster, were highly induced in 1R1A (*recA*) with the exception of $DR1235$, a dynamin-like GTPase, which is only repressed 4-fold. The Pilin IV cluster includes a GTPase assigning this operon a possible regulatory role, probably responsible for DNA transformation [Makarova et al., 2001].

In *E. coli* the rate of DNA synthesis could be correlated to replication-arresting lesion removal when the cells were irradiated with a moderate fluence of 254 nm-UV radiation. One efficient mechanism identified in *E. coli* to remove UV-254 nm-induced lesions that lead to an arrest of replication is the RecF pathway (Figure 1.2 in chapter 1.3.1.2, p. 24).

Absence of any RecF pathway-associated protein results in gaps that persist in the synthesized DNA and in degradation of nascent DNA at the replication fork [Courcelle et al., 2005]. This has been confirmed by the delayed post-irradiation repair kinetics of 1R1A (*recA*) obtained in this study (chapter 4). Furthermore, the remaining components of the RecF-mediated pathway are repressed as well Table 5.7, though to a lesser extent than expected, an exemplary disclosure of RecA's co-protease activity in distinct pathways.

[3] **E**nzyme **C**ommission Numbers (EC #) are made up of four numbers separated by periods. The first number represents the Main Function of the enzyme, the second number represents the Sub One Function, the third number is the Sub Two Function and the third number is the Sub Three Function. http://rice.tigr.org/tigr-scripts/CMR2/ECSearch.spl

Tab. 5.6: The table comprises PEG exhibiting a fold-change of $\geq$ 10. For comparison the calculated fold-values of UVs78 (*uvrA-1 uvsE*) are listed in a separate column. In total this list is predominated by PEG designated as hypothetical proteins, mainly with unknown function (54%) and the second main functional group comprise PEG related to nucleotide transport and ABC transport membrane proteins (11%).

Gene	Biological process DNA damage repair/stress response proteins	f-value 1R1A	f-value UVs78
*DRA*0181	GGDEF family protein	-29.41	2.61
*DR*1572	helicase-related protein uvrD	-10.93	1.70
*DRB*0067	extracellular nuclease, putative; involved in intracellular signaling	-10.18	2.23
*DR*0798	putative Gcn5-related acetyltransferases (GNATs) involved in in transcription and DNA repair	-10.02	1.88
Nucleotide transport and ABC transport membrane protein genes (ca. 11%)			
*DRA*0176	xanthine permease, putative	-34.24	3.17
*DRB*0119	Na+/H+ antiporter, putative	-12.91	2.02
*DR*2121	branched-chain amino acid ABC transporter, permease protein	-12.28	1.10
*DR*1569	peptide ABC transporter, permease protein	-12.03	1.05
*DR*2053	phosphate transport system regulatory protein PhoU, putative	-11.80	1.80
*DR*2120*	branched-chain amino acid ABC transporter, permease protein	-11.48	-1.16
*DRA*0210	ABC transporter, periplasmic peptide-binding protein	-10.94	2.01
*DR*1570*	peptide ABC transporter, permease protein	-10.28	-1.12
*DR*2395	Na+/H+ antiporter, putative; integral to membrane	-10.17	1.63

Tab. 5.6b (continued): Genes with a fold-change $\geq$ 10

Gene	Biological process Protein Fate	f-value 1R1A	f-value UVs78
*DRA*0206	oligoendopeptidase F, putative; proteolysis	-16.09	2.14
*DR*2484	trp repressor binding protein WrbA, putative (oxidoreductase activity)	-14.73	1.13
*DRA*0214	trp repressor binding protein WrbA, putative	-11.03	1.76
*DR*0717	leucyl aminopeptidase, putative; proteolysis	-10.40	2.27
*DR*1725*	WD-repeat family protein, regulates modules in processing and cytoskeleton assembly	-10.20	-1.05
Central intermediary metabolism			
*DR*0963	N-acetyl-γ-glutamyl-phosphate reductase; arginine synthesis	-14.11	1.68
*DRB*0079	N-acylamino acid racemase	-13.45	1.65
*DR*1742	glucose-6-phosphate isomerase	-11.78	1.52
*DRB*0033	arylesterase/monoxygenase; inorganic ion transport	-11.36	1.97
*DR*1637	4-α-glucanotransferase	-10.18	2.05
*DRB*0101	amine oxidase-related protein	-10.18	2.19
Cellular process and signaling			
*DR*1232	pilin, type IV, putative§	-15.22	1.56
*DR*1233	pilin, type IV, putative§	-11.25	1.49
*DR*1361	endopeptidase-related protein; cell wall biogenesis	-10.99	1.46
*DR*1560*	Sphingosine kinase and enzymes related to eukaryotic diaclglycerol kinase (contain regulatory domains)	-18.20	-1.05

Tab. 5.6c (continued): Genes with a fold-change ≥ 10

Gene	Biological process Energy acquisition	f-value 1R1A	f-value UVs78
*DR*1506	NADH dehydrogenase I, A subunit	-11.08	2.45
*DR*1493	NADH dehydrogenase I, M subunit	-12.20	1.39
	Translation		
*DR*1759	tRNA (5-methylaminomethyl-2-thio-uridylate)-methyltransferase; tRNA modification	-10.21	1.93
	Transcription and transcriptional regulators		
*DRA*0204	response regulator	-20.71	2.10
	Transposase (6%)		
*DR*1523	putative transposase	-18.44	1.77
*DRB*0056	putative transposase	-14.17	1.92
*DRB*0019.1	transposase	-12.74	2.59
*DRB*0019.2	transposase	-16.45	2.81
*DRB*0055	transposase, pseudogene	-10.71	2.38
	Hypotheticals (54%)		
*DR*0539	hypothetical protein	-11.40	1.95
*DR*0545	hypothetical protein	-11.34	1.63
*DR*0839	hypothetical protein	-11.71	1.08
*DR*0841	hypothetical protein	-10.17	1.12
*DR*0923	hypothetical protein	-14.75	1.41
*DR*0955	hypothetical protein	-10.34	2.04
*DR*0996	hypothetical protein	-16.98	1.69
*DR*1044	hypothetical protein	-10.69	1.79
*DR*1186	hypothetical protein	-13.46	2.08
*DR*1231	hypothetical protein	-13.04	1.65
*DR*1234	hypothetical protein – bioinformatic-based affiliation to Pilin IV cluster§	-11.46	1.16
*DR*1280	hypothetical protein	-10.51	1.73
*DR*1297	hypothetical protein	-10.29	1.59
*DR*1429*	hypothetical protein	-10.44	-1.11
*DR*1441	hypothetical protein	-10.67	1.98

Tab. 5.6d (continued): Genes with a fold-change ≥ 10

Gene	Biological process Hypotheticals (54%)	f-value 1R1A	f-value UVs78
*DR*1533	hypothetical protein	-10.75	1.52
*DR*1591	hypothetical protein	-14.86	2.05
*DR*1603	hypothetical protein	-10.04	1.67
*DR*1636	hypothetical protein	-10.10	2.36
*DR*1653	hypothetical protein	-11.26	1.56
*DR*1686	hypothetical protein	-10.57	1.48
*DR*1722	hypothetical protein	-13.02	2.58
*DR*1726	hypothetical protein	-16.76	1.42
*DR*1774	hypothetical protein	-11.60	1.88
*DR*1951	hypothetical protein	-11.51	2.02
*DR*1956	hypothetical protein	-16.77	2.38
*DR*2037	hypothetical protein	-10.47	2.37
*DR*2038	hypothetical protein	-11.74	2.27
*DR*2061*	hypothetical protein	-10.33	-1.74
*DR*2456	hypothetical protein	-12.04	1.69
*DRA*0090	hypothetical protein	-11.58	2.93
*DRA*0095	hypothetical protein	-10.68	2.74
*DRA*0119.1	hypothetical protein	-10.61	2.44
*DRA*0189	hypothetical protein	-11.41	1.75
*DRB*0004	hypothetical protein	-10.51	2.14
*DRB*0032	hypothetical protein	-10.04	1.92
*DRB*0035	hypothetical protein	-13.02	1.83
*DRB*0051	hypothetical protein	-11.36	2.08
*DRB*0068	hypothetical protein	-11.06	2.10
*DRB*0084	hypothetical protein	-11.98	2.67
*DRB*0085	hypothetical protein	-11.00	2.28
*DRB*0127	hypothetical protein	-14.28	1.76
*DRB*0131	hypothetical protein	-13.89	2.04
*DRB*0145	hypothetical protein	-10.32	1.95

*PEG, which are down regulated in both UV-sensitive *D. radiodurans* mutant strains

§[Makarova et al., 2001] – Predicted unusual operon Pilin IV cluster comprising *DR*1232 to *DR*1235

Sheng and coworkers (2005) provided evidence that *recX*, designated *DR*1310, down regulates the transcription of *recA* and reported that *recX* was required for an elevated expression level of RecA. Moreover, Sheng and coworkers (2005) determined that RecX is involved in antioxidant mechanism of *D. radiodurans* and had a negative effect on the transcription of catalase (*DRA*0146) and superoxide dismutase (*DR*1279), that along with RecA are involved in the SOS reaction caused by irradiation. But they were unable to state whether RecX exerts its repressor activity directly on the SOS process or if it is an indirect result of its negative regulation of RecA activity. The microarray data obtained in this dissertation, showed a 4-fold repression of *recX* in a $\Delta recA$[4] background. Hence, RecA can be regarded as trigger protein for RecX' regulation activity.

Tab. 5.7: The components of the RecF-pathway as outlined in the model of [Lee et al., 2004]. In *E. coli* the RecF-mediated pathway is primarily required to repair fork-arresting lesions, which block DNA polymerases [Courcelle et al., 2005]. Listed are the fold-change values of 1R1A (*recA*).

Gene name		f-value 1R1A
*DR*0198	recombinase R (RecR)	1.50
*DR*1089	RecF	1.25
*DR*1289	RecQ (processing of dsbs)	1.08
*DR*1126	RecJ (processing of dsbs)	1.08
*DR*0819	RecO (strand-annealing enzyme)	-1.35
*DR*2340	RecA	-1.51

It was expected to find some novel key players among these highly repressed genes in 1R1A (*recA*), that have been identified in recent studies.

Although Earl postulated in her dissertation [Earl, 2003] that the gene product of *DR*0167, designated *irrE* by [Earl et al., 2002a] and [Jolivet et al., 2006], but *pprI* by [Gao et al., 2006], plays a critical role in *D. radiodurans'* ability to survive UV irradiation, the analyzed microarray data of either strain in this study showed no significant induction fold of this PEG.

[4] The greek letter Δ is commonly used to express the deleted loci in a mutant.

Tab. 5.8: The fold-change values solely of 1R1A (*recA*) compared to wild-type strain R1 are opposed to the literature data obtained by [Earl, 2003]. Of these overlapping PEG, nine have already been listed in Table 5.1 and are highlighted with an asterisk in this table.

Gene	Biological process Transposase	f-value 1R1A	†Earl 0.5 h	†Earl 1 h
⋆*DRC*0004*	putative transposase	1.12	4.00	3.00
⋆*DR*0255*	putative transposase	-1.04	3.00	
*DRB*0018*	putative transposase	-6.07	3.00	
Energy acquisition				
*DRB*0109	ribonucleotide-diphosphate reductase, β-subunit	-9.31		4.00
Protein synthesis				
*DR*0101*	30S ribosomal protein S18 (rpsR); small subunit	1.41		4.00
*DR*0102*	50S ribosomal protein L9 (rplI); large subunit	1.23		4.00
*DR*1309	ribosomal protein S20	1.18	4.00	
*DR*0755	50S ribosomal protein L19	1.14		4.00
*DR*0309*	elongation factor EF-TU	1.07		4.00
Protein Fate				
*DR*0349	ATP-dependent protease LA	1.67		4.00
ABC Transport proteins				
*DRB*0121	iron transporter, ATP-binding	-4.51		3.00
*DRB*0125	iron transporter, periplasmic substrate-binding	-4.01		3.00
Outer structure proteins				
*DR*0383	S-layer-like array-related	4.17		4.00
*DR*1185	S-layer-like array-related	2.08		6.00
Hypotheticals				
*DR*1954	hypothetical protein	-6.86		4.00
*DR*2003	hypothetical protein	-5.73		4.00
*DRC*0024	hypothetical protein	-4.57		4.00

⋆PEG denote the genes induced in all three investigated strains as inferred from their signal intensity (cf. chapter 5.1, p. 78)

†Earl 0.5 h and 1 h are related to the recovery time points, that were analyzed for the recovery profile (data derived from [Earl, 2003]).

Still, comparison of the highly expressed genes following ionizing radiation [Earl, 2003] revealed 17 genes that overlap in $\Delta irrE$ and UVC irradiated 1R1A (*recA*) microarray data analyses, the overlapping gene loci are listed in Table 5.8.

To assign these 17 genes some kind of a role in radiation-induced damage repair would be a preterm jump to conclusion. Because they have been mainly denoted hypothetical proteins with unknown function, are involved in protein synthesis, in protein fate, cell membrane biogenesis or belong to the transposases. Interestingly, the two transposase that have been induced in all three investigated strains ($DR0255$ and $DRC0004$, Table 5.1) are among the overlapping PEG listed in Table 5.8. Therefore, further corroborating their potential relevance in response to radiation-induced damage.

5.2.1 Top-induced genes in 1R1A

As pointed out previously, the most highly expressed genes induced following UVC-irradiation are rather down regulated. Still about 200 PEG are up regulated in 1R1A (*recA*), which are listed in Table 5.9. Due to the high threshold-value set as starting condition, these PEG were not included before.

$DR1200$ and $DR1891$ rank among the most highly up regulated genes in 1R1A (*recA*), being promising candidates that may trigger the proposed bypass repair system. Both belong to the tetratricopeptide repeats (TPR) and have been assigned to play a role in signal processes in *D. radiodurans* [Makarova et al., 2001], which has been inferred from their documented mediation of protein-protein interaction within molecular complexes in eukaryotic systems. Both PEG possess a TPR-like helical domain as the response regulator aspartate phosphatase protein RapA. Rap proteins comprise a group of sequence-related proteins that regulate protein activity either by specifically binding to regulatory proteins or by acting as peptide phosphatase that target the phosphorylated forms of response regulators of two-component phosphorelay systems [Budde et al., 2006]. Phosphotransfer-mediated signaling pathways allow cells to sense and respond to environmental stimuli. Autophosphorylating histidine protein kinases provide phosphoryl groups for response regulator proteins which, in turn, function as molecular switches that control diverse effector activities [West & Stock, 2001].

According to [Makarova et al., 2001] the best analog of the hypothetical protein $DRA0334$ was found in *Mycobacterium tuberculosis* (NCBI gene identification number: 1552573). The hypothetical protein, designated $DRA0334$, belongs to the predicted unusual operon of serine/threonine protein kinase based regulatory system that may have been acquired by *D. radiodurans* through horizontal gene transfer [Makarova et al., 2001]. Components encoded by this operon $DRA0331 - DRA0335$ are proteins involved in the kinase-dependent regulatory pathway, but except for $DRA0334$ the other operon members have been down regulated and exhibit 5–3-fold values.

Though not among the highly up regulated genes, $DR2444$ encoding a helicase of the HRDC[5]-family has been further investigated and comparative genomic analysis was performed, because $DR2444$ has been assigned a member of the RNAse H-clan but also many genes in close proximity are up regulated as well. Particularly, the concomitance of endonuclease III, designated $DR2438$, and a homolog of Din[6]B of *Bacillus subtilis* [Thompson et al., 2006] $DR2439$ in the gene neighborhood of $DR2444$ suggested that an ortholog of the thermophile-specific repair system may exist [Makarova et al., 2002]. Furthermore, the hypothetical protein $DR2441$ holds similarity to Gcn5-related acetyltransferases (GNAT), which are involved in transcription and DNA repair. Since no gene ortholog could be determined for $DR2445, DR2446$ and $DR2450$, it is assumed that they may be part of this putative repair core.

$DR2448 - DR2452$ can be ruled out to be involved in this putative repair core, because comparative genomic analysis revealed that the designated hypothetical proteins $DR2448, DR2449$ and $DR2451, DR2452$ are rather gene orthologs of the copper homeostasis regulation operon in *Deinococcus geothermalis* DSM11300 and *Thermus thermophilus* HB27.

It is interesting to note that many of the up regulated genes (cf. Table 5.9) have been either assigned to belong to the heat shock regulon of the ECF (extracytoplasmatic funcion) subfamily member Sig1 ($DR0180$) or are directly regulated by the negative regulator HspR ($DR0934$) via binding directly to a 7 bp inverted repeat HAIR sequence (HAIR, HspR-associated inverted repeat), [Schmid et al., 2005a] and [Schmid et al., 2005b].

[5] Helicase and RNAse D C-terminal (HRDC), see chapter 1.3.1.2 (p. 16).
[6] **D**NA damage-**in**ducible gene

Tab. 5.9: The **up** regulated genes in 1R1A (*recA*) were grouped according to their assigned biological function in the cellular organism.

Gene	Biological process DNA damage repair/stress response proteins	Gene name	f-value 1R1A
*DR*2415	DNA-binding response regulator		2.58
*DR*2220	tellurium resistance protein, putative	TerB	2.02
*DR*0335	ATP-dependent RNA helicase, putative		2.02
*DR*2128	DNA-directed RNA polymerase, α-subunit	RpoA	1.85
*DR*0326	hypothetical protein	DdrD	1.68
*DR*0423	hypothetical protein; DNA single strand annealing	DdrA	1.47
*DR*2339	$2' - 5'$ RNA ligase, putative; representative of LigT protein family		1.32
*DR*1262	ribonucleoprotein Ro-related protein	Rsr	1.31
*DRA*0346	DNA damage repair protein	PprA	1.21
*DR*0099	single-stranded DNA-binding protein		1.12
*DR*2444	putative HRDC family-recQ (Helicase), nucleic acid-binding protein		1.05
*DR*2438	endonuclease III	Nth-2	1.05
*DR*0070	hypothetical protein	DdrB	1.04
*DR*1998	catalase (antioxidant enzyme)	KatA	1.01
Outer structure proteins			
*DR*1115	S-layer-like array-related		6.92
*DR*0382	O-sialoglycoprotein endopeptidase, putative		6.16
*DR*0383	S-layer-like array-related		4.17
*DR*1185	S-layer-like array-related –*Sig1R*		2.08
*DR*2096	endopeptidase IV-related protein		1.90
*DR*2070	membrane lipoprotein		1.61
*DR*1124	SLH (S-layer homology domain) family protein		1.21
*DR*0379	outer membrane protein		1.17
*DR*1369	minicell-associated protein	DivIVA	1.03

Tab. 5.9b (continued): Up regulated PEG in 1R1A

Gene	Biological process Protein Fate	Gene name	f-value 1R1A
*DR*0492	hypothetical protein –*Sig1R*		5.79
*DR*0907	cold shock protein, CSD family		3.54
*DR*1459	serine protease, subtilase family		2.91
*DR*1815	hypothetical protein –*Sig1R*		2.71
*DR*0128	heat shock protein –*Sig1R*	GrpE	2.44
*DR*0607	heat shock protein –*Sig1R*	GroEL	2.35
*DR*2572	hypothetical protein –*Sig1R*		2.20
*DR*0227	hypothetical protein –*Sig1R*		2.19
*DR*1937	serine protease –*Sig1R*		2.23
*DR*1473	phage shock protein A –*Sig1R*		2.07
*DR*0972	hypothetical protein –*Sig1R*		1.86
*DR*0129	chaperone protein dnaK –*Sig1R*	DnaK	1.83
*DR*1314	hypothetical protein –*Sig1R*		1.76
*DR*0127	hypothetical protein –*Sig1R*		1.70
*DR*0349	ATP-dependent protease –*HspR*	Lon2	1.67
*DR*0482	putative suppressor gene; B-cell receptor associated protein		1.43
*DR*1974	ATP-dependent protease	Lon1	1.25
*DRA*0290	cell division protein FtsH –*HspR*	FtsH-3	1.18
*DR*0606	chaperonin –*Sig1R*	GroES	1.16
Two-component phosphorelay system			
*DR*2416	sensor histidine kinase		3.06
*DR*1891	tetratricopeptide repeat family protein; binds nucleic acids		2.68
*DRB*0091	response regulator		2.11
*DR*2327	response regulator		1.95
*DR*0892	sensor histidine kinase		1.82

Sig1R – PEG that have been assigned to be part of the sigma factor Sig1 (*DR*0180) heat shock regulon [Schmid et al., 2005a].

HspR – The transcription of these PEG are directly regulated by HspR (*DR*0934), a negative regulator of heat shock genes [Schmid et al., 2005b].

Tab. 5.9c (continued): Up regulated PEG in 1R1A

Gene	Biological process Signaling process (general)	Gene name	f-value 1R1A
*DR*0139	GTP-binding protein HflX		1.90
*DR*2518	serine/threonine protein kinase, putative		1.59
*DR*1814	hypothetical, predicted phosphodiesterase of LigT protein family		1.27
*DRA*0334	hypothetical inactive kinase (phosphoprotein phosphatase)		1.21
*DR*2161	protein-tyrosine phosphatase-related protein		1.05
Protein Synthesis			
*DR*2109	ribosomal protein S14	RpsN	2.50
*DR*0318	50S ribosomal protein L16		2.37
*DR*2115	ribosomal protein L15	RplO	2.31
*DR*2110	ribosomal protein S8	RpsH	2.20
*DR*0312	50S ribosomal protein L4	RplD	2.20
*DR*1294	ribosomal protein S16		2.05
*DR*0311	ribosomal protein L3	RplC	2.02
*DR*2114	ribosomal protein L30	RpmD	1.61
*DR*0098	ribosomal protein S6		1.53
*DR*0319	ribosomal protein L29	RpmC	1.52
*DR*2111	50S ribosomal protein L6	RplF	1.48
*DR*0101	ribosomal protein S18		1.41
*DR*0086	ribosomal protein L21	RplU	1.40
*DR*0341	ribosomal protein S15	RpsO	1.24
*DR*0102	ribosomal protein L9		1.23
*DR*0313	ribosomal protein L23		1.18
*DR*1309	ribosomal protein S20	RpsT	1.18
*DR*2005	ribosomal protein L35		1.18
*DR*0755	50S ribosomal protein L19	RplS	1.14
*DR*0175	ribosomal protein S9	RpsI	1.13
*DR*0306	30S ribosomal protein S7	RpsG	1.12
*DR*2050	elongation factor TU	EF-Tu	1.08
*DR*1983	ribosomal protein S1, putative		1.08
*DR*0309	elongation factor TU	EF-Tu	1.07
*DR*0317	ribosomal protein S3	RpsC	1.02
*DR*2129	ribosomal protein L17	RplQ	1.02

Tab. 5.9d (continued): Up regulated PEG in 1R1A

Gene	Biological process Transcription and transcriptional regulators	Gene name	f-value 1R1A
*DR*2574	transcriptional regulator, HTH_3 family		2.41
*DR*1918	aminoglycoside acetyltransferase; information storage/processing		1.65
*DRC*0012	transcriptional regulator, GerE family		1.59
*DR*2168	rRNA small subunit methyltransferase B [EC 2.1.1.-]; tRNA modification		1.51
*DR*0997	transcriptional regulator, FNR/CRP family		1.44
*DR*2148	transcriptional regulator, TetR family		1.41
*DR*2448	transcriptional regulator, MerR family		1.24
*DR*2357	phenylalanyl-tRNA synthetase, β-subunit	PheT	1.19
*DR*0834	nitrogen regulator, putative		1.07
*DR*2539	Fe-dependent repressor, putative		1.05
*DR*0026	methyltransferase, putative		1.03
Nucleotide transport and ABC transport membrane proteins			
*DR*0788	putative branched-chain amino acid transporter, periplasmic binding protein		2.36
*DR*0986	extracellular solute binding protein, family 5; dipeptide transport		1.52
*DR*2588	putative Fe-transporter, periplasmic substrate-binding protein		1.49
*DR*2589	putative Fe-transporter, permease protein		1.40
*DR*2590	Fe-transporter, ATP-binding protein		1.21
*DR*1188	permease, putative		1.01
*DR*2413	chromate transport protein		1.01

Tab. 5.9e (continued): Up regulated PEG in 1R1A

Gene	Biological process Metabolism/Energy acquisition	Gene name	f-value 1R1A
*DR*2594	magnesium protoporphyrin chelatase, putative		2.11
*DR*1968	nitroreductase		2.00
*DR*0970	electron transfer flavoprotein, α-subunit		1.98
*DR*0112	glutamine cyclotransferase		1.86
*DR*0944	thioredoxin	TrxA	1.69
*DR*2442	N-acetylglutamate kinase; arginine biosynthesis	ArgB-1	1.21
*DR*2406	comA protein; aromatic compounds catabolism	ComA	1.16
*DR*1812	aminomethyltransferase, putative		1.14
*DR*1467	short chain dehydrogenase		1.12
*DR*2626	carboxylesterase, type B		1.12
*DR*2364	L-lactate dehydrogenase	Ldh	1.11
*DR*0215	aminotransferase, class V		1.08
*DR*0377	L-serine dehydratase, α-subunit		1.06
*DRA*0037	glycosyltransferase		1.05
*DR*0623	aspartate aminotransferase	AspC	1.04
Riboflavin metabolism			
*DRA*0243	flavohemoprotein		1.83
*DR*0153	Diaminohydroxyphosphoribosylaminopyrimidine deaminase [EC: 3.5.4.26] / 5-amino-6-(5-phosphoribosylamino) uracil reductase [EC: 1.1.1.193]	RibD	1.42
*DR*0156	6,7-dimethyl-8-ribityllumazine synthase [EC: 2.5.1.9] (riboflavin synthase, β-subunit)	RibH	1.22
*DR*0154	riboflavin synthase, α-subunit [EC: 2.5.1.9]	ribE	1.09

Tab. 5.9f (continued): Up regulated PEG in 1R1A

Gene	Biological process Transposase	Gene name	f-value 1R1A
*DRC*0004	putative transposase		1.12
Protein with homology but unknown function			
*DR*1480	alginate regulatory protein (AlgP-related)		1.16
*DR*0439	HesB/YadR/YfhF family protein		1.14
Hypotheticals			
*DR*2489	hypothetical protein		5.57
*DR*1200	hypothetical protein		4.08
*DR*0025	hypothetical protein		4.04
*DR*2451	hypothetical protein		3.56
*DR*2573	hypothetical protein		3.38
*DR*1465	hypothetical protein		3.28
*DR*2450	hypothetical protein		3.27
*DR*1940	hypothetical protein		3.03
*DR*1925	hypothetical protein		2.96
*DR*1370	hypothetical protein		2.91
*DR*0714	hypothetical protein		2.90
*DR*0138	hypothetical protein		2.86
*DR*2229	hypothetical protein		2.81
*DR*0491	hypothetical protein		2.54
*DR*1924	hypothetical protein		2.44
*DR*0459	hypothetical protein		2.39
*DR*2494	hypothetical protein		2.39
*DR*2142	hypothetical protein		2.36
*DR*2146	hypothetical protein		2.26
*DR*1623	hypothetical protein		2.17
*DR*2593	hypothetical protein		2.07
*DR*1926	hypothetical protein		2.04
*DR*0622	hypothetical protein		2.03
*DR*1331	hypothetical protein		2.00
Hypotheticals with a fold change < 2 are listed in appendix D.2 (p. 152)			

The deinococcal sigma factor Sig1 belongs to the σ^{70} class, also known as major sigma factor that is in charge of the transcription of housekeeping promoters and general stress-protective genes [Schmid et al., 2005a]. This observation corroborates studies of [Zou et al., 1998], who provided evidence that molecular chaperonins are involved in NER. In particular, DnaK ensures thermal stability of UvrA, the catalytic loading of UvrB, enhances repair and increases UV resistance in *D. radiodurans*.

A further group abound in Table 5.9 are PEG involved in intermediary central metabolism and protein synthesis. This concomitant phenomenon has been observed in heat shocked *D. radiodurans* cells as well. Schmid inferred a hypothesis of cross protection [Schmid et al., 2005a] implying that the increased production of genes linked to glycolysis and carbon metabolism are induced in response to heat shock as means to cross-protect the cell against the impending nutritional stress. The authors found in the first 2–3 h a dramatic increase in growth rate following the shift to heat shock [Schmid et al., 2005a]. The obtained data confirmed this hypothesis and can be extended and rephrased universally that the increased production of genes linked to metabolism are induced in response to DNA damaging stressors as means to cross-protect the cell against the impending demand of protein building blocks.

5.2.2 Broad stress-induced genes common in expression pattern

The most prevalent result of the expression pattern of 1R1A (*recA*) post-UVC-irradiation is the abundance of broad stress-induced PEG Table 5.10. Especially, PEG of interest as inferred from their signal intensity (cf. chapter 5.1, p. 78) and most of the up regulated genes (chapter 5.2.1) respond almost entirely to a diverse range of environmental stressors.

The qualitative induction response was derived from the supplementary material provided by [Lipton et al., 2002], who compiled a predetermined set of accurate mass tags (AMT) of biomarkers in *D. radiodurans* that were induced under varied culture conditions and different environmental stressors. These data corroborate assumptions that *D. radiodurans* has rather improved its intrinsic DNA damage response by expanding the response scope of diverse genes to ensure an efficient repair process.

As a result of the programme settings the majority of PEG with broad stress response exhibit a rather low fold-change value corroborating their importance for *D. radiodurans'* UV radiation tolerance, because the measured intensities in wild-type and mutant strain are comparable. On the other hand, *DR*1233 and *DR*1603 are among the highly repressed genes in 1R1A (*recA*) Table 5.10 and Table 5.1. These PEG seem to be directly regulated

by RecA because their expression is very distinct compared to that of the wild-type strain R1.

The most intriguing finding was that the core genes of the postulated bypass repair system respond to a wide range of environmental stressors as well, indicating the requirement to further investigate their potential biological role.

Further examples of either up regulated genes or genes linked to the postulated bypass repair, protein fate and synthesis can be found in the appendix Table D.3 (p. 154). Moreover, the abundance of ribosomal proteins with a broad stress response (Table D.3) provide further evidence to the hypothesis of cross protection (chapter 5.2.1).

Tab. 5.10: Abundance of broad stress response genes post-UV-(254 nm) radiation. The qualitative induction response to the environmental stressors of these selected genes has been derived from [Lipton et al., 2002].

Gene	f-value	Table	Environmental stress conditions									
*DRC*0004	1.1	5.1										UV
*DR*0099	1.1	5.1	N	T	OX	ST		pH				UV
*DR*0100	-1.0	5.1										UV
*DR*0255	-1.0	5.1										UV
*DR*1697	-2.3	5.1	N									UV
*DR*2344	-1.4	5.1	N	T	OX	ST	CS	pH				UV
*DR*1115	6.9	5.1	N	T	OX	ST	CS	pH	HS			UV
*DR*0383	4.2	5.1	N	T	OX	ST	CS	pH				UV
*DR*2128	1.8	5.1	N	T	OX	ST	CS	pH				UV
*DR*0326	1.7	5.1	N	Th						D	IR	UV
*DR*1262	1.3	5.9	N	T	OX		CS	pH				UV
*DR*2446	1.7	5.9	N	T				pH				UV
*DR*2445	1.4	5.9	N	T		ST		pH				UV
*DR*2444	1.0	5.9	N	T	OX	ST	CS	pH				UV
*DR*1233	-11.2	5.6	N	T	OX		CS	pH				UV
*DR*1603	-10.0	5.6	N	T	OX	ST	CS	pH				UV

N – Nutrient constraints, T – Temperature shock (heat "h" and cold), OX – Oxidative stress by adding H_2O_2, ST – Starvation period, CS – Chemical shock, pH – Alkaline shock, HS – Heat shock [Schmid et al., 2005a], D – Desiccation and IR – Ionizing radiation exposure [Tanaka et al., 2004], UV – UV-(254 nm) irradiation (this work)

5.3 Ultrastructural UV-radiation protection evidenced by TEM

The existing mutant strains of *D. radiodurans* R1 have always been utilized to elucidate the radiation-induced repair mechanisms by means of their repair capability. None of the mutant strains has been completely sequenced or physiologically characterized. Therefore, transmission electron microscopy (TEM) was applied as an additional tool to obtain insight into the cellular composition of the mutant strains and to compare them to the wild-type strain R1 (details to specimen preparation cf. chapter 2.2, p. 27). By this approach, a more complex view was aimed at, i.e. a combined reference of biochemical, cellular and ultrastructural experimental techniques, for interpreting the results in the context of enlightening the UV-induced repair mechanism of *D. radiodurans*.

The gene expression analysis of 1R1A (*recA*) provided evidence that in the absence of *recA* cell wall biogenesis is severeley affected as inferred from the highly up regulated PEG *DR*1115 and *DR*0382 (fold-change values: 7 and 6.2, respectively) and other functionally-related but moderately up regulated PEG (chapter 5.2.1 and Table 5.11). The micrographs obtained via transmission electron microscopy (TEM) provided insight into the micro-anatomy of the *D. radiodurans* strains investigated in this work.

5.3.1 Cell wall thickness correlates to UV-protection level in mutants

First screening of the obtained micrographs suggested that the intrinsic cell wall thickness of the *D. radiodurans* strains differing in repair ability might function as UV-protection measure. Early studies have already suggested that the cell wall may be involved in repair or protective mechanisms ([Baumeister et al., 1981] and references therein). As determined by [Schuerger et al., 2003] already $10 - 50\ \mu m$ non-contiguous layers of Mars soil analogue offered a moderate protection from UV-irradiation, whereas the smallest soil fraction ($2 - 8\ \mu m$) failed to protect the investigated *Bacillus subtilis* endospores, that are similar in size as *D. radiodurans*. But a contiguous layer was more effective in protecting the bacteria of the biocidal effects of UV. In contrast, this study has shown that a contiguous layer of Goldenrod B-6090, the hematite with a grain size of $0.3\ \mu m$, was sufficient to provide UV protection (chapter 3.2.1, p. 56). Therefore, it is assumed that significant differences in cell wall thickness rather function as a first barrier to attenuate incident UV-photons and to contribute to *D. radiodurans'* UV-protection mechanism than contributing to its repair systems.

Tab. 5.11: The up regulated PEG of 1R1A (*recA*) following 254 nm-UV radiation that are associated to cell wall biogenesis in the broadest sense.

Gene	Cell wall biogenesis	f-value 1R1A
*DR*1115	S-layer-like array-related protein	6.92
*DR*0382	O-sialoglycoprotein endopeptidase, putative	6.16
*DR*0383	S-layer-like array-related protein	4.17
*DR*1185	S-layer-like array-related protein – *Sig1R*	2.08
*DR*2096	endopeptidase IV-related protein	1.90
*DR*2070	membrane lipoprotein	1.61
*DR*1124	SLH (S-layer homology domain) family protein	1.21
*DR*0379	outer membrane protein	1.17
*DR*1369	minicell-associated protein; *B. subtilis* homolog – septum misplacement§	1.03

Sig1R – PEG that have been assigned to be part of the sigma factor Sig1 (*DR*0180) heat shock regulon [Schmid et al., 2005a]; §[Thompson et al., 2006]

The deinococcal cell envelope has a complex multilayered profile:
"a plasma membrane (8 nm thick), a peptidoglycan layer (50 nm thick), a compartimentalized layer ($30 - 70$ nm thick), an outer membrane (6.5 nm thick), an electron-transparent zone (10 nm thick), and a superficial hexagonal protein array (10 nm thick)" [Thompson & Murray, 1981].

Since the aim of the TEM approach was to gain insight into the microanatomy of the different UV-susceptible mutant strains compared to wild-type strain, specimen preparation was aimed at preserving the whole cell.

Tab. 5.12: Average cell wall measures of the investigated *D. radiodurans* strains. The values were calculated of at least 60 measurements of the obtained TEM micrographs.

	S-Layer				Murein sacculus			
Average value [nm]	R1	262	1R1A	UVs78	R1	262	1R1A	UVs78
total	53.82	58.86	44.13	49.77	30.72	34.60	28.78	22.45
deviation	7.23	8.34	4.54	5.19	3.60	7.60	7.68	2.69

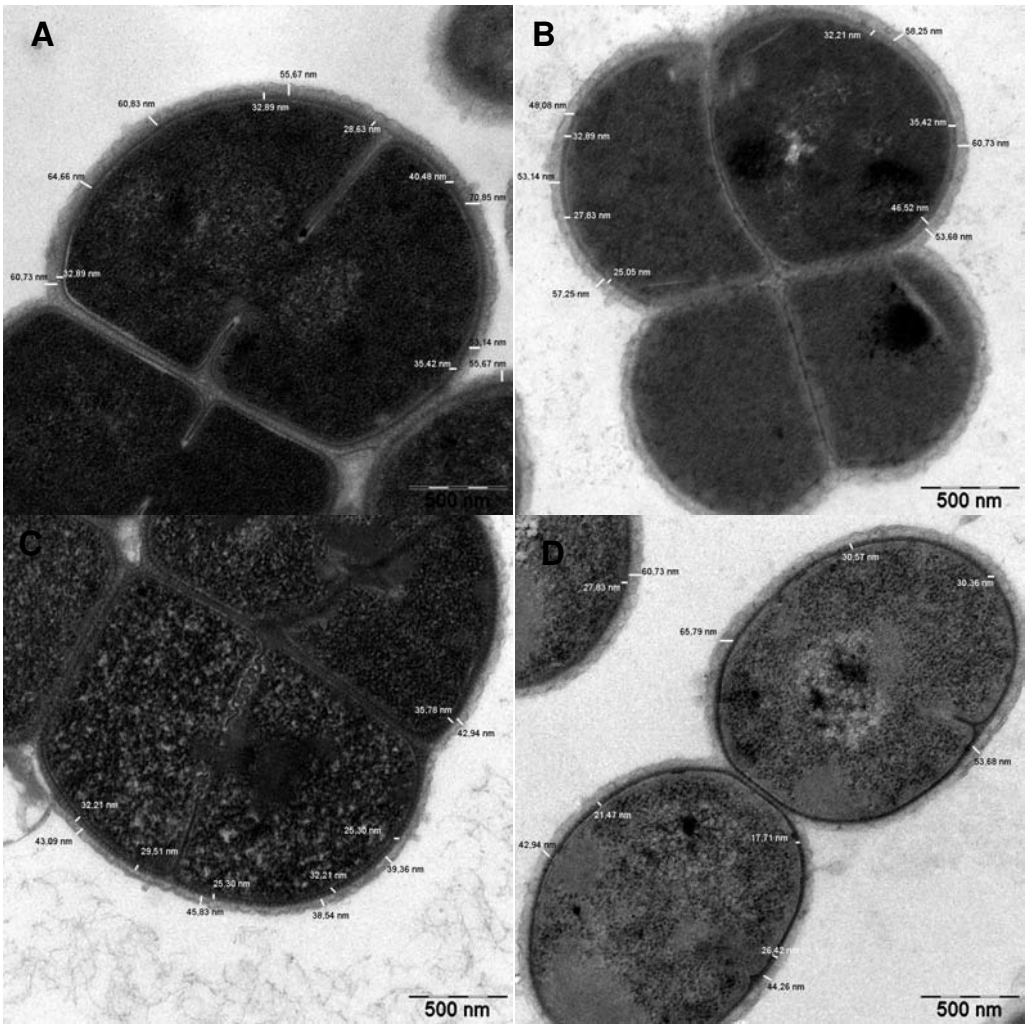

Fig. 5.2: TEM micrographs of the *D. radiodurans* strains differing in their UV-susceptibility. For each strain a micrograph was chosen that reflects the average obtained cell wall measures. A: Wild-type strain, B: 262 (*uvrA-2*), C: 1R1A (*recA*) and D: UVs78 (*uvrA-1 uvsE*).

Therefore, the multiple cell layers are not easily distinguishable under the applied specimen preparation (chapter 2.2, p. 27). The preparation protocol allows to distinguish between the crystalline bacterial cell surface layer (*S-layer*) and the so-called *murein sacculus*.

The S-layer measured here is composed of the hexagonally-packed intermediate (HPI) layer, the outer membrane, the compartimentalized layer and the electron-transparent zone resulting in a total thickness between 60 and 100 nm [Baumeister et al., 1986]. Whereas the murein sacculus comprises the peptidoglycan layer and the plasma membrane (the latter being the inner-

most layer) with a total thickness up to 60 nm [Thompson & Murray, 1981]. These measures have been derived from investigations of the *D. radiodurans* strain Sark [Thompson & Murray, 1981], which was isolated by Murray and Robinow in 1958. Since solely these two composed cell wall structures were distinguishable at the operated TEM-settings the obtained measures comprised in Table 5.12 list the average thickness of each investigated *D. radiodurans* strain. The significance of the cell wall measures Table 5.12 of the *D. radiodurans* strains differing in their UV-susceptibility was tested via t-statistics with a P-value set at $P \leq 0.05$.

As expected both measured cell wall structures of the designated UV-resistant class (R1 and 262 (*uvrA-2*)) showed no heterogenous thickness (cf. Figure 5.2). Compared to the wild-type strain R1 solely mutant strain 1R1A (*recA*) exhibited significant differences in S-layer thickness. Particularly, the mutant strains among each other showed significant variation in thickness. However, comparing the murein sacculus of the *D. radiodurans* strains determined that the most UV-sensitive strain UVs78 (*uvrA-1 uvsE*) possesses the narrowest inner barrier Table 5.12.

5.4 Discussion

The transcriptional profiling of the irradiated *D. radiodurans* strains R1 (wild-type), UVs78 (*uvrA-1 uvsE*) and 1R1A (*recA*) provided results that were unexpectedly confined concerning their biological interpretation. Significant differential gene expression was anticipated, but the obtained profile of UVs78 (*uvrA-1 uvsE*) yielded a similar transcription profile as wild-type strain R1, suggesting that nucleotide excision repair (NER) was compensated by homologous recombination repair (HR) or an unidentified bypass system and that the deleted gene loci possess no regulatory function. In contrast, *recA* is a key protein to *D. radiodurans'* radiation resistance and stress response because the transcription profile of 1R1A (*recA*) differs significantly from wild-type strain's gene expression profile. Corroborating the crucial role of *recA* for *D. radiodurans'* exceptional resistance phenotype, the results obtained provided evidence that deletion of *recA* has a severe impact on cell wall biogenesis and septum formation (chapter 5.3.1). Taken together, the results imply four possiblities of the hypothesized bypass repair process, which firstly, had been inferred from the enhanced survival capability of the UV-sensitive strains following irradiation with the longer UV wavelength spectrum [Pogoda de la Vega et al., 2005].

Activation of bypass repair process:

1. Entire compensation for nucleotide excision repair (NER), only activated if the UV endonuclease α-mediated system and the UV endonuclease β-mediated system are off-state (chapter 1.3.2.2).

2. Bridge the role of UvrA as molecular matchmaker, so that the protein complex of *uvrB* and *uvrC* may form and resume the UV endonuclease $\alpha-$mediated system.

3. An unidentified enzyme that can compensate for UV endonuclease β.

4. An unidentified, NER- and HR-independent repair pathway.

The obtained data favor the existence of an unidentified, NER- and HR-independent repair pathway based on the subsequent outlined conclusions. The microarray data analysis provided evidence that rather a regulatory function should be attributed to the two transposases $DR0255$ and $DRC0004$. By reason of their concomitant induction in all investigated *D. radiodurans* strains and yielding the highest measured signal intensity compared to all PEG in the three differing UV-susceptible strains. According to their proposed involvement in signal processing and their elevated induction post-0.5 h-irradiation, $DR1200$ and $DR1891$ are apt to initiate the bypass repair system. Potential core genes of the postulated bypass repair system comprise: $DR2438, DR2439, DR2441$ and $DR2444$. The core genes were determined by comparative genomic analyses, which fortified their biological function as DNA repair proteins. Whereas $DR2445, DR2446$ and $DR2450$ may be associated proteins that support the course of repair action. But this is highly speculative because alignment of these PEG to close genomes failed to reveal ortholog genes, or to ascertain any kind of cellular function.

Lastly, the question arises whether *D. radiodurans* may have developed some kind of mechanism that regulates the pyrimidine pool and determines the fate of excised dinucleotides. Following acute ionizing irradiation, *D. radiodurans* exhibits a dose-dependent delay of cellular replication (period of stasis) featured by phases of repair [Makarova et al., 2001]. It has been suggested that during the first phase cellular cleansing takes places, which amongst others is associated with export of damaged DNA components into the cytoplasm and surrounding growth medium [Battista, 1997]. In this respect, the fate of excised free dinucleotide dimers is rather deemed of being disposed off than recycled.

In contrast, recycling building blocks of especially pyrimidines seem desirable and obligatory to ensure rapid repair of DNA photoproducts (chapter 4).

Recently a hidden pathway for pyrimidine catabolism has been identified by Loh and coworkers (2006). This equipment is composed of seven unidentified ORF, formerly known as b1012 operon of *E. coli* K-12, now denoted as *rut* operon. The operon is under regulation of the novel repressor RutR (former *ycdC* gene). It has been suggested that this machinery contributes to the control of the internal pyrimidine pool [Osterman, 2006, Loh et al., 2006]. Though, first comparative genome studies by [Loh et al., 2006] could expand this pathway beyond the model *E. coli*, with gene orthologs corresponding to a broad range of taxonomic groups (α-proteobacteria; β-proteobacteria; γ-proteobacteria and firmicutes), no orthologs were found in *D. radiodurans'* genome. Still, in depth database search may reveal homolog machinery existing in *D. radiodurans* because this microarray study showed significant fold-change values for PEG involved rather in pyrimidine metabolism than purine metabolism Table 5.13.

Tab. 5.13: Selected representatives of enzymes involved in pyrimidine metabolism. Random selection focused on enzymes directly linked to the *de novo* synthesis of Thymine and Cytosine. For the sake of completeness, the related purine enzymes are listed as well.

Gene	Biological process Pyrimidine metabolism	f-value 1R1A
*DR*2177	Cytidine deaminase [EC: 3.5.4.5]	-5.30
*DR*2543	Cytidilate kinase [EC: 2.7.4.14]	-4.00
*DR*0443	Pyrimidine nucleosidase phosphorylase [EC 2.4.2.2]	-3.80
*DR*0159	Uridine kinase [EC: 2.7.1.48]	-2.50
*DR*1984	Thymidine kinase [EC: 2.7.1.21]	-1.70
Purine metabolism		
*DRA*0180	Guanine deaminase [EC: 3.5.4.3]	-2.23
*DRA*0185	Exopolyphosphatase [EC: 3.6.1.11]	-6.13
*DR*2289	Guanylate kinase [EC: 2.7.4.8]	-3.40
*DR*2499	Nucleoside diphosphate kinase [EC 2.7.4.6]	-3.00
*DR*2117	Adenylate kinase [EC: 2.7.4.3]	-1.90
*DR*0403	Purine nucleosidase [EC: 3.2.2.1]	-1.40
Involved in both		
*DR*0505	5'-nucleotidase [EC: 3.1.3.5]	-6.80
*DR*2166	Purine nucleoside phosphorylase	-6.30

6. CONCLUDING COMMENTS

The aim of this dissertation was to make use of the differing UV-susceptibility and UV-damage repair capability of the investigated *D. radiodurans* strains and to identify components of the hypothesized bypass UV-induced damage repair system that conferred an enhanced survival to repair-deficient strains. Specifically, I anticipated to identify proteins involved in the postulated bypass repair system. My objective was to gain a more complex view of the deinococcal UV-resistance, therefore I attempted to achieve this aim by i) combining biochemical, survival assessment by cultivation and ultrastructural experimental techniques, ii) monitoring repair kinetics of bipyrimidine photoproducts induced by 254 nm-UV radiation and iii) examining and comparing the gene expression profiles of the differing UV-susceptible *D. radiodurans* strains post-0.5 h-UV irradiation recovery.

I demonstrated that a post-0.5 h-recovery phase was sufficient for wild-type strain R1 to repair up to 80% of the total induced DNA photoproducts and that nucleotide excision repair (NER) is given priority over homologeous recombination repair (HR), based on the fact that 1R1A (*recA*) resumed repair of bipyrimidine dimers but UVs78 (*uvrA-1 uvsE*) was unable to repair any photoproduct type not even after 2 h, the utmost post-irradiation recovery time point analyzed.

My attempt to identify key players of the predicted bypass UV-induced damage repair system was successful, though further studies are necessary by virtue of the vast abundance of induced hypothetical proteins and transposases, of which many were repressed in a $\Delta recA$ background. Therefore extended comparative genomic analysis focusing on protein features should be next step to identify the cellular function of the transposases, especially those belonging to the IS4-family. The core genes of this novel bypass pathway being $DR2438, DR2439$, $DR2441$ and $DR2444$ as well as $DR2445, DR2446$. Whereas the assertion that $DR1200$ and $DR1891$ may act as putative signal factors to initiate this NER- and HR-independent bypass still has to be verified. One approach to experimentally verify the role of some of the indicated new key players would be real-time QPCR analysis associated with additional microarray studies. A further approach to experimentally educe their role in UV-resistance should start by inactivating the loci of the genes

of interest and determining their response to UV radiation.

First step would be deleting the core genes, then the loci of the overlapping PEG, determined when comparing the signal intensities of the three *D. radiodurans* strains. Hereof, the PEG with unknown or transposase function are preferred. Further auspicious candidates are genes, designated hypothetical proteins, which have been both highly repressed and highly up regulated in 1R1A (*recA*). Transcripts of genes belonging to the highly up regulated determined in this study: *DR*0492, *DR*2489 and *DR*0025. The most highly repressed PEG following 254 nm-UV radiation: *DR*0923, *DR*0996, *DR*1591, *DR*1726, *DR*1956 and *DRB*0127. Since these genes have been repressed in a Δ*recA* background, it would be interesting to determine whether they are solely under RecA-regulation or if they indeed can be linked to the UV radiation resistance of *D. radiodurans*. Furthermore, *DR*0492, *DR*2489 and *DR*0025 are up regulated in both UV-sensitive mutant strains, apparently showing no relation to either excision or homologeous recombination repair, therefore indicating their involvement in the novel bypass system facilitating tolerance to UV-induced DNA damage.

Additionally, mutants that have not been exposed to UV radiation, but have been shown to contribute to *D. radiodurans'* ionizing radiation resistance are promising as well. Especially, because on one hand, *D. radiodurans* seems to have utilized mechanisms that enhance the effectiveness of its novel and traditional DNA repair proteins. On the other hand, this study has provided evidence that a suit of PEG is cross-induced in *D. radiodurans* irrespective of the applied environmental stressor to ensure an efficient and rapid repair progress.

Tanaka and coworkers (2004) determined five novel PEG that were most highly induced in response to ionizing radiation and desiccation: *ddrA*[1] (*DR*0423), *ddrB* (*DR*0070), *ddrC* (*DR*0003), *ddrD* (*DR*0326) and *pprA* (*DRA*0346). In this study *pprA*, *ddrA*, *ddrB* and *ddrD* were significantly induced. Moreover, Tanaka et al. (2004) not only studied the above mentioned single mutants but by deleting the five loci in all possible combinations, created double mutants with either similar response as the single mutants or in some cases (e.g. Δ*pprA*Δ*ddrA* and Δ*pprA*Δ*ddrB*) demonstrated increased ionizing radiation sensitivity. Especially, combinations of the UVC-induced Ddr-PEG are auspicious candidates to start with. Additionally, other UV-conferring resistance PEG, especially combinations with Δ*rsr* (*DR*1262, **R**o **s**ixty **r**elated PEG) [Chen et al., 2000] and Δ*uvrA-2* of the UvrABC system, which up to date seems to play a rather minor role in UV-resistance, could provide further insigths into the novel bypass pathway.

[1] **D**NA **d**amage **r**esponse

LIST OF FIGURES

LIST OF TABLES

BIBLIOGRAPHY

[Agostini et al., 1996] Agostini, H., Carroll, J., & Minton, K. (1996). Identification and characterization of uvrA, a DNA repair gene of *Deinococcus radiodurans*. *J. Bacteriol.*, 178(23), 6759–6765.

[Airo et al., 2004] Airo, A., Chan, S. L., Martinez, Z., Platt, M. O., & Trent, J. D. (2004). Heat shock and cold shock in *Deinococcus radiodurans*. *Cell Biochemistry and Biophysics*, 40(3), 277–288.

[Anderson et al., 1956] Anderson, A. W., Nordan, H. C., Cain, R. F., Parrish, G., & Duggan, D. (1956). Studies on a radio-resistant *Micrococcus*. I. isolation, morphology, cultural characteristics, and resistance to gamma radiation. *Food Technology*, 10, 575–578.

[Arnold & Kowalczykowski, 2000] Arnold, D. A. & Kowalczykowski, S. C. (2000). Facilitated loading of RecA protein is essential to recombination by RecBCD enzyme. *J. Biol. Chem.*, 275(16), 12261–12265.

[Barrett et al., 2007] Barrett, T., Troup, D. B., Wilhite, S. E., Ledoux, P., Rudnev, D., Evangelista, C., Kim, I. F., Soboleva, A., Tomashevsky, M., & Edgar, R. (2007). NCBI GEO: mining tens of millions of expression profiles–database and tools update. *Nucl. Acids Res.*, 35(Supplement 1), D760–765.

[Battista, 1997] Battista, J. (1997). Against all odds: the survival strategies of *Deinococcus radiodurans*. *Annu Rev Microbiol*, 51, 203–224.

[Battista & Rainey, 2001] Battista, J. & Rainey, F. (2001). Phylum BIV. *Deinococcus–Thermus* family 1. deinococcaceae Brooks and Murray 1981, 356,vp emend. Rainey, Nobre, Schumann, Stackebrandt and da Costa 1997, 513. *Bergey's Manual of Systematic Bacteriology*, 1, 395–414.

[Baumeister et al., 1986] Baumeister, W., Barth, M., Hegerl, R., Guckenberger, R., Hahn, M., & Saxton, W. O. (1986). Three-dimensional structure of the regular surface layer (HPI layer) of *Deinococcus radiodurans*. *Journal of Molecular Biology*, 187(2), 241–250.

[Baumeister et al., 1981] Baumeister, W., Kübler, O., & Zingsheim, H. P. (1981). The structure of the cell envelope of *Micrococcus radiodurans* as revealed by metal shadowing and decoration. *Journal of Ultrastructure Research*, 75(1), 369–376.

[Berger, 2003] Berger, T. (2003). *Dose assessment in mixed radiation fields: special emphasis on space dosimetry*. PhD thesis, Technical University of Vienna, Austria.

[Bernstein et al., 2004] Bernstein, D. A., Eggington, J. M., Killoran, M. P., Misic, A. M., Cox, M. M., & Keck, J. L. (2004). Crystal structure of the *Deinococcus radiodurans* single-stranded DNA-binding protein suggests a mechanism for coping with DNA damage. *Proceedings of the National Academy of Sciences*, 101(23), 8575–8580.

[Bieger-Dose et al., 1992] Bieger-Dose, A., Dose, K., Meffert, R., Mehler, M., & Risi, S. (1992). Extreme dryness and DNA-protein cross-links. *Advances in Space Research*, 12(4), 265–270.

[Bockrath & Li, 1997] Bockrath, R. & Li, B. H. (1997). Photoreversal of UV-potentiated glutamine tRNA suppressor mutations in excision proficient *Escherichia coli*. *Current Protocols in Molecular Biology*, 383(3), 231–242.

[Boling & Setlow, 1966] Boling, M. E. & Setlow, J. K. (1966). The resistance of *Micrococcus radiodurans* to ultraviolet radiation III. a repair mechanism. *Biochimica et Biophysica Acta (BBA) - Nucleic Acids and Protein Synthesis*, 123(1), 26–33.

[Bolstad et al., 2003] Bolstad, B., Irizarry, R., Astrand, M., & Speed, T. (2003). A comparison of normalization methods for high density oligonucleotide array data based on variance and bias. *Bioinformatics*, 19(2), 185–193.

[Brooks & Murray, 1981] Brooks, B. W. & Murray, R. G. E. (1981). Nomenclature for *Micrococcus radiodurans* and other radiation resistant cocci: deinococcaceae fam. nov. and *Deinococcus* gn. nov., including five species. *Int. J. Syst. Bacteriol.*, 31, 353–360.

[Bucker et al., 1972] Bucker, H., Horneck, G., Facius, R., Schwager, M., Thomas, C., Turcu, G., & Wollenhaupt, H. (1972). Effects of simulated space vacuum on bacterial cells. *Life Sci. Space Res.*, 10, 191–195.

[Budde et al., 2006] Budde, I., Steil, L., Scharf, C., Volker, U., & Bremer, E. (2006). Adaptation of *Bacillus subtilis* to growth at low temperature:

a combined transcriptomic and proteomic appraisal. *Microbiology*, 152(3), 831–853.

[Cadet et al., 2005] Cadet, J., Sage, E., & Douki, T. (2005). Ultraviolet radiation-mediated damage to cellular DNA. *Mutation Research/Fundamental and Molecular Mechanisms of Mutagenesis*, 571(1-2), 3–17.

[Carbonneau et al., 1989] Carbonneau, M. A., Melin, A. M., Perromat, A., & Clerc, M. (1989). The action of free radicals on *Deinococcus radiodurans*' carotenoids. *Archives of Biochemistry and Biophysics*, 275(1), 244–251.

[Carr, 1981] Carr, M. H. (1981). *The surface of Mars*. Yale University Press, New Haven, first edition.

[Chen et al., 2000] Chen, X., Quinn, A. M., & Wolin, S. L. (2000). Ro ribonucleoproteins contribute to the resistance of *Deinococcus radiodurans* to ultraviolet irradiation. *Genes Dev.*, 14(7), 777–782.

[Chow & Courcelle, 2004] Chow, K.-H. & Courcelle, J. (2004). RecO acts with RecF and RecR to protect and maintain replication forks blocked by UV-induced DNA damage in *Escherichia coli*. *Journal of Biological Chemistry*, 279(5), 3492–3496.

[Cockell, 2000] Cockell, C. S. (2000). Biological effects of high ultraviolet radiation on early Earth-a theoretical evaluation. *Journal of Theoretical Biology*, 193(4), 717–729.

[Cockell & Andrady, 1999] Cockell, C. S. & Andrady, A. (1999). The martian and extraterrestrial UV radiation environment—1. biological and closed-loop ecosystem considerations. *Acta Astronaut.*, 44(1), 53–62.

[Cockell et al., 2000] Cockell, C. S., Catling, D. C., Davis, W. L., Snook, K., Kepner, R. L., Lee, P., & McKay, C. P. (2000). The ultraviolet environment of Mars: Biological implications past, present, and future. *Icarus*, 146(2), 343–359.

[Cockell & Horneck, 2001] Cockell, C. S. & Horneck, G. (2001). The history of the UV radiation climate of the Earth; theoretical and space-based observations. *Photochemistry and Photobiology*, 73(4), 447–451.

[Correction & Clarifications, 2003] Correction & Clarifications (2003). Letters to science. *Science*, 303(5659), 766.

[Courcelle et al., 2005] Courcelle, C. T., Belle, J. J., & Courcelle, J. (2005). Nucleotide excision repair or polymerase V-mediated lesion bypass can act to restore UV-arrested replication forks in *Escherichia coli*. *J. Bacteriol.*, 187(20), 6953–6961.

[Cox, 2003] Cox, M. M. (2003). The bacterial RecA protein as a motor protein. *Annual Review of Microbiology*, 57(1), 551–577.

[Cox & Battista, 2005] Cox, M. M. & Battista, J. R. (2005). *Deinococcus radiodurans* — the consummate survivor. *Nat Rev Micro*, 3(11), 882–892.

[Daly et al., 2004] Daly, M., Gaidamakova, E., Matrosova, V., Vasilenko, A., Zhai, M., Venkateswaran, A., Hess, M., Omelchenko, M., Kostandarithes, H., Makarova, K., Wackett, L., Fredrickson, J., & Ghosal, D. (2004). Accumulation of Mn(II) in *Deinococcus radiodurans* facilitates gamma-radiation resistance. *Science*, 306(5698), 1025–1028.

[Daly & Minton, 1995] Daly, M. & Minton, K. (1995). Interchromosomal recombination in the extremely radioresistant bacterium *Deinococcus radiodurans*. *J. Bacteriol.*, 177(19), 5495–5505.

[Daly & Minton, 1996] Daly, M. & Minton, K. (1996). An alternative pathway of recombination of chromosomal fragments precedes recA-dependent recombination in the radioresistant bacterium *Deinococcus radiodurans*. *J. Bacteriol.*, 178(15), 4461–4471.

[Daly et al., 2007] Daly, M. J., Gaidamakova, E. K., Matrosova, V. Y., Vasilenko, A., Zhai, M., Leapman, R. D., Lai, B., Ravel, B., Li, S.-M. W., Kemner, K. M., & Fredrickson, J. K. (2007). Protein oxidation implicated as the primary determinant of bacterial radioresistance. *PLoS Biology*, 5(4), e92.

[Daly et al., 1994] Daly, M. J., Ouyang, L., Fuchs, P., & Minton, K. W. (1994). In vivo damage and recA-dependent repair of plasmid and chromosomal DNA in the radiation-resistant bacterium *Deinococcus radiodurans*. *J. Bacteriol.*, 176(12), 3508–3517.

[Dartnell et al., 2007] Dartnell, L. R., Desorgher, L., Ward, J. M., & Coates, A. J. (2007). Modelling the surface and subsurface martian radiation environment: Implications for astrobiology. *Geophysical Research Letters*, 34(L02207), 1–6.

[de Groot et al., 2005] de Groot, A., Chapon, V., Servant, P., Christen, R., Saux, M. F.-L., Sommer, S., & Heulin, T. (2005). *Deinococcus* deserti

sp. nov., a gamma-radiation-tolerant bacterium isolated from the Sahara desert. *Int J Syst Evol Microbiol*, 55(6), 2441–2446.

[de la Vega, 2004] de la Vega, U. (2004). *Studien zur UV-Strahlen- und Trockenresistenz von Deinococcus radiodurans(master thesis)*. PhD thesis, University of Cologne, Germany.

[Diaz & Schulze-Makuch, 2006] Diaz, B. & Schulze-Makuch, D. (2006). Microbial survival rates of *Escherichia coli* and *Deinococcus radiodurans* under low temperature, low pressure, and UV-irradiation conditions, and their relevance to possible martian life. *Astrobiology*, 6(2), 332–347.

[Dose et al., 1992] Dose, K., Bieger-Dose, A., Labusch, M., & Gill, M. (1992). Survival in extreme dryness and DNA-single-strand breaks. *Advances in Space Research*, 12(4), 221–229.

[Douki & Cadet, 2001] Douki, T. & Cadet, J. (2001). Individual determination of the yield of the main UV-induced dimeric pyrimidine photoproducts in DNA suggests a high mutagenicity of CC photolesions. *Biochemistry*, 40(8), 2495–2501.

[Douki & Cadet, 2003] Douki, T. & Cadet, J. (2003). Formation of the spore photoproduct and other dimeric lesions between adjacent pyrimidines in UVC-irradiated dry DNA. *Photochem. Photobiol. Sci.*, 2, 433–436.

[Douki et al., 2000] Douki, T., Court, M., Sauvaigo, S., Odin, F., & Cadet, J. (2000). Formation of the main UV-induced thymine dimeric lesions within isolated and cellular DNA as measured by high performance liquid chromatography-tandem mass spectrometry. *J. Biol. Chem.*, 275(16), 11678–11685.

[Draghici et al., 2003] Draghici, S., Kulaeva, O., Hoff, B., Petrov, A., Shams, S., & Tainsky, M. A. (2003). Noise sampling method: an ANOVA approach allowing robust selection of differentially regulated genes measured by DNA microarrays. *Bioinformatics*, 19(11), 1348–1359.

[Earl, 2003] Earl, A. M. (2003). *Global Expression Analysis of Deinococcus radiodurans' response to ionizing radiation: IrrE is a novel regulator of this response*. PhD thesis, Louisiana State University, USA.

[Earl et al., 2002a] Earl, A. M., Mohundro, M. M., Mian, I. S., & Battista, J. R. (2002a). The IrrE protein of *Deinococcus radiodurans* R1 is a novel regulator of recA expression. *J. Bacteriol.*, 184(22), 6216–6224.

[Earl et al., 2002b] Earl, A. M., Rankin, S. K., Kim, K.-P., Lamendola, O. N., & Battista, J. R. (2002b). Genetic evidence that the uvsE gene product of *Deinococcus radiodurans* R1 is a UV damage endonuclease. *J. Bacteriol.*, 184(4), 1003–1009.

[Eggington et al., 2004] Eggington, J., Haruta, N., Wood, E., & Cox, M. (2004). The single-stranded DNA-binding protein of *Deinococcus radiodurans*. *BMC Microbiology*, 4(1), 2.

[Eggington et al., 2006] Eggington, J., Kozlov, A., Cox, M., & Lohman, T. (2006). Polar destabilization of DNA duplexes with single-stranded overhangs by the *Deinococcus radiodurans* SSB protein. *Biochemistry*, 45(48), 14490–14502.

[Eltsov & Dubochet, 2005] Eltsov, M. & Dubochet, J. (2005). Fine structure of the *Deinococcus radiodurans* nucleoid revealed by cryoelectron microscopy of vitreous sections. *J. Bacteriol.*, 187(23), 8047–8054.

[Englander et al., 2004] Englander, J., Klein, E., Brumfeld, V., Sharma, A., Doherty, A., & Minsky, A. (2004). DNA toroids: framework for DNA repair in *Deinococcus radiodurans* and in germinating bacterial spores. *J Bacteriol*, 186(18), 5973–5977.

[Evans & Moseley, 1985] Evans, D. & Moseley, B. (1985). Identification and initial characterisation of a pyrimidine dimer UV endonuclease (UV endonuclease beta) from *Deinococcus radiodurans*; a DNA-repair enzyme that requires manganese ions. *Mutat. Res.*, 145(3), 119–128.

[Evans & Moseley, 1988] Evans, D. & Moseley, B. (1988). *Deinococcus radiodurans* UV endonuclease beta DNA incisions do not generate photoreversible thymine residues. *Mutat. Res.*, 207(3-4), 117–119.

[Evans & Moseley, 1983] Evans, D. M. & Moseley, B. E. (1983). Roles of the uvsC, uvsD, uvsE, and mtcA genes in the two pyrimidine dimer excision repair pathways of *Deinococcus radiodurans*. *J. Bacteriol.*, 156(2), 576–583.

[Ferreira et al., 1997] Ferreira, A., Nobre, M., Rainey, F., Silva, M., Wait, R., Burghardt, J., Chung, A., & da Costa, M. (1997). *Deinococcus* geothermalis sp. nov. and *Deinococcus* murrayi sp. nov., two extremely radiation-resistant and slightly thermophilic species from hot springs. *Int J Syst Bacteriol*, 47(4), 939–947.

[Frenkiel-Krispin et al., 2004] Frenkiel-Krispin, D., Ben-Avraham, I., Englander, J., Shimoni, E., Wolf, S. G., & Minsky, A. (2004). Nucleoid restructuring in stationary-state bacteria. *Molecular Microbiology*, 51(2), 395–405.

[Frenkiel-Krispin & Minsky, 2006] Frenkiel-Krispin, D. & Minsky, A. (2006). Nucleoid organization and the maintenance of DNA integrity in *Escherichia coli*, *Bacillus subtilis* and *D. radiodurans*. *Journal of Structural Biology*, 156(2), 311–319.

[Friedberg, 2003] Friedberg, E. C. (2003). DNA damage and repair. *Nature*, 421(6921), 436–440.

[Gao et al., 2006] Gao, G., Le, D., Huang, L., Lu, H., Narumi, I., & Hua, Y. (2006). Internal promoter characterization and expression of the *Deinococcus radiodurans* pprI-folP gene cluster. *FEMS Microbiology Letters*, 257(2), 195–201.

[Gasteiger et al., 2001] Gasteiger, E., Jung, E., & Bairoch, A. (2001). SWISS-PROT: Connecting biomolecular knowledge via a protein database. *Curr. Issues Mol. Biol.*, 3(3), 47–55.

[Ghosal et al., 2005] Ghosal, D., Omelchenko, M. V., Gaidamakova, E. K., Matrosova, V. Y., Vasilenko, A., Venkateswaran, A., Zhai, M., Kostandarithes, H. M., Brim, H., Makarova, K. S., Wackett, L. P., Fredrickson, J. K., & Daly, M. J. (2005). How radiation kills cells: Survival of *Deinococcus radiodurans* and Shewanella oneidensis under oxidative stress. *FEMS Microbiology Reviews*, 29(2), 361–375.

[Grant et al., 2007] Grant, G. R., Manduchi, E., & Stoeckert Jr., C. J. (2007). UNIT 19.6: Analysis and management of microarray gene expression data. *Current Protocols in Molecular Biology*, Supplement 77, 19.6.1–19.6.29.

[Griffiths & Gupta, 2004] Griffiths, E. & Gupta, R. S. (2004). Distinctive protein signatures provide molecular markers and evidence for the monophyletic nature of the *Deinococcus–Thermus* phylum. *J. Bacteriol.*, 186(10), 3097–3107.

[Griffiths, 1996] Griffiths, G. (1996). *Fine Structure Immunocytochemistry*. Springer, first edition.

[Gutman et al., 1994] Gutman, P., Carroll, J., Masters, C., & Minton, K. (1994). Sequencing, targeted mutagenesis and expression of a recA gene

required for the extreme radioresistance of *Deinococcus radiodurans*. *Gene*, 141(1), 31–37.

[Gutman et al., 1993] Gutman, P. D., Fuchs, P., Ouyang, L., & Minton, K. W. (1993). Identification, sequencing, and targeted mutagenesis of a DNA polymerase gene required for the extreme radioresistance of *Deinococcus radiodurans*. *J. Bacteriol.*, 175(11), 3581–3590.

[Hablanian, 1997] Hablanian, M. H. (1997). *High-Vacuum Technology (Mechanical Engineering)*. Marcel Dekker Inc., second edition.

[Hajibagheri, 1999] Hajibagheri, M. A. N. (1999). *Electro Microscopy Methods and Protocols (Methods in Molecular Biology)*. Humana Press, first edition.

[Hansen, 1978] Hansen, M. T. (1978). Multiplicity of genome equivalents in the radiation-resistant bacterium *Micrococcus radiodurans*. *J. Bacteriol.*, 134(1), 71–75.

[Hansen, 1980] Hansen, M. T. (1980). Four proteins synthesized in response to deoxyribonucleic acid damage in *Micrococcus radiodurans*. *J. Bacteriol.*, 141(1), 81–86.

[Harris et al., 2004] Harris, D. R., Tanaka, M., Saveliev, S. V., Jolivet, E., Earl, A. M., Cox, M. M., & Battista, J. R. (2004). Preserving genome integrity: The DdrA protein of *Deinococcus radiodurans* R1. *PLoS Biology*, e304, 2–10.

[Harsojo et al., 1981] Harsojo, Kitayama, S., & Matsuyama, A. (1981). Genome multiplicity and radiation resistance in *Micrococcus radiodurans*. *J Biochem (Tokyo)*, 90(3), 877–880.

[Haruta et al., 2003] Haruta, N., Yu, X., Yang, S., Egelman, E. H., & Cox, M. M. (2003). A DNA pairing-enhanced conformation of bacterial RecA proteins. *J. Biol. Chem.*, 278(52), 52710–52723.

[Hayat, 1981] Hayat, M. H. (1981). *Fixation for Electron Microscopy*. Academic Press, New York, first edition.

[Hensel et al., 1986] Hensel, R., Demharter, W., Kandler, O. amd Kroppenstedt, R., & Stackebrandt, E. (1986). Chemotaxonomic and molecular-genetic studies of the genus *Thermus*: evidence for a phylogenetic relationship of *Thermus* aquaticus and *Thermus* ruber to the genus *Deinococcus*. *Int. J. Syst. Bacteriol.*, 36, 444–453.

[Hickman et al., 2000] Hickman, A. B., Li, Y., Mathew, S. V., May, E. W., Craig, N. L., & Dyda, F. (2000). Unexpected structural diversity in DNA recombination: The restriction endonuclease connection. *Molecular Cell*, 5(6), 1025–1034.

[Hirsch et al., 2004] Hirsch, P., Gallikowski, C., Siebert, J., Peissl, K., Kroppenstedt, R., Schumann, P., Stackebrandt, E., & Anderson, R. (2004). *Deinococcus* frigens sp. nov., *Deinococcus* saxicola sp. nov., and *Deinococcus* marmoris sp. nov., low temperature and draught-tolerating, UV-resistant bacteria from continental antarctica. *Syst Appl Microbiol*, 27(6), 636–645.

[Horneck, 2006] Horneck, G. (2006). Search for life in the universe - what can we learn from our own biosphere? In S. Roeser (Ed.), *Reviews in Modern Astronomy: The Many Facets of the Universe - Revelations by New Instruments*, volume 19 (pp. 215–235). University of Cologne, Germany: Astronomical Society's International Scientific Conference on: The many facets of the universe - Revelations by New Instruments Wiley-VCH.

[Horneck et al., 1998] Horneck, G., Rettberg, P., Rabbow, E., Strauch, W., Seckmeyer, G., Facius, R., Reitz, G., Strauch, K., & Schott, J. (1998). Biological dosimetry of solar radiation for different simulated ozone column thicknesses. *Journal of Photochemistry and Photobiology B: Biology*, 32(3), 189–196.

[Horneck et al., 2001] Horneck, G., Rettberg, P., Reitz, G., Wehner, J., Eschweiler, U., Strauch, K., Panitz, C., Starke, V., & Baumstark-Khan, C. (2001). Protection of bacterial spores in space, a contribution to the discussion on panspermia. *Origins of Life and Evolution of Biospheres*, 31(6), 527–547.

[Ivancic-Bace et al., 2003] Ivancic-Bace, I., Peharec, P., Moslavac, S., Skrobot, N., Salaj-Smic, E., & Brcic-Kostic, K. (2003). RecFOR function is required for DNA repair and recombination in a RecA loading-deficient recB mutant of *Escherichia coli*. *Genetics*, 163(2), 485–494.

[Jolivet et al., 2006] Jolivet, E., Lecointe, F., Coste, G., Satoh, K., Narumi, I., Bailone, A., & Sommer, S. (2006). Limited concentration of RecA delays DNA double-strand break repair in *Deinococcus radiodurans* R1. *Molecular Microbiology*, 59(1), 338–349.

[Killoran & Keck, 2006] Killoran, M. P. & Keck, J. L. (2006). Three HRDC domains differentially modulate *Deinococcus radiodurans* RecQ DNA helicase biochemical activity. *J. Biol. Chem.*, 281(18), 12849–12857.

[Kim & Cox, 2002] Kim, J.-I. & Cox, M. M. (2002). The RecA proteins of *Deinococcus radiodurans* and *Escherichia coli* promote DNA strand exchange via inverse pathways. *Proceedings of the National Academy of Sciences*, 99(12), 7917–7921.

[Kim et al., 2002] Kim, J.-I., Sharma, A. K., Abbott, S. N., Wood, E. A., Dwyer, D. W., Jambura, A., Minton, K. W., Inman, R. B., Daly, M. J., & Cox, M. M. (2002). RecA protein from the extremely radioresistant bacterium *Deinococcus radiodurans*: Expression, purification, and characterization. *J. Bacteriol.*, 184(6), 1649–1660.

[Knudsen et al., 2003] Knudsen, S., Workman, C., Sicheritz-Ponten, T., & Friis, C. (2003). GenePublisher: automated analysis of DNA microarray data. *Nucl. Acids Res.*, 31(13), 3471–3476.

[Lai et al., 2006] Lai, W.-A., Kampfer, P., Arun, A. B., Shen, F.-T., Huber, B., Rekha, P. D., & Young, C.-C. (2006). *Deinococcus* ficus sp. nov., isolated from the rhizosphere of Ficus religiosa L. *Int J Syst Evol Microbiol*, 56(4), 787–791.

[Lecointe et al., 2004] Lecointe, F., Shevelev, I. V., Bailone, A., Sommer, S., & Hubscher, U. (2004). Involvement of an X family DNA polymerase in double-stranded break repair in the radioresistant organism *Deinococcus radiodurans*. *Molecular Microbiology*, 53(6), 1721–1730.

[Lee et al., 2004] Lee, B. I., Kim, K. H., Park, S. J., Eom, S. H., Song, H. K., & Suh, S. W. (2004). Ring-shaped architecture of RecR: implications for its role in homologous recombinational DNA repair. *The EMBO Journal*, 23, 2029–2038.

[Leiros et al., 2005] Leiros, I., Timmins, J., Hall, D. R., & McSweeney, S. (2005). Crystal structure and DNA-binding analysis of RecO from *Deinococcus radiodurans*. *The EMBO Journal*, 24, 906–918.

[Leplae et al., 2004] Leplae, R., Hebrant, A., Wodak, S. J., & Toussaint, A. (2004). ACLAME: A classification of mobile genetic elements. *Nucl. Acids Res.*, 32(Supplement 1), D45–49.

[Levin-Zaidman et al., 2003] Levin-Zaidman, S., Englander, J., Shimoni, E., Sharma, A. K., Minton, K. W., & Minsky, A. (2003). Ringlike structure of the *Deinococcus radiodurans* genome: A key to radioresistance? *Science*, 299(5604), 254–256.

[Lin et al., 1999] Lin, J., Qi, R., Aston, C., Jing, J., Anantharaman, T. S., Mishra, B., White, O., Daly, M. J., Minton, K. W., Venter, J. C., & Schwartz, D. C. (1999). Whole-genome shotgun optical mapping of *Deinococcus radiodurans*. *Science*, 285(5433), 1558–1562.

[Lipton et al., 2002] Lipton, M. S., Pasa-Tolic', L., Anderson, G. A., Anderson, D. J., Auberry, D. L., Battista, J. R., Daly, M. J., Fredrickson, J., Hixson, K. K., Kostandarithes, H., Masselon, C., Markillie, L. M., Moore, R. J., Romine, M. F., Shen, Y., Stritmatter, E., Tolic', N., Udseth, H. R., Venkateswaran, A., Wong, K.-K., Zhao, R., & Smith, R. D. (2002). From the cover: Global analysis of the *Deinococcus radiodurans* proteome by using accurate mass tags. *Proceedings of the National Academy of Sciences*, 99(17), 11049–11054.

[Loh et al., 2006] Loh, K. D., Gyaneshwar, P., Markenscoff Papadimitriou, E., Fong, R., Kim, K.-S., Parales, R., Zhou, Z., Inwood, W., & Kustu, S. (2006). From the cover: A previously undescribed pathway for pyrimidine catabolism. *Proceedings of the National Academy of Sciences*, 103(13), 5114–5119.

[Makarova et al., 2002] Makarova, K. S., Aravind, L., Grishin, N. V., Rogozin, I. B., & Koonin, E. V. (2002). A DNA repair system specific for thermophilic Archaea and bacteria predicted by genomic context analysis. *Nucl. Acids Res.*, 30(2), 482–496.

[Makarova et al., 2001] Makarova, K. S., Aravind, L., Wolf, Y. I., Tatusov, R. L., Minton, K. W., Koonin, E. V., & Daly, M. J. (2001). Genome of the extremely radiation-resistant bacterium *Deinococcus radiodurans* viewed from the perspective of comparative genomics. *Microbiol. Mol. Biol. Rev.*, 65(1), 44–79.

[Makharashvili et al., 2005] Makharashvili, N., Koroleva, O., Bera, S., Grandgenett, D. P., & Korolev, S. (2005). A novel structure of DNA repair protein RecO from *Deinococcus radiodurans*. *Structure*, 12, 1881–1889.

[Mattimore & Battista, 1996] Mattimore, V. & Battista, J. (1996). Radioresistance of *Deinococcus radiodurans*: functions necessary to survive ionizing radiation are also necessary to survive prolonged desiccation. *J. Bacteriol.*, 178(3), 633–637.

[Mennecier et al., 2004] Mennecier, S., Coste, G., Servant, P., Bailone, A., & Sommer, S. (2004). Mismatch repair ensures fidelity of replication

and recombination in the radioresistant organism *Deinococcus radiodurans*. *Molecular Genetics and Genomics*, 272(4), 460–469.

[Minsky, 2003] Minsky, A. (2003). Structural aspects of DNA repair: the role of restricted diffusion. *Molecular Microbiology*, 50(2), 367–376.

[Minsky et al., 2006] Minsky, A., Shimoni, E., & Englander, J. (2006). Ring-like nucleoids and DNA repair through error-free nonhomologous end joining in *Deinococcus radiodurans*. *J. Bacteriol.*, 188(17), 6047–6051.

[Minton & Daly, 1995] Minton, K. & Daly, M. (1995). A model for repair of radiation-induced DNA double-strand breaks in the extreme radiophile *Deinococcus radiodurans*. *Bioessays*, 17(5), 457–464.

[Minton, 1994] Minton, K. W. (1994). DNA repair in the extremely radioresistant bacterium *Deinococcus radiodurans*. *Mol Microbiol.*, 13(1), 9–15.

[Moehlmann, 2005] Moehlmann, D. (2005). Adsorption water-related potential chemical and biological processes in the upper martian surface. *Astrobiology*, 5(6), 770–777.

[Moehlmann, 2004] Moehlmann, D. T. F. (2004). Water in the upper martian surface at mid- and low-latitudes: presence, state, and consequences. *Icarus*, 168(2), 318–323.

[Moeller, 2007] Moeller, R. (2007). *Characterization of different types of radiation- and pressure-induced DNA damage in Bacillus subtilis spores and their global transcriptional response during spore germination*. PhD thesis, Technical University Carolo-Wilhelmina of Braunschweig, Germany.

[Morris & Golden, 1998] Morris, R. V. & Golden, D. C. (1998). Goldenrod pigments and the occurrence of hematite and possibly goethite in the Olympus–Amazonis region of Mars. *Icarus*, 134(1), 1–10.

[Moseley & Copland, 1978] Moseley, B. & Copland, H. (1978). Four mutants of *Micrococcus radiodurans* defective in the ability to repair DNA damaged by mitomycin-C, two of which have wild-type resistance to ultraviolet radiation. *Mol Gen Genet.*, 160(3), 331–337.

[Moseley & Evans, 1983] Moseley, B. & Evans, D. (1983). Isolation and properties of strains of *Micrococcus* (*Deinococcus*) *radiodurans* unable to excise ultraviolet light induced pyrimidine dimers from DNA: Evidence for two excision pathways. *J Gen Microbiol.*, 129(8), 2437–2445.

[Moseley, 1983] Moseley, B. E. B. (1983). Photobiology and radiobiology of *Micrococcus* (*Deinococcus*) *radiodurans*. *Photochem Photobiol Rev*, 7, 223–274.

[Moseley & Laser, 1965] Moseley, B. E. B. & Laser, H. (1965). Repair of X-ray damage in *Micrococcus radiodurans*. *Proc. Roy. Soc. (London) Ser. B*, 162, 210–222.

[Mrazek, 2002] Mrazek, J. (2002). New technology may reveal mechanisms of radiation resistance in *Deinococcus radiodurans*. *Proceedings of the National Academy of Sciences*, 99(17), 10943–10944.

[Mulder et al., 2007] Mulder, N. J., Apweiler, R., Attwood, T. K., Bairoch, A., Bateman, A., Binns, D., Bork, P., Buillard, V., Cerutti, L., Copley, R., Courcelle, E., Das, U., Daugherty, L., Dibley, M., Finn, R., Fleischmann, W., Gough, J., Haft, D., Hulo, N., Hunter, S., Kahn, D., Kanapin, A., Kejariwal, A., Labarga, A., Langendijk-Genevaux, P. S., Lonsdale, D., Lopez, R., Letunic, I., Madera, M., Maslen, J., McAnulla, C., McDowall, J., Mistry, J., Mitchell, A., Nikolskaya, A. N., Orchard, S., Orengo, C., Petryszak, R., Selengut, J. D., Sigrist, C. J. A., Thomas, P. D., Valentin, F., Wilson, D., Wu, C. H., & Yeats, C. (2007). New developments in the InterPro database. *Nucl. Acids Res.*, 35(Supplement 1), D224–228.

[Narumi et al., 1997] Narumi, I., Cherdchu, K., Kitayama, S., & Watanabe, H. (1997). The *Deinococcus radiodurans* uvrA gene: identification of mutation sites in two mitomycin-sensitive strains and the first discovery of insertion sequence element from deinobacteria. *Gene*, 198(1-2), 115–126.

[Narumi et al., 2004] Narumi, I., Satoh, K., Cui, S., Funayama, T., Kitayama, S., & Watanabe, H. (2004). PprA: a novel protein from *Deinococcus radiodurans* that stimulates DNA ligation. *Molecular Microbiology*, 54(1), 278–285.

[Nicholson et al., 2005] Nicholson, W. L., Schuerger, A. C., & Setlow, P. (2005). The solar UV environment and bacterial spore UV resistance: considerations for Earth-to-Mars transport by natural processes and human spaceflight. *Mutation Research/Fundamental and Molecular Mechanisms of Mutagenesis*, 571(1-2), 249–264.

[Ohba et al., 2005] Ohba, H., Satoh, K., Yanagisawa, T., & Narumi, I. (2005). The radiation responsive promoter of the *Deinococcus radiodurans* pprA gene. *Gene*, 363, 133–141.

[Osterman, 2006] Osterman, A. (2006). A hidden metabolic pathway exposed. *Proceedings of the National Academy of Sciences*, 103(15), 5637–5638.

[Patel et al., 2003] Patel, M. R., Berces, A., Kolb, C., Lammer, H., Rettberg, P., Zarnecki, J. C., & Selsis, F. (2003). Seasonal and diurnal variations in martian surface ultraviolet irradiation: biological and chemical implications for the martian regolith. *International Journal of Astrobiology*, 2(01), 21–34.

[Pitcher et al., 2007] Pitcher, R. S., Brissett, N. C., & Doherty, A. J. (2007). Nonhomologous end-joining in bacteria: A microbial perspective. *Annual Review of Microbiology*, 61(1), 259–282.

[Pogoda de la Vega et al., 2005] Pogoda de la Vega, U., Rettberg, P., Douki, T., Cadet, J., & Horneck, G. (2005). Sensitivity to polychromatic UV-radiation of strains of *Deinococcus radiodurans* differing in their DNA repair capacity. *International Journal of Radiation Biology*, 81(8), 601–611.

[Pogoda de la Vega et al., 2007] Pogoda de la Vega, U., Rettberg, P., & Reitz, G. (2007). Simulation of the environmental climate conditions on martian surface and its effect on *Deinococcus radiodurans*. *Advances in Space Research*, 40(11), 1672–1677.

[Rainey et al., 1997] Rainey, F., Nobre, M., Schumann, P., Stackebrandt, E., & da Costa, M. (1997). Phylogenetic diversity of the Deinococci as determined by 16S ribosomal DNA sequence comparison. *Int J Syst Bacteriol*, 47(2), 510–514.

[Rainey et al., 2005] Rainey, F. A., Ray, K., Ferreira, M., Gatz, B. Z., Nobre, M. F., Bagaley, D., Rash, B. A., Park, M.-J., Earl, A. M., Shank, N. C., Small, A. M., Henk, M. C., Battista, J. R., Kampfer, P., & da Costa, M. S. (2005). Extensive diversity of ionizing-radiation-resistant bacteria recovered from Sonoran desert soil and description of nine new species of the genus *Deinococcus* obtained from a single soil sample. *Appl. Environ. Microbiol.*, 71(9), 5225–5235.

[Ravanat et al., 2001] Ravanat, J.-L., Douki, T., & Cadet, J. (2001). Direct and indirect effects of UV radiation on DNA and its components. *Journal of Photochemistry and Photobiology B: Biology*, 63(1-3), 88–102.

[Rettberg et al., 1998] Rettberg, P., Horneck, G., Strauch, W., Facius, R., & Seckmeyer, G. (1998). Simulation of planetary UV radiation climate

on the example of the early Earth. *Advances in Space Research*, 22(3), 335–339.

[Rettberg et al., 2004] Rettberg, P., Rabbow, E., Panitz, C., & Horneck, G. (2004). Biological space experiments for the simulation of martian conditions: UV radiation and martian soil analogues. *Advances in Space Research*, 33(8), 1294–1301.

[Ronto et al., 2003] Ronto, G., Berces, A., Lammer, H., Cockell, C. S., Molina-Cuberos, G. J., Patel, M. R., & Selsis, F. (2003). Solar UV irradiation conditions on the surface of Mars. *Photochemistry and Photobiology*, 77(1), 34–40.

[Sancar, 1996] Sancar, A. (1996). DNA excision repair. *Annual Review of Biochemistry*, 65(1), 43–81.

[Sancar, 1999] Sancar, A. (1999). Excision repair invades the territory of mismatch repair. *Nat Genet*, 21(3), 247–249.

[Schmid et al., 2005a] Schmid, A. K., Howell, H. A., Battista, J. R., Peterson, S. N., & Lidstrom, M. E. (2005a). Global transcriptional and proteomic analysis of the Sig1 heat shock regulon of *Deinococcus radiodurans*. *J. Bacteriol.*, 187(10), 3339–3351.

[Schmid et al., 2005b] Schmid, A. K., Howell, H. A., Battista, J. R., Peterson, S. N., & Lidstrom, M. E. (2005b). HspR is a global negative regulator of heat shock gene expression in *Deinococcus radiodurans*. *Molecular Microbiology*, 55(5), 1579–1590.

[Schuerger et al., 2003] Schuerger, A. C., Mancinelli, R. L., Kern, R. G., Rothschild, L. J., & McKay, C. P. (2003). Survival of endospores of *Bacillus subtilis* on spacecraft surfaces under simulated martian environments: implications for the forward contamination of Mars. *Icarus*, 165(2), 253–276.

[Schuerger et al., 2006] Schuerger, A. C., Richards, J. T., Newcombe, D. A., & Venkateswaran, K. (2006). Rapid inactivation of seven Bacillus spp. under simulated Mars UV irradiation. *Icarus*, 181(1), 52–62.

[Servinsky & Julin, 2007] Servinsky, M. D. & Julin, D. A. (2007). Effect of a recD mutation on DNA damage resistance and transformation in *Deinococcus radiodurans*. *J. Bacteriol.*, (pp. JB.00409–07).

[Shashidhar & Bandekar, 2006] Shashidhar, R. & Bandekar, J. R. (2006). *Deinococcus* mumbaiensis sp. nov., a radiation-resistant pleomorphic bacterium isolated from Mumbai, India. *FEMS Microbiology Letters*, 254(2), 275–280.

[Sheng et al., 2005] Sheng, D., Gao, G., Tian, B., Xu, Z., Zheng, Z., & Hua, Y. (2005). RecX is involved in antioxidant mechanisms of the radioresistant bacterium *Deinococcus radiodurans*. *FEMS Microbiology Letters*, 244(2), 251–257.

[Slot et al., 1989] Slot, J. W., Geuze, H. J., & Weerkamp, A. H. (1989). Localization of macromolecular components by application of the immunogold technique on cryosectioned bacteria. In F. Mayer (Ed.), *Methods in Microbiology: Electron Microscopy in Microbiology, Vol. 20* (pp. 211–236).: Academic Press.

[Southworth & Perler, 2002] Southworth, M. W. & Perler, F. B. (2002). Protein splicing of the *Deinococcus radiodurans* strain R1 Snf2 intein. *J. Bacteriol.*, 184(22), 6387–6388.

[Spacek et al., 1995] Spacek, W., Bauer, R., & Heisler, G. (1995). Heterogeneous and homogeneous wastewater treatment - comparison between photodegradation with TiO_2 and the photo-fenton reaction. *Chemosphere*, 30(3), 477–484.

[Spurr, 1969] Spurr, A. R. (1969). A low-viscosity epoxy resin embedding medium for electron microscopy. *Journal of Ultrastructure Research*, 26(1-2), 31–43.

[Suresh et al., 2004] Suresh, K., Reddy, G. S. N., Sengupta, S., & Shivaji, S. (2004). *Deinococcus* indicus sp. nov., an arsenic-resistant bacterium from an aquifer in West Bengal, India. *Int J Syst Evol Microbiol*, 54(2), 457–461.

[Tanaka et al., 2004] Tanaka, M., Earl, A. M., Howell, H. A., Park, M.-J., Eisen, J. A., Peterson, S. N., & Battista, J. R. (2004). Analysis of *Deinococcus radiodurans*' transcriptional response to ionizing radiation and desiccation reveals novel proteins that contribute to extreme radioresistance. *Genetics*, 168(1), 21–33.

[Tanaka et al., 2005] Tanaka, M., Narumi, I., Funayama, T., Kikuchi, M., Watanabe, H., Matsunaga, T., Nikaido, O., & Yamamoto, K. (2005). Characterization of pathways dependent on the uvsE, uvrA1, or uvrA2

gene product for UV resistance in *Deinococcus radiodurans*. *J. Bacteriol.*, 187(11), 3693–3697.

[Thompson & Murray, 1981] Thompson, B. G. & Murray, R. G. (1981). Isolation and characterization of the plasma membrane and the outer membrane of *Deinococcus radiodurans* strain Sark. *Canadian Journal of Microbiology*, 27(7), 729–734.

[Thompson et al., 2006] Thompson, L. S., Beech, P. L., Real, G., Henriques, A. O., & Harry, E. J. (2006). Requirement for the cell division protein DivIB in polar cell division and engulfment during sporulation in *Bacillus subtilis*. *J. Bacteriol.*, 188(21), 7677–7685.

[van Dongen, 2000] van Dongen, S. (2000). *Graph Clustering by Flow Simulation*. PhD thesis, University of Utrecht, Netherlands.

[Venkateswaran et al., 2000] Venkateswaran, A., McFarlan, S. C., Ghosal, D., Minton, K. W., Vasilenko, A., Makarova, K., Wackett, L. P., & Daly, M. J. (2000). Physiologic determinants of radiation resistance in *Deinococcus radiodurans*. *Appl. Environ. Microbiol.*, 66(6), 2620–2626.

[Vogel, 1995] Vogel, H. (1995). *Gerthsen Physik*. Springer, 18th edition.

[Wagner et al., 2003] Wagner, D., Kobabe, S., Pfeiffer, E.-M., & Hubberten, H.-W. (2003). Microbial controls on methane fluxes from a polygonal tundra of the Lena Delta, Siberia. *Permafrost and Periglacial Processes*, 14(2), 173–185.

[Wang & Julin, 2004] Wang, J. & Julin, D. A. (2004). DNA helicase activity of the RecD protein from *Deinococcus radiodurans*. *J. Biol. Chem.*, 279(50), 52024–52032.

[Ward, 1975] Ward, J. (1975). Molecular mechanisms of radiation-induced damage to nucleic acids. *Adv Rad Biol*, 5, 181–239.

[Weisburg et al., 1989] Weisburg, W. G., Giovannoni, S. J., & Woese, C. R. (1989). The *Deinococcus–Thermus* phylum and the effect of rRNA composition on phylogenetic tree construction. *Syst Appl Microbiol*, 11, 128–134.

[West & Stock, 2001] West, A. H. & Stock, A. M. (2001). Histidine kinases and response regulator proteins in two-component signaling systems. *Trends in Biochemical Sciences*, 26(1), 369–376.

[White et al., 1999] White, O., Eisen, J. A., Heidelberg, J. F., Hickey, E. K., Peterson, J. D., Dodson, R. J., Haft, D. H., Gwinn, M. L., Nelson, W. C., Richardson, D. L., Moffat, K. S., Qin, H., Jiang, L., Pamphile, W., Crosby, M., Shen, M., Vamathevan, J. J., Lam, P., McDonald, L., Utterback, T., Zalewski, C., Makarova, K. S., Aravind, L., Daly, M. J., Minton, K. W., Fleischmann, R. D., Ketchum, K. A., Nelson, K. E., Salzberg, S., Smith, H. O., Craig, J., Venter, A., & Fraser, C. M. (1999). Genome sequence of the radioresistant bacterium *Deinococcus radiodurans* R1. *Science*, 286(5444), 1571–1577.

[Witte et al., 2005] Witte, G., Urbanke, C., & Curth, U. (2005). Single-stranded DNA-binding protein of *Deinococcus radiodurans*: a biophysical characterization. *Nucl. Acids Res.*, 33(5), 1662–1670.

[Woese, 1987] Woese, C. R. (1987). Bacterial evolution. *Microbiol. Mol. Biol. Rev.*, 51(2), 221–271.

[Zahradka et al., 2006] Zahradka, K., Slade, D., Bailone, A., Sommer, S., Averbeck, D., Petranovic, M., Lindner, A. B., & Radman, M. (2006). Reassembly of shattered chromosomes in *Deinococcus radiodurans*. *Nature*, 443(7111), 569–573.

[Zhang et al., 2007] Zhang, Y.-Q., Sun, C.-H., Li, W.-J., Yu, L.-Y., Zhou, J.-Q., Zhang, Y.-Q., Xu, L.-H., & Jiang, C.-L. (2007). *Deinococcus* yunweiensis sp. nov., a gamma- and UV-radiation-resistant bacterium from China. *Int J Syst Evol Microbiol*, 57(2), 370–375.

[Zimmerman & Battista, 2005] Zimmerman, J. & Battista, J. (2005). A ring-like nucleoid is not necessary for radioresistance in the Deinococcaceae. *BMC Microbiology*, 5(1), 17.

[Zou et al., 1998] Zou, Y., Crowley, D. J., & Van Houten, B. (1998). Involvement of molecular chaperonins in nucleotide excision repair. DnaK leads to increased thermal stability of uvrA, catalytic uvrB loading, enhanced repair, and increased UV resistance. *J. Biol. Chem.*, 273(21), 12887–12892.

APPENDIX

A. SUMMARY

The aim of this dissertation was to make use of the differing UV-susceptibility and UV-damage repair capability of the investigated *D. radiodurans* strains and to identify components of the hypothesized bypass UV-induced damage repair system. This aim was achieved by i) combining biochemical, survival assessment by cultivation and ultrastructural experimental techniques, ii) monitoring repair kinetics of bipyrimidine photoproducts induced by 254 nm-UV radiation and iii) examining and comparing the gene expression profiles of the differing UV-susceptible *D. radiodurans* strains post-0.5 h-UV irradiation recovery.

Previous studies have corroborated UV radiation to be the primary biocidal factor. The results obtained in this dissertation provide evidence that UV radiation engenders synergistic effects in combination with other stressors like temperature, humidity and desiccation (vacuum, respectively). Together with its inherent biocidal activity UV radiation potentiates the biological effectiveness of the associated parameters. Whereas low temperature and vacuum exhibited a moderate biological effectiveness. Supported by the results obtained from the simulated harsh environment, in which desiccated *D. radiodurans* cells survived 7 d Mars-like cycles of temperature and water activity without UV radiation. Chances of survival for the strains are enlarged, if shielded by dust particles or covered by soil, suggesting that residing in microhabitats below the surface is most probable in a harsh UV climate.

Not only genetic equipment but also the applied wavelengths influence *D. radiodurans'* repair efficiency, especially polychromatic UV radiation enables the UV-sensitive class to repair the UV-induced lesions and retain their vitality. A possible explanatory approach for this observed increase in repair efficiency suggests that the wavelength range $\lambda = 315 - 400$ nm activates a photosensitive gene or gene cluster that is involved in UV-induced damage repair.

A post-0.5 h-recovery phase was sufficient for wild-type strain R1 to repair up to 80% of the total induced DNA photoproducts. Nucleotide excision repair (NER) is given priority over homologeous recombination repair (HR), based on the fact that 1R1A (*recA*) resumed repair of bipyrimidine dimers but UVs78 (*uvrA-1 uvsE*) was unable to repair any photoproduct type not

even after 2 h, the utmost post-irradiation recovery time point analyzed.

The proposed UV-repair process flow: NER efficiently removes both cyclobutane bipyrimidine dimers (CPDs) and $6-4$ bipyrimidine adducts. HR assists removal of CPD from UV-irradiated DNA, but plays a minor role in removal of $6-4$ adducts. Though the NER is not existent in UVs78 (*uvrA-1 uvsE*) up to 70% of both bipyrimidine photoproduct types were equally repaired post-UV ($>$ 315 nm)-irradiation. If the repair ability were due to the existent HR-pathway, a minimum repair of at least CPD should be measurable following UV-254 nm- and UV-($>$ 200 nm)-radiation. Hence, an additional pathway must be available that allows repair of both photoproduct classes. The core genes of this novel bypass pathway identified $DR2438, DR2439, DR2441$ and $DR2444$ as well as $DR2445, DR2446$. Whereas the assertion that $DR1200$ and $DR1891$ may act as putative signal factors to initiate this NER- and HR-independent bypass still has to be verified.

B. ZUSAMMENFASSUNG

UV-Strahlung verursacht DNA-Schäden in Form von Cyclobutan-Pyrimidin-Dimeren (CPD) und $6-4$ Dipyrimidin Addukte. *D. radiodurans* zeigt eine ausgeprägte UV-Strahlenresistenz, selbst UV-empfindliche reparaturdefiziente Mutantenstämme zeigen einen ähnlichen Verlauf des Überlebens wie der Wildtyp-Stamm nach Bestrahlung mit polychromatischer langwelliger UV-Strahlung. Zur weiteren Erforschung und Aufklärung eines vorhandenen unbekannten UV-Reparaturprozesses wurden i) eingehende biochemische, elektronenmikroskopische und physiologische Untersuchungen getätigt, ii) die Reparaturverläufe der DNA Photoprodukte jedes Stammes beobachtet und iii) die Schadensauswirkungen mit Hilfe von DNA Microarrays auf Genexpressionsebene analysiert.
Die untersuchten Umweltparameter Niedrig-Temperaturen und Vakuum zeigten im gewählten Bereich ein eher moderates Inaktivierungspotential. Dagegen belegen die durchgeführten Studien, dass UV-Strahlung als synergistischer Umweltfaktor fungiert. Im Zusammenspiel mit anderen abiotischen Faktoren wie Temperatur, Feuchtigkeit, Trocknung und Vakuum potenziert UV-Strahlung die individuell vorhandene Schadenswirkung in erheblichem Maße. Dies bestätigte sich bei der Simulation eines unwirtlichen Milieus, bei dem getrocknete *D. radiodurans* Zellen zwar einem 7-Tage-Zyklus von Temperatur- und Feuchtigkeitschwankungen bei 7 hPa und CO_2-haltiger Atmosphäre überlebten, jedoch nur unter Ausschluss von UV-Strahlung. Bereits Stäube mit geringer Korngröße schützten die Zellen vor UV-Strahlung.

Es stellte sich heraus, daß nicht die genetische Ausstattung allein, sondern auch die applizierte Wellenlänge erheblich die Reparaturfähigkeit der einzelnen *D. radiodurans* Stämme beeinflußt. Vor allem polychromatische langwellige UV-Strahlung ermöglicht den UV-empfindlichen Stämmen, DNA Photoprodukte zu beheben. Ein möglicher Erklärungsansatz hierfür postuliert die Aktivierung eines photoinduzierten Gens oder einer Gengruppe, deren Korrelationswellenlängenbereich bei $\lambda = 315 - 400$ nm liegt.
Nach einem Erholungszeitraum von 0.5 h nach UV-(254 nm)-Bestrahlung erzielte *D. radiodurans* Wildtyp-Stamm bereits eine Reparaturrate von bis zu 80% der gesamten induzierten DNA Photoprodukte. Aufgrund der moderat vorhandenen Reparaturrate des Mutantenstammes 1R1A (*recA*) und der

anhaltenden Reparaturunfähigkeit der Doppelmutante UVs78 (*uvrA-1 uvsE*) erfolgt die UV-Schadenbehebung bevorzugt durch "nucleotide excision repair (NER)" (Ausschneiden von Nukleotiden). Demnach beseitigt NER in effizienter Weise sowohl CPD als auch $6-4$ Addukte. Trotz des fehlenden NER-Mechanismus in UVs78 (*uvrA-1 uvsE*) erzielt diese Mutante eine 70%-ige Reparaturrate der Gesamt-Photoproduktanzahl nach UV-($>$ 315 nm)-Bestrahlung. Wäre ausschließlich homologe Rekombination für diesen Reparaturerfolg verantwortlich, so müsste sich zumindest teilweise die Anzahl der Gesamt-CPD nach UV-254 nm- und UV-($>$ 200 nm)-Bestrahlung im Verlauf der Erholungsphase verringern. Aus diesem Grunde, muss ein weiterer Mechanismus vorhanden sein, der beide DNA Photoprodukte gleichermaßen reparieren kann. Aussichtsreiche Kandidaten sind $DR2438$, $DR2439$, $DR2441$ und $DR2444$ sowie $DR2445$, $DR2446$, wobei noch experimentell verifiziert werden muss, ob $DR1200$ und $DR1891$ mögliche Auslösefaktoren dieses bisher unbekannten UV-Reparaturprozesses sind.

C. LIST OF ABBREVIATIONS

Tab. C.1: List of abbreviations

$6-4$ PPs	– Pyrimidine $(6-4)$ pyrimidone photoproducts
CO_2	– Carbon dioxide
aa	– Amino acids
ACLAME	– A CLAssification of Mobile genetic Elements
AG	– Aktien-Gesellschaft
AMT	– Accurate mass tag
AP	– Apurinic/apyrimidinic sites
ATCC	– American Type Culture Collection
ATP	– Adenosine-triphosphate
biP	– UV-induced bipyrimidine dimers (CPD and $6-4$ PP)
C	– Cyotosine
cDNA	– Complementary DNA
cfu	– Colony forming units
Cm	– Chloramphenicol (Antibiotic)
CP	– Chromosomal plasmid
CPD	– Cyclobutane pyrimidine dimer
Cy3	– 5-Amino-propargyl-2′-deoxyuridine or deoxycytidine 5′-triphosphate coupled to Cy3 fluorescent dye
ddr	– DNA damage response protein
DER 736	– Diglycidyl ether of polypropylene glycol
DFG	– Deutsche Forschungsgemeinschaft (German Research Foundation)
DIN	– Deutsche Iso-Norm
Din	– DNA damage-inducible gene
DLR	– Deutsches Zentrum für Luft- und Raumfahrt e.V.
DMAE S-1	– Dimethylaminoethanol (S-1)
DMM	– chemically Defined synthethetic Minimal Media

Tab. C.1b (continued): List of abbreviations

DNA	– Deoxynucleic Acid
DR	– Gene loci of *D. radiodurans*
dsb	– Double strand breaks
EBI	– European Bioinformatics Institute (an outstation of EMBL)
EC	– Enzyme Commission Numbers
ECF	– Extracytoplasmatic funcion
EDTA	– Ethylenediamine-tetraacetic acid
ELISA	– Enzyme-linked immunosorbent assays
EMBL	– European Molecular Biology Laboratory
ER	– Excision repair pathway
ERL 4206	– Vinyl cyclohexen dioxide (a cycloaliphatic diepoxide)
ESDSA	– Extended synthesis-dependent strand annealing
FIG	– Fellowship for Interpretation of Genomes (University of Chicago, USA)
GC [content]	– Guanine cytosine content (mostly expressed as mol%)
GCR	– Galactic cosmic rays
GmbH	– Gesellschaft mit beschränkter Haftung
GTPase	– Enzyme that cleaves Guanine-triphospate
HAIR	– HspR-associated inverted repeat sequence
HIMAC	– Heavy Ion Medical Accelerator
HPI	– Hexagonally-packed intermediate layer (component of cell wall)
HPLC	– High performance liquid chromatography
HR	– Homologous recombination repair
HRDC	– Helicase and RNAse D C-terminal domain
HspR	– Heat stress protein regulator
HTH	– Helix-turn-helix motif
InterPro	– Integrated resource of protein families, domains and functional sites
IS	– Insertion sequence in genome
KEGG	– Kyoto Encyclopedia of Genes and Genomes
KG	– Kommanditgesellschaft
KGaA	– Kommanditgesellschaft auf Aktien

Tab. C.1c (continued): List of abbreviations

LHR – Liquid holding recovery
Lig – DNA ligase
Mb – Mega base pairs
MCL – Markov clustering algorithm
MD – Maryland (a state in USA)
MESS – Mars-Environment-Simulation Studies
MGE – Mobile genetic elements
MMC – Mitomycin C
MMR – Mismatch repair pathway
Mn – Manganese
MNNG – $N-$methyl$-N'-$nitro$-N-$nitrosoguanidine
MP – Megaplasmid
mRNA – Messenger RNA
MS/MS– Tandem mass spectrometry
NAD – Nicotinamide adenine dinucleotide
NCBI – National Center for Biotechnology Information
NCH – Nano-crystalline hematite
NER – Nucleotide excision repair
NHEJ – Non-homologous end joining (DNA damage repair pathway)
NIH – National Institute of Health
NIRS – National Institute for Radiological Sciences
NLM – National Library of Medicine
NSA – Nonenyl succinic anhydride
OH – Hydroxyl molecule
ORF – Open reading frames
PEG – Protein encoding genes
PIR – Protein Information Resource
Pol – Polymerase
PSI – Planetary and Space Simulation Facilities
PVA – Polyvinyl alcohol
QPCR – Real-time polymerase chain reaction
Rec – *Recombinase*, enzyme linked to homologous recombinational repair
RIN – RNA integrity number
RMA – Robust Multichip Average algorithm

Tab. C.1d (continued): List of abbreviations

RNA	– Ribonucleic Acid
RNAse	– RNA degrading enzyme
ROS	– Reactive oxygen species
rRNA	– Ribosomal RNA
RSR	– Ro sixty related protein
RZPD	– German Resource Center for Genome Research
SDSA	– Synthesis-dependent strand annealing (most recent model for HR)
SEM	– Scanning electron microscopy
SER	– Standard error
SI	– Systéme international d'unités
SMC	– Structural maintenance-of-chromosomes proteins
SSA	– Single-strand annealing (aberrant HR)
SSB	– Single-strand-binding protein
ssDNA	– Single-stranded DNA
Swiss-Prot	– Swiss Institute of Bioinformatics
T	– Thymine
TE	– Tris-EDTA buffer solution
TEM	– Transmission electron microscopy
TGY	– Tryptone Yeast and Glucose (nutrient broth)
TPR	– Tetratricopeptide repeats
UHV	– Ultrahigh vacuum
UniProt	– Universal Protein Resource
UniPRotKB	– UniProt Knowledgebase
USA	– United States of America
USUHS	– Uniformed Services University of the Health Sciences
UV	– Ultra violet
UVA	– $315 - 400$ nm
UVB	– $280 - 315$ nm
UVC	– $100 - 280$ nm
UVDE	– UV-induced dimer endonucleases
UVP	– Ultra-Violet Products (instrument to measure the UV radiation flux)
VUV	– Vacuum UV, $\lambda < 100 - 200$ nm
WT	– Wild-type strain

D. ADDITIONAL TABLES

Tab. D.1: Transposase affiliated to the IS4-family including E-values and the grade of homology. The proteins encoded by this group of MGE resulted in sequence pairs within the *D. radiodurans* genome. The list of sequence pairs is transformed into a scoring matrix with the E-value (expected value) as distance.

IS4-family			
Aligne index	E-value	ID%	Organism
*DRC*0029			
584	1.e-168	98	*DRB*0057
583	1.e-167	98	*DRB*0117
581	1.e-167	97	*DRB*0020
581	1.e-166	97	*DRB*0102
581	1.e-166	97	*DRB*0005
578	1.e-166	97	*DRB*0134
134	3.e-32	80	*DRC*0032
*DRB*0020			
674	0.e+00	99	*DRB*0102
674	0.e+00	99	*DRB*0005
667	0.e+00	98	*DRB*0057
666	0.e+00	98	*DRB*0134
660	0.e+00	97	*DRB*0117
581	1.e-167	97	*DRC*0029
130	7.e-31	78	*DRC*0032
*DRB*0055			
82	3.e-17	87	*DRB*0059
65	4.e-12	97	*DRB*0018
65	4.e-12	97	*DRB*0113
65	4.e-12	97	*DRB*0132
65	4.e-12	97	*DRB*0058
65	4.e-12	97	*DRB*0103

Tab. D.1b (continued): IS4-family

IS4-family			
Aligne index	E-value	ID%	Organism
*DR*1196			
593	1.e-170	99	*DRC*0029
587	1.e-168	98	*DRB*0057
586	1.e-168	98	*DRB*0117
583	1.e-167	97	*DRB*0020
583	1.e-167	97	*DRB*0102
583	1.e-167	97	*DRB*0005
581	1.e-166	97	*DRB*0134
134	3.e-32	80	*DRC*0032
*DRB*0057			
667	0.e+00	98	*DRB*0134
667	0.e+00	98	*DRB*0020
667	0.e+00	98	*DRB*0102
667	0.e+00	98	*DRB*0005
652	0.e+00	96	*DRB*0117
584	1.e-167	98	*DRC*0029
130	7.e-31	78	*DRC*0032
*DRB*0134			
670	0.e+00	99	*DRB*0102
670	0.e+00	99	*DRB*0005
667	0.e+00	98	*DRB*0057
666	0.e+00	98	*DRB*0020
651	0.e+00	96	*DRB*0117
578	1.e-166	97	*DRC*0029
126	1.e-29	76	*DRC*0032
*DR*0144			
678	0.e+00	100	*DRB*0102
678	0.e+00	100	*DRB*0005
674	0.e+00	99	*DRB*0020
670	0.e+00	99	*DRB*0134
667	0.e+00	98	*DRB*0057
659	0.e+00	97	*DRB*0117
581	1.e-166	97	*DRC*0029
130	7.e-31	78	*DRC*0032

Tab. D.1c (continued): IS4-family

IS4-family			
Aligne index	E-value	ID%	Organism
*DRB*0102			
678	0.e+00	100	*DRB*0005
674	0.e+00	99	*DRB*0020
670	0.e+00	99	*DRB*0134
667	0.e+00	98	*DRB*0057
659	0.e+00	97	*DRB*0117
581	1.e-166	97	*DRC*0029
130	7.e-31	78	*DRC*0032
*DRC*0019			
120	1.e-28	96	*DRB*0102
120	1.e-28	96	*DRB*0005
120	1.e-28	96	*DRB*0117
120	1.e-28	96	*DRB*0020
118	6.e-28	95	*DRB*0134
114	1.e-26	91	*DRB*0057
*DR*1618			
701	0.e+00	90	*DRB*0018
701	0.e+00	90	*DRB*0113
687	0.e+00	89	*DRB*0103
684	0.e+00	89	*DRB*0058
655	0.e+00	84	*DRB*0059
392	1.e-109	93	*DRB*0132
*DRB*0018 and *DRA*0253			
699	0.e+00	90	*DRB*0113
686	0.e+00	89	*DRB*0103
683	0.e+00	89	*DRB*0058
392	1.e-109	93	*DRB*0132
*DR*0010			
701	0.e+00	90	*DRB*0018
701	0.e+00	90	*DRB*0113
687	0.e+00	89	*DRB*0103
684	0.e+00	89	*DRB*0058
655	0.e+00	84	*DRB*0059
392	1.e-109	93	*DRB*0132

Tab. D.1d (continued): IS4-family

IS4-family			
Aligne index	E-value	ID%	Organism
*DRB*0058			
749	0.e+00	93	*DRB*0103
732	0.e+00	94	*DRB*0018
732	0.e+00	94	*DRB*0113
684	0.e+00	88	*DRB*0059
414	1.e-116	93	*DRB*0132
*DRB*0113			
414	1.e-116	93	*DRB*0132
412	1.e-116	92	*DRB*0018
412	1.e-116	92	*DRB*0058
412	1.e-116	92	*DRB*0103
379	1.e-106	86	*DRB*0059
*DRB*0103			
749	0.e+00	93	*DRB*0058
735	0.e+00	95	*DRB*0018
735	0.e+00	95	*DRB*0113
687	0.e+00	89	*DRB*0059
414	1.e-116	93	*DRB*0132
*DRB*0132			
414	1.e-116	93	*DRB*0018
414	1.e-116	93	*DRB*0058
414	1.e-116	93	*DRB*0103
412	1.e-116	92	*DRB*0113
378	1.e-106	85	*DRB*0059
*DR*1762			
412	1.e-116	8 4	*DRB*0018
412	1.e-116	84	*DRB*0058
412	1.e-116	84	*DRB*0103
411	1.e-116	84	*DRB*0113
392	1.e-110	93	*DRB*0132
380	1.e-106	79	DRB005

*An ACLAME family is defined as a set of similar sequences sharing one or more functions.

Tab. D.2: Up regulated hypothetical proteins with a fold change < 2 . Induced hypotheticals with a fold change ≥ 2 are listed in table 5.9 (chapter 5, p. 102).

Gene	Hypotheticals	f-value 1R1A
*DR*0007	hypothetical protein	1.98
*DR*2449	hypothetical protein	1.96
*DR*1919	hypothetical protein	1.95
*DR*0988	hypothetical protein	1.92
*DR*0008	hypothetical protein	1.90
*DR*2318	hypothetical protein	1.84
*DR*1574	hypothetical protein	1.83
*DR*0381	hypothetical protein	1.82
*DR*2150	hypothetical protein	1.81
*DR*0380	hypothetical protein	1.74
*DR*1818	hypothetical protein	1.72
*DR*1715	hypothetical protein	1.71
*DR*2452	hypothetical protein	1.70
*DR*2446	hypothetical protein	1.66
*DR*1388	hypothetical protein	1.65
*DR*2436	hypothetical protein	1.63
*DR*2517	hypothetical protein	1.62
*DR*0488	hypothetical protein	1.61
*DR*0481	hypothetical protein	1.58
*DR*1936	hypothetical protein	1.54
*DR*2167	hypothetical protein	1.43
*DR*2319	hypothetical protein	1.40
*DR*1821	hypothetical protein	1.39
*DR*2445	hypothetical protein	1.36
*DR*2437	hypothetical protein	1.33
*DR*0392	hypothetical protein	1.31
*DR*2505	hypothetical protein	1.31
*DR*0600	hypothetical protein	1.31

Tab. D.2b (continued): Proteins with a fold change < 2

Gene	Hypotheticals	f-value 1R1A
*DR*1138	hypothetical protein	1.30
*DRA*0292	hypothetical protein	1.28
*DR*1135	hypothetical protein	1.22
*DR*1575	hypothetical protein	1.22
*DR*0214	hypothetical protein	1.22
*DR*1466	hypothetical protein	1.20
*DR*0357	hypothetical protein	1.19
*DR*0915	hypothetical protein	1.15
*DRA*0294	hypothetical protein	1.15
*DR*1249	hypothetical protein	1.15
*DRA*0293	hypothetical protein	1.14
*DR*0337	hypothetical protein	1.14
*DR*2441	hypothetical protein	1.14
*DR*2143	hypothetical protein	1.13
*DR*0787	hypothetical protein	1.12
*DR*1484	hypothetical protein	1.12
*DR*0800	hypothetical protein	1.12
*DR*1021	hypothetical protein	1.11
*DR*0368	hypothetical protein	1.11
*DR*0737	hypothetical protein	1.10
*DR*1422	hypothetical protein	1.09
*DR*2411	hypothetical protein	1.06
*DR*2159	hypothetical protein	1.06
*DR*1119	hypothetical protein	1.05
*DRA*0129	hypothetical protein	1.04
*DR*1576	hypothetical protein	1.02
*DR*2472	hypothetical protein	1.02
*DRA*0006	hypothetical protein	1.01

Tab. D.3: Abundance of broad stress response genes post-UV-(254 nm) radiation. The qualitative induction response to the environmental stressors of these selected genes has been derived from [Lipton et al., 2002].

Gene		f-value 1R1A	table	Environmental stress conditions								
*DRB*0051	HP	-11.4	5.6	N		OX	ST	CS	pH			UV
*DRB*0067	extra-cellular nuclease	-10.2	5.6	N	Th	OX	ST		pH			UV
*DR*1279	SodA	-7.0	5.1	N	T	OX	ST	CS	pH			UV
*DR*1459	serine protease	2.9	5.1	N	T	OX	ST	CS	pH		IR	UV
*DR*2588	Fe-complex trans-porter	1.5	5.1	N	T	OX	ST	CS	pH			UV
Protein Fate												
*DR*1473	phage shock protein	2.1	5.1	N	T	OX	ST	CS	pH	HS		UV
*DR*0129	DnaK	1.8	5.1	N	T	OX	ST	CS	pH	HS		UV
*DR*1314	heat shock protein	1.8	5.1	N	T	OX	ST	CS	pH	HS		UV
*DR*0606	GroES	1.2	5.9	N	T	OX	ST	CS	pH	HS		UV
*DR*0309	EF-Tu	1.1	5.1	N	T	OX	ST	CS	pH			UV

Tab. D.3b (continued): Broad stress response genes

Gene		f-value 1R1A	table	Environmental stress conditions								
Outer structure proteins												
*DR*1185	S-layer-like array	2.1	5.1	N	T	OX	ST	CS	pH	HS		UV
*DR*2070	membrane lipoprotein	1.6	5.1	N	T	OX	ST	CS	pH			UV
*DR*1124	S-layer homolog	1.2	5.9	N	T	OX	ST	CS	pH			UV
*DR*0379	outer membrane	1.2	5.9	N	T	OX	ST	CS	pH			UV
Protein Synthesis, ribosomal proteins												
*DR*2115	rplO	2.3	5.9	N	T	OX	ST	CS	pH			UV
*DR*0098	rpsF	1.5	5.1	N	T	OX	ST	CS	pH			UV
*DR*0101	rpsR	1.4	5.1	N	T	OX		CS	pH		IR	UV
*DR*0102	rpll	1.2	5.1	N	T	OX	ST	CS	pH			UV
Potential core genes of bypass repair												
*DR*2450	HP	3.3	5.9		T	OX	ST					UV
*DR*2438	endonuclease	1.0	5.9		Tc		ST					UV

HP – hypothetical protein, N – Nutrient constraints, T – Temperature shock (heat "h") and cold), OX – Oxidative stress by adding H_2O_2, ST – Starvation period, CS – Chemical shock, pH – Alkaline shock, HS – Heat shock [Schmid et al., 2005a], D – Desiccation and IR – Ionizing radiation exposure [Tanaka et al., 2004], UV – UV-(254 nm) irradiation (this work)

E. ACKNOWLEDGMENTS

Well, how to start this, when you don't want to forget anyone and wish to give everyone enough room to acknowledge his or her contribution to the success of this dissertation...
First of all - DLR, because the most part of the experiments for this dissertation were performed at the labs of the Radiation Biology division of the Institute of Aerospace Medicine.

But I also want to thank Dr. Anna Gorbushina and her working group at the Carl-von-Ossietzky University of Oldenburg for welcoming me so warmly and helping to facilitate the affiliation to this university and the familarization to their labs.

Furthermore, I would like to express my gratitude to Prof. Dr. Luise Berthe-Corti for her assent to act as assessor of my dissertation.

I extend thanks to those that have had a direct impact to my dissertation: Dr. Thierry Douki (DRFMC/SCIB, Laboratory "Lésions des Acides Nucléiques", CEA-Grenoble, France) for his support and readiness to answer any questions, but especially for the analysis of the bipyrimidine DNA photoproducts.

I want to appreciate the help of Dr. Natalie Leys (Laboratory for Molecular and Cellular Biology (MCB), Belgian Nuclear Research Centre, Mol, Belgium) and her working group, who fostered the transcription profile analysis due to their expertise on the DNA microarray field — special thanks go to Felice.

Though DLR is such a big facility there was this one little island that allowed me to feel comfortable. This island is the Radiation Biology division of the Institute of Aerospace Medicine in Köln-Porz, where I worked the past 5 years.

Each and every staff member as well as guests (scientists, students, former collegues) contributed to this absolutely unusual and special atmosphere. Especially our two non-scientists (Britta and Frau Pütz) were always eager to help whenever bureaucratic stuff or deadlines seemed insuperable and supported me. Not to forget our recent head Dr. Günther Reitz and my supervisor Dr. Petra Rettberg who provided the conditions to work and concentrate on my studies and to consume lab material as much as I needed.

Moreover, I don't want to miss to thank and express my sincere gratitude to Dr. Gerda Horneck, THE role model for all young astrobiologists, always prompting us to plunge deeper into this fascinating and broad scientific field.

Looking back with mixed feelings I will definitely miss our Docs, the new and the old. Here, I would like to single out Ralf and Patrick, with whom I on one hand attended a few business trips filled with fun memories but on the other hand could always exchange my thoughts, fears, frustration and every minor or grave ups or downs.

Now, I want to appreciate the background players:

my family — my blood and my in-law :-)

It's impossible to express their extensive share throughout my scientific path and their unfailing encouragement.

But most of all, my deepest gratitude goes to my husband who endured the agony of my writing phase but still took care of me, especially during the past months of finalizing my dissertation. Without his understanding and belief in me, this work wouldn't have been achievable.

Curriculum Vitae

Personal data

Born	April 20th 1976 in New York, USA
	USA citizenship

Education

2005 - 2008	Matriculation at Carl von Ossietzky University Oldenburg, Germany
1997 - 2004	Matriculation at University of Cologne, Germany
2004 - 2007	PhD-thesis at DLR, Institute of Aerospace Medicine, Radiation Biology Department, Cologne
2003 - 2004	Academic degree *Diploma* in Biology Master thesis at DLR, Institute of Aerospace Medicine, Radiation Biology Department, titled "Characterization of the UV-radiation and desiccation tolerance of *Deinococcus radiodurans*" (German)
1997 - 2003	General Biology, University of Cologne, Germany

Research Experience

2007	Participation at the Biopan 6 experiment
2005 - 2006	DLR project *HUMILAB* (Co-Investigator)
2005	Participation at the Biopan 5 experiment
2005	IX Int. School for Pure and Applied Biophysics
2003	Temporary research training at the laboratory "Lésions des Acides Nucléiques", CEA-Grenoble, France (supervised by Dr. T. Douki)
2002	Lab internship at the DLR, Institute of Aerospace Medicine, Radiation Biology Department, Cologne
2002	Sample preparation for Biopan 4

Research projects and workshop organization

2004 - 2007	DFG project RE 1574/1-1 and 1-2 "Adaptive strategies of microorganisms to extreme environmental conditions: Molecular mechanisms of desiccation and UV-radiation resistance in the extremophile bacterium *Deinococcus radiodurans*"
2004 - 2007	ESA project *HighRad* (Co–Investigator)
2006	DFG workshop *Viability in Space* at DLR, Cologne, Germany (Co–Organizer)